Institut für Neurowissenschaften

Technische Universität München

Structure and function studies in layer 5 pyramidal neurons of the mouse vibrissal cortex

Elvira Sharifullina

Vollständiger Abdruck der von der Fakultät für Medizin der Technischen Universität München zur Erlangung des akademischen Grades eines

Doctor of Philosophy (Ph.D.)

genehmigten Dissertation.

Vorsitzende/r: Univ.- Prof. Dr. Thomas Misgeld

Prüfer der Dissertation:

1. Univ.- Prof. Dr. Arthur Konnerth

2. Priv.- Doz. Dr. Jana Eveline Hartmann

Die Dissertation wurde am 20.09.2011 bei der Fakultät für Medizin der Technischen Universität München eingereicht und durch die Fakultät für Medizin am 23.09.2011 angenommen.

Table of contents

Glossary

AAV	Adeno- associated virus
AMPA	α-amino-3-hydroxy-5-methyl-4-isoxazolepropionic acid
AMPAR	AMPA receptor
AOD	Acousto - optical deflector
APV	2 -amino-5-phosphonovaleric acid
BAC	Bacterial artificial chromosomes
bAP	Back- propagating action potential
Ca^{2+}	Calcium ions
CC	Current clamp mode
CCD	Charge-coupled device
ChR	Channelrhodopsin
ΔF/F	Relative fluorescence change
DAB	Diaminobenzidine
di – ANEPEQ	di- amino naphthyl ethenyl pyridinium
DIC	Differential interference contrast
EGFP	Enhanced green fluorescent protein
EPSP	Excitatory postsynaptic potential
etv	ets variant gene
EYFP	Enhanced yellow fluorescent protein
Fs	Femto second (10^{-15}s)
glt	Glycosyltransferase
HRP	Horseradish peroxidase
Hz	Hertz
K_d	Dissociation constant
L(5)	Layer (5)
LTD	Long- term depression
LTP	Long- term potentiation

MCBL	Multi- cell bolus loading
mM	Millimolar (10^{-3} mol)
MΩ	Megaohm (10^{6} ohm)
ms	Millisecond (10^{-3} s)
mV	Millivolt (10^{-3} V)
mW	Milliwatt (10^{-3} W)
µm	Micrometer (10^{-6} m)
NA	Numerical aperture
NBQX	1, 2, 3, 4-Tetrahydro-6-nitro-2, 3-dioxo-benzo quinoxaline-7-sulfonamide
nm	Nanometer (10^{-9} m)
NMDA	N-Methyl-D-aspartic acid
NMDAR	NMDA receptor
OGB1	Oregon Green Bapta 1
pA	Picoampere (10^{-12} A)
PBS	Phosphate buffered saline
PFA	Paraformaldehyde
PMT	Photomultiplier
POm	Posteromedial nucleus of thalamus
PPT	Patch power tools
p_r	Release probability
RAMM	Regenerative amplification multiphoton microscopy
ROI	Region of interest
S1	Primary somatosensory cortex
SNR	Signal- to- noise ratio
STDP	Spike- timing dependent plasticity
Ti:Sa	Titan:Saphire
VGCC	Voltage- gated Ca^{2+} channels
VPM	Ventral posteromedial nucleus of thalamus

VSD	Voltage- sensitive dye
WM	White matter
3D	Three dimension

Chapter1

Introduction

1.1 The functional organization of the mouse primary somatosensory cortex

The rodent primary somatosensory cortex (vibrissal cortex, barrel cortex, S1) is a widely used model for the analysis of the mammalian cortical circuit. The scientific efforts to describe the functional and morphological properties of the vibrissal cortex in detail date back to work of Woolsey and Van der Loos in 1970. The systematic organization of the vibrissall cortex provides advantages for characterization of the mechanisms of neural transduction from single cellular to circuit level. Thus, it was described that neural activity in the barrel cortex occurs during obtaining of sensory information, in the process of free whisking (Fee et al., 1979). This finding suggests further investigations of the mechanisms underlying the information flow in the thalamocortical pathways.

Most research studies concerning investigation of the vibrissal cortex were performed on rodents such as rats and mice referring to these mammals as nocturnal animals. Therefore the specialized development of their whisker system as sensory signaling compared to other species presents advantages for performing studies in these animals (Petersen, 2003).

The systematic organization of the vibrissal cortex is based on its cytoarchitectonic structure, where every whisker has its own representation in the barrels in layer 4 (L4). The mystacial vibrissae are highly developed tactile organ of the mouse and they are arranged in rows as well as barrels in the cortex (Woolsey and Van der Loos, 1970) (Fig.1.1).

In acute brain slices barrels can be visualized with the bright field microscopy separated from each other with septa and forming the barrel column (Lübke and Feldmeyer, 2007). Each cortical column spreads into approximately 100-400µm in diameter (Woolsey and Van der Loos, 1970). This is another advantage for the studies performed in the barrel cortex, because the direct identification of the barrel column in acute slice preparations gives the possibility to restrict the region of the recording to the individual barrel. That allows study of the synaptic connectivity in the defined barrel field or in particular cell populations.

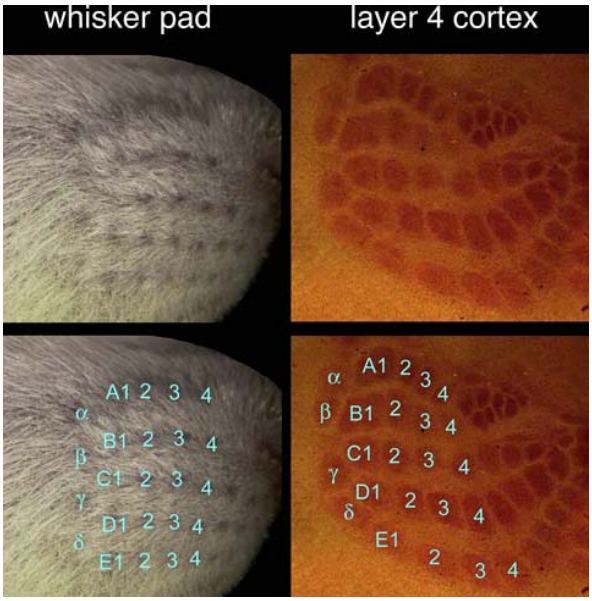

Figure 1.1 Representation of the mouse whiskers and barrel fields of L4 in the slice (Petersen, 2003).
The slice (right) was stained for cytochrome oxidase. The barrels of L4 in the slice show the match with the vibrissae (left).

Although the structure of the vibrissal cortex appears to be highly organized with identified barrels, the functional connections represent the complex system of the cortical synaptic interactions with the signaling flow in different spatial directions. Within the single barrel column the information flow can be local (intracolumnar) or connecting the other columns, transcolumnar. The synaptic contacts can involve a particular layer (intralaminar) or provide connections between cortical layers (Lübke and Feldmeyer, 2007).

1.2 The structure of thalamocortical pathways

Sensory information is transported to the vibrissal cortex through two major thalamocortical pathways (Fig.1.2). The thalamocortical pathway that transmits signals about whisker movements is specified as lemniscal pathway (Lu and Lin, 1993; Yu et al., 2006). It transfers information from ventral posterior medial nucleus of the thalamus (VPM). This pathway contains axons to the neurons of cortical layer 4 (L4), L5, L6, L3 (Wise and Jones, 1978; Agmon et al., 1993; Brecht, 2007; Petreanu et al., 2007).

The second thalamocortical pathway is represented by paralemniscal inputs that transport information about tactile exploration during whisking (Yu et al., 2006).

The afferents arrive from posteromedial nucleus of thalamus (POm) (Diamond et al., 1992; Lu and Lin, 1993; Deschenes et al., 1998; Petreanu et al., 2009) and project to L5A, L4, L3, L2 neurons (Deschenes et al., 1998; Petreanu et al., 2009; Meyer et al., 2010).

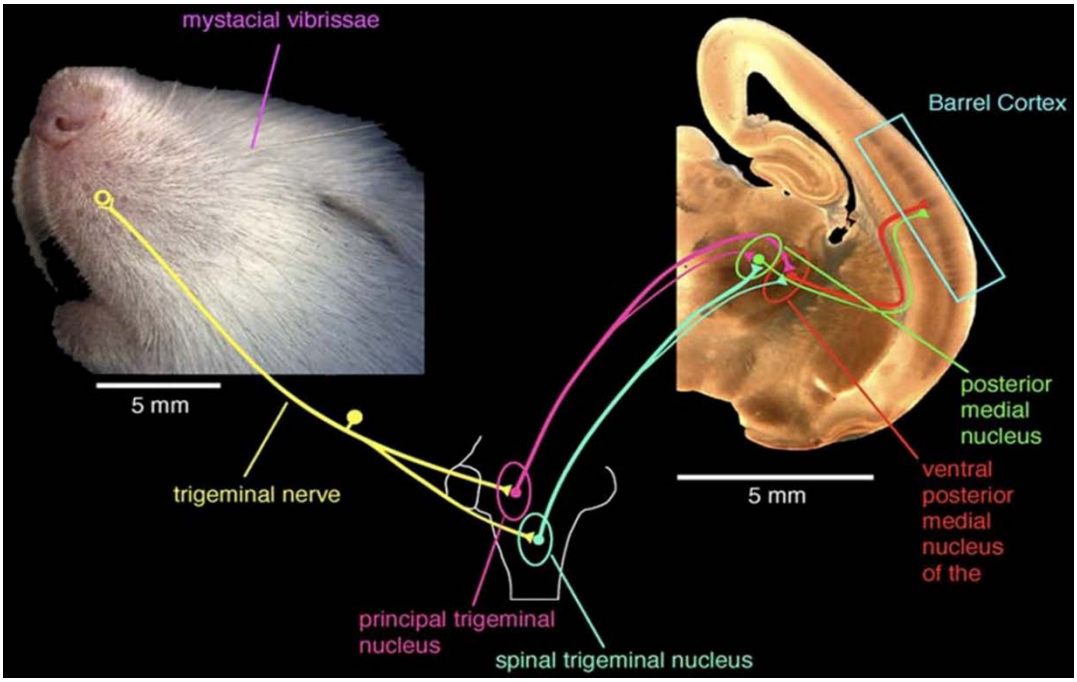

Figure 1.2 The signaling transfer pathway from whisker to barrel cortex (Lübke and Feldmeyer, 2007).
Whisker receptors convert sensory signaling through trigeminal nerve to the trigeminal nuclei in the brainstem. From brainstem the information is transferred to the thalamic nuclei (VPM and POm) that project to the barrels in the somatosensory cortex.

Furthermore, it was shown in experimental studies *in vitro* that the transduction of somatosensory information from thalamus to cortex is bidirectional (Reichova and Sherman, 2004; Theyel et al., 2010). That means, that the projections from thalamic nuclei is not the single direction of the signaling flow and cortex is not the terminal destination of the thalamocortical inputs. The projections of thick- tufted L5B pyramidal neurons to POm form the corticothalamic pathway and support the connections from cortex to subcortical structures (Reichova and Sherman, 2004) organizing the back-forward direction of the signaling flow.

1.3 Characteristics of L5 pyramidal neurons in the vibrissal cortex

Pyramidal neurons are the most abundant cells in all cortical areas of the mammalian brain. They represent approximately 70 to 85% of the whole population of neurons (DeFelipe and Farinas, 1992). The pyramidal neurons have distinct morphology and can be found in different layers of the cerebral cortex. Pyramidal neurons located in L5 are considered to be output neurons with projection targets to the subcortical structures (Wang and McCormick, 1993, Kasper et al. 1994).

1.3.1 Morphological properties of L5 pyramidal neurons

L5 pyramidal neurons have defined features that distinguish them from other pyramidal neurons in the cortex. L5 pyramidal neurons have pyramidal or ovoid shaped somata. From the upper part of the soma the extending apical dendrite protrudes and directs towards pia matter. Several oblique branches direct laterally from apical dendrite (Fig.1.3). The apical dendrite of L5 pyramidal neuron forms a bifurcation and ends in L1 of the cortex forming the apical tuft of the dendritic branching. The length of the apical dendrite in the cortex of adult mice from soma to pia surface can reach over 700-800µm. Hence this represents the difficulty of obtaining data from these structures with the number of widely used methods. *In vivo* study of this population of neurons encounters problems due to the location of L5 pyramidal neurons in deep cortical layers and therefore the limitations of cellular approach with widely- used methods of 2- photon microscopy (Denk et al., 1990). *In vitro* examinations of L5 pyramidal neurons allow the morphological and functional characterization of this type of neurons. Still calcium (Ca^{2+}) imaging and electrophysiological recordings are restricted to the proximal branches of L5 pyramidal neurons due to the inaccessibility of the fine distal dendrites and terminal spines with the electrodes.

Subsequently the lack of knowledge about the possible functions of the apical tuft of L5 pyramidal neurons remains. Performing a study on this topic requires development of new methods of cell loading and use of high- resolution imaging techniques.

The other structures of typical L5 pyramidal neuron also include the basal dendrites. Basal dendrites arise from soma and have lateral or downward directions. The axon originates from the distal part of the soma and passes towards subcortical

structures through the cortex leaving the several branches and projecting to the sub cortical structures (Wang and McCormick, 1993, Kasper et al. 1994).

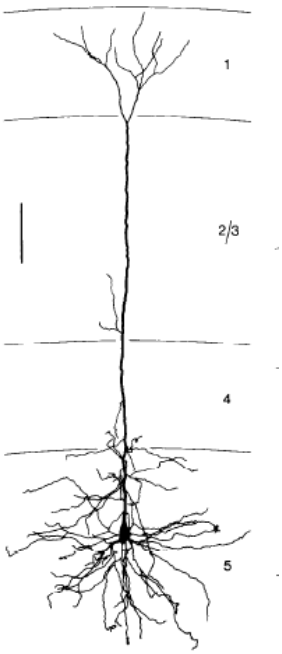

Figure 1.3. Example of a cortical L5 pyramidal neuron (Larkman and Mason, 1990). The image of the reconstructed L5 pyramidal neuron shows the dendritic branching pattern. The axon is not represented. Scale bar 100µm.

1.3.2 Classification of L5 pyramidal neurons

The population of L5 pyramidal neurons is heterogeneous. Several studies dating back to the works of Golgi 1886, Ramon y Cajal, 1911 reveal the scientific attempts to classify the cortical pyramidal neurons on the basis of their morphological differences. The more recent studies concerning this topic have defined several cell- specific groups within the population of L5 pyramidal neurons according to their location in the cortex, the site of the projection (Chagnac- Amitai et al., 1990, Larkman and Mason, 1990, Wang and McCormick, 1993, Kasper et al., 1994), the pattern of the dendritic branching, functional properties (Connors and Gutnick, 1990; Kasper et al., 1994) and gene expression (Stanfield and Jacobowitz, 1990, Feng et al., 2000, Arlotta et al.,2005, Groh et al., 2010).

The classification parameters of this population of pyramidal neurons in the visual cortex of rats have revealed their distinct properties (Kasper et al., 1994). This led to established studies showing two similar populations of L5 pyramidal neurons

in somatosensory and auditory cortex (Chagnac- Amitai et al., 1990). Similar results are described in other works performed within the mice cortex (Mittchell and Macklis, 2005).

The one class described are L5B pyramidal neurons with somata located in the lower part of L5 in the cortex, whereas the upper part of L5 is populated with somata of L5A pyramidal neurons. However, this classification based on the location within L5 is not absolute due to the possible overlap of the cell bodies in different cortices (Molnar and Cheung, 2006).

L5B pyramidal neurons correspond to thick- tufted L5 pyramidal neurons. This class features large somata and thick apical dendrite that terminates within L1 forming the elaborated tuft of dendritic branching (Fig.1.4). L5A pyramidal neurons are subdivided into slender- tufted pyramidal neurons that have smaller size of the soma and thin apical dendrite that terminate without extended tuft branching in the lower part of L1 or L2/3 (Fig.1.4). This classification of the cell types in L5 determining two groups of L5 pyramidal neurons based on the morphological differences appears to be simplified. Though this simple morphological classification has revealed cell- specific functional characteristics (Angulo et al., 2003) with defined projection targets, genes expression and according to the recent studies additionally differences in the input sources (Petreanu et al., 2009; Meyer, Wimmer et al., 2010).

Studying the physiological properties of two morphologically different classes of L5 pyramidal neurons indicated also differences in membrane structure with specific organization of ion channels on the membrane of soma and dendrites of each cell class. Intracellular recordings revealed cell- type specific firing patterns (Connors and Gutnick, 1990, Chagnac- Amitai et al., 1990; Larkman and Mason, 1990; Wang and McCormick, 1993; Kasper et al., 1994).

L5 pyramidal neurons can be divided into bursting and non- bursting cells. Slender- tufted L5 pyramidal neurons have a regular spiking pattern (Chagnac-Amitai et al., 1990; Kasper et al., 1994) to the prolonged current injection (Fig.1.5 A). This cell class has a slow rate of repolarization with long- lasting spikes. The adaptation of the spike frequency is in the prolongation of the interspike interval to response of the longer current injection (Kasper et al., 1994).

Figure 1.4 Reconstructions with camera lucida of slender- tufted (left) and thick- tufted (right) L5 pyramidal neurons of rat visual cortex. Scale bar 100µm. (Kasper et al., 1994).
The image of the reconstructed neurons depicts the differences in dendritic branching of two classes of L5 pyramidal neurons of the rat visual cortex.

Thick- tufted L5 pyramidal neurons are characterized by two distinct firing modes. First, fast- spiking cells (Fig. 1.5 C) produce initial high- frequency bursts to a prolonged stimulus and have a fast repolarization. Second firing mode of thick-tufted L5 pyramidal neurons consist of intrinsic bursts (Fig.1.5 B). In this mode the neurons respond to prolonged current injection with the bursts of spikes at high frequencies (Kasper et al., 1994). Spikes within the burst gradually decrease in amplitude due to the inactivation of the sodium channels during the prolonged stimulus (Connors and Gutnick, 1990).

Corresponding to the morphological, electrophysiological properties of thick- and slender- tufted L5 pyramidal neurons it is essential to mention their output targets. The method of neuroanatomical tract tracing has allowed the description of the projections of defined cell classes of L5 pyramidal neurons. Hattox and Nelson (2007) described L5 pyramidal neurons projections to corticostriatal and corticothalamic targets.

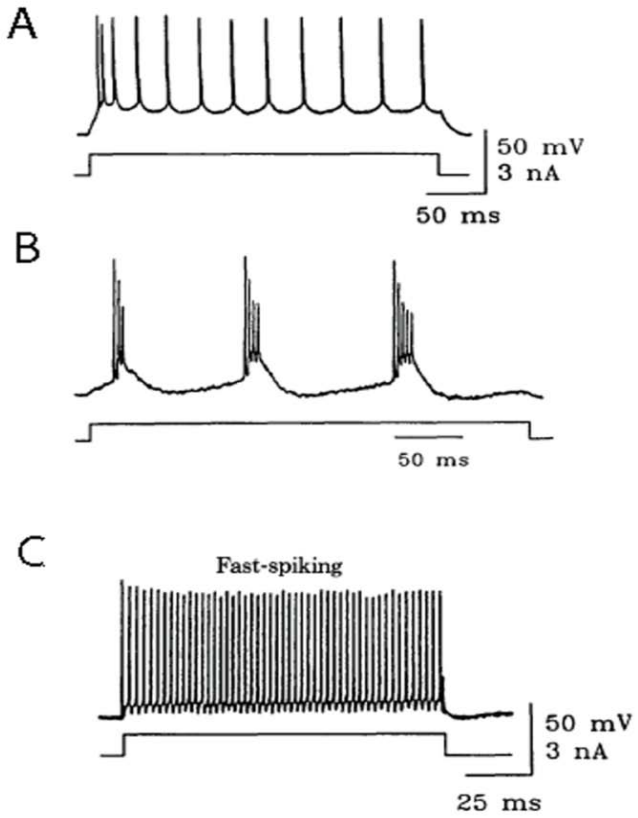

Figure 1.5 Intrinsic firing patterns of slender- tufted L5A and thick- tufted L5B pyramidal neurons (Connors and Gutnick, 1990).
A. Slender – tufted L5A pyramidal neurons respond to depolarizing current with regular spiking pattern.
B. Thick – tufted L5B pyramidal neurons show firing pattern of intrinsically – bursting neurons
C. The other firing mode of L5B pyramidal neurons is fast- spiking pattern. The spikes have high frequency during the whole stimulus.

By contrast, slender- tufted L5 pyramidal neurons send their axons to the cortex of the contralateral hemisphere, to striatum, also ipsilaterally, thick- tufted L5 pyramidal neurons project to ipsilateral subcortical targets such as thalamus, tectum, spinal cord, to the structures of the brainstem (Larkman and Mason, 1990, Wang and McCormick, 1993, Kasper et al., 1994, Le Bé et al., 2007, Groh et al., 2010).

The use of histological markers and transgenic mice expressing fluorescent proteins in specific cell classes will extend in the future the characterization of L5 pyramidal neurons. That will provide a deeper understanding of the role of the defined cell populations in the mechanisms of the sensorymotor signaling transfer.

The recent studies performed by Groh et al., 2010 provided a detailed histological and physiological description of two types of L5 pyramidal neurons dependent on gene expression. The experiments carried out on two lines of transgenic mice developed on the base of BAC (bacterial artificial chromosome) have determined two populations of genetically- labeled L5 pyramidal neurons with the expression of enhanced green fluorescent protein (EGFP). One mouse line expressing EGFP under the control of promoter for transcription factor (ets variant gene (*etv*)) revealed labeling of a subpopulation (16% of neurons in L5) of slender-tufted L5A pyramidal neurons with characteristic morphological, electrophysiological properties and projections to the ipsilateral and contralateral striatum (Fig.1.6 A, C). The second mouse line expressing EGFP under control of glycosyltransferase (glycosyltransferase -25 – domain containing (*glt*)) revealed the properties of the subpopulation (9% of L5 neurons) of thick- tufted L5B pyramidal neurons with projecting targets to the ipsilateral pons and thalamic nuclei POm (Fig.1.6 B, D).

Considering the contributions of the described above slender – and thick-tufted L5 pyramidal neurons to thalamocortical network mechanisms, it is essential to mention that these two different cell classes presumably provide different functions in the cortex. Thick- tufted L5 pyramidal neurons being fast- spiking and intrinsically- bursting neurons at high frequencies suggest their possible role as driving cells of the cortex to the subcortical structures (Reichova and Sherman, 2004). Additionally thick- tufted L5 pyramidal neurons due to their extending apical tufts in L1 can receive inputs from higher cortical regions. That without a doubt is an interesting topic for future investigations, especially regarding the inaccessibility of the distal branches to direct examinations with available techniques and therefore lack of the recordings from these cellular compartments.

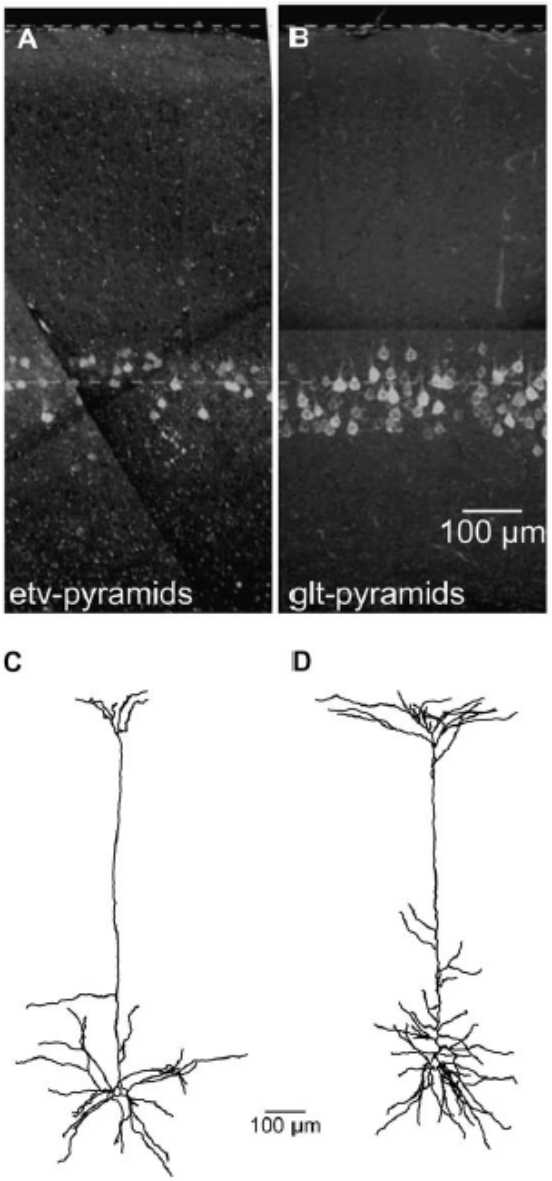

Figure 1.6 Distribution in layer 5 of etv (left) and glt (right) pyramids. Dendritic morphology of two cell- types in the visual cortex. Scale bar 100µm. (Groh et al. 2010)
A. Confocal image of the region in the slice with EGFP- positive etv pyramidal neurons.
B. Confocal image of the slice region with EGFP- positive glt pyramids.
C. Biocytin- filled reconstruction of etv neuron shows L5A slender- tufted neuron with few oblique branches.
D. Biocytin- filled reconstruction of glt pyramid with the properties of L5B thick- tufted pyramidal neuron and several oblique branches.

1.4 Thalamocortical inputs to L5 pyramidal neurons

Several scientific attempts were made to map the inputs in the cortex from subcortical structures. The recent data with the application of ChR2 and the use of the fluorescent targets determines not only morphological staining of the selective input sources, but also provides the elaborated functional mapping of the afferents

to L5 pyramidal neurons. These neurons with its complex dendritic structure appear to receive inputs from distinct thalamic targets to different dendritic compartments of the cell (Fig.1.7). Referring to the experiments (Petreanu et al., 2007; Petreanu et al., 2009; Meyer, Wimmer et al., 2010) the inputs also differ dependent on the cell types. Thus, two classes of L5 pyramidal neurons: thick-tufted (L5B) and slender – tufted (L5A) pyramidal neurons receive afferents from distinct nuclei of thalamus.

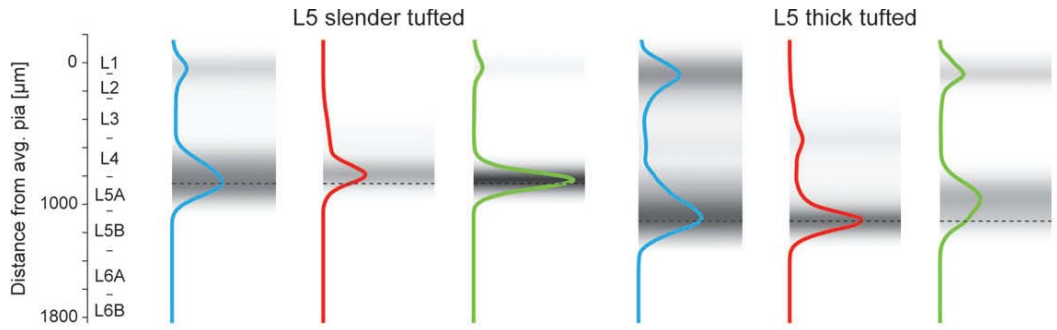

Figure 1.7 Thalamocortical innervations of L5 slender-tufted and L5 thick-tufted pyramidal neurons (Meyer, Wimmer et al., 2010).
Dendritic length density (µm/bin) is depicted on the left panel of each image and is represented with the blue color. VPM innervations (red) per average neuron (contacts/bin), POm innervation (green) respectively (contacts/bin).

Corresponding to observations in the series of studies performed by Meyer, Wimmer et al., 2010 (Fig.1.7) slender-tufted (L5A) pyramidal neurons receive thalamocortical inputs to the basal dendrites: a small fraction from VPM and a large fraction from POm. The apical tuft dendrites of L5A receive no input from VPM and slight input from POm.

The thalamocortical innervation of basal dendrites of thick-tufted L5 pyramidal neurons (L5B) is provided by majority of innervation from VPM and minority from POm. The apical tuft dendrites of L5B receive innervations only from POm.

In contrast, another group (Petreanu et al., 2007; Petreanu et al., 2009) has described the absence of input from the site of POm to the apical dendrites of thick-tufted L5 pyramidal neurons. The previous notion raises the question about innervation of the apical tuft of L5B pyramidal neurons, which are considered as the output neurons providing corticothalamic connections (Reichova and Sherman, 2004).

1.5 Applications of channelrhodopsin2 in selective activation and mapping of neuronal circuits

Channelrhodopsin 2 (ChR2) represents an effective method to optically control neural activity in the milliseconds timescale (Boyden et al., 2005). ChR2 provides means of accurate manipulations of the cellular circuitry activation in the intact brain with the investigation of the network *in vivo* (Adamantis et al., 2007). The application of ChR2 with the use of the special promoters and targeting methods has allowed the functional examinations of defined cell- types and mapping of the specific projection targets with the input sources to distinct cellular compartments.

The multifunctional applications of ChR activation have become possible due to the finding of the light- activated proton channel (ChR1) from the green algae *Chlamydomonas reinhardtii* in 2002 *(*Nagel et al., 2002). The further studies with the use of light- gated cation channel ChR2 have revealed the temporally precise control of the activity of the neuronal cells *in vitro* (Boyden et al., 2005) and possibilities for genetic targeting (Zhang et al., 2007).

The mechanism of ChR2 activation is based on its structure. It contains a seven- transmembrane ion channel from *Chlamydomonas reinhardtii.* The application of blue light (excitation maximum 470nm) evolves a non - selective cation influx (Suzuki et al., 2003; Nagel et al., 2003) (Fig.1.8).

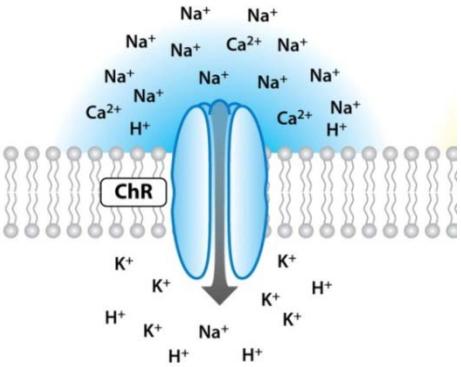

Figure 1.8 Mechanism of channelrhodopsin (ChR) activation (Fenno et al., 2011). The application of light flashes with blue light causes the conformational changes in the structure of the transmembrane ion channel that opens the channel and provides influx of ions (Nagel et al., 2003).

The effective photostimulation of ChR2 requires several conditions. The light intensity that activates ChR2 is minimum 5mW/mm^2. The source of the light for ChR2 stimulation can be provided by laser light. ChR2 protein expression level also determines the efficacy of the optical response (Zhang et al., 2006). The temporal

and spatial conditions of the applied optical stimulus additionally regulate ChR2 activation. Thus, the area of the stimulation and pulse duration additionally define the light- activated response.

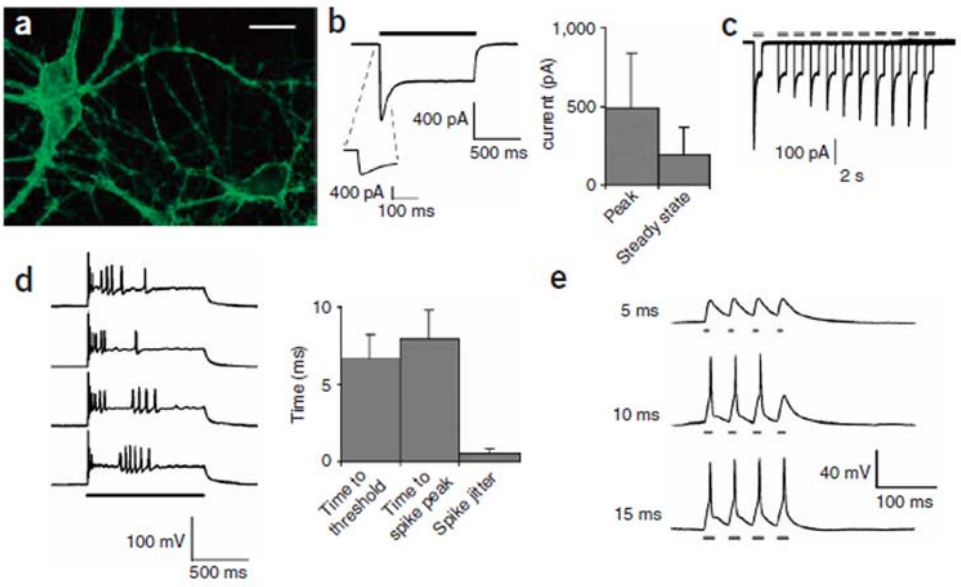

Figure 1.9 ChR2 response to the optical stimulation in cultured hippocampal neurons (Boyden et al., 2005).
A. ChR2- YFP- positive hippocampal neurons. Scale bar 30µm
B.(Left) Inward current evoked by optical stimulation with a duration of 1s. (Right)Summary of the initial phase of the current transient.
C.Current traces evoked by the light pulses in duration of 0.5s each.
D.(Left)Spikes evoked by light stimulus for 1s in the current clamp mode. (Right) Properties of the first spike.
E.Voltage traces evoked by light pulses with duration of 5ms, 10ms, 15ms.

The investigation and analysis of ChR2 kinetics characterize the response of the light-gated cation channel to the optical illumination. The kinetics of ChR2 light-activated response to the prolonged flash show rapid depolarizing current with further inactivation (Fig.1.9B). The short pulses also evoke the depolarizing current, but with recovery of the peak within the trials (Fig.1.9C). The prolonged light stimulation of ChR2- expressing neuron elicits irregular spiking pattern of the cell (Fig.1.9D), whereas the application of brief light pulses evokes reliable responses (Fig.1.9E). The use of 15 ms light pulses educes single spikes more successfully than light flashes in shorter duration.

Thus, ChR2 has become a useful tool for controlling neuronal activity on different levels of the brain structures starting from investigation of the behavior of

single cell of defined cell population and selective synaptic contacts to the studies of the neuronal networks in the whole brain.

The future implications of channelrhodopsin present the comprehensive prediction in the investigation of detailed mapping of neuronal circuits (Stroh et al., 2011) and possible application in the treatment of some neurological diseases, such as Parkinson's disease (Gradinaru et al., 2009; Kravitz et al., 2010).

1.6. Significance of Ca^{2+} signaling in the brain

Calcium ions (Ca^{2+}) play an important role in the physiological processes in the brain. The function of Ca^{2+} in the developmental cell growth and in the apoptosis was described (Catterall, 2000; Augustine et al., 2003). Numerous neurological and psychiatric disorders are related to the pathological changes in Ca^{2+} signaling (Braunewell, 2005; Brown, 2008; Hovnanian, 2008).

Ca^{2+} ions play major role in the integration of neuronal signaling. The interaction between neurons is provided by complex mechanisms of release of the neurotransmitter in the synapses that is activated by Ca^{2+} ions entry into the cellular membrane. Thus, the dynamical changes in intracellular Ca^{2+} are important for the communication between neuronal cellular compartments. Ca^{2+} ions are also crucial in the changes of the synaptic strength and evoking of synaptic plasticity that is fundamental in learning and memory processes (Zucker, 1989; Zucker, 1999; Yang et al., 1999, Bailey et al., 2004; Hawkin et al., 2006).

Several attempts were made for describing Ca^{2+} dynamics in past years. Only the breakthrough in mid 1980s in the invention of chemical fluorescent Ca^{2+} indicators has allowed characterization of intracellular Ca^{2+} changes (Grynkiewicz et al., 1985; Minta et al., 1989). The number of nowadays available fluorescent indicators together with the applied new techniques of imaging provides the possibility for extension of understanding in Ca^{2+} dynamics mechanisms. The future detailed investigation of Ca^{2+} signaling in different areas of the brain will extend the knowledge in the complex system of the information flow between billion of neurons.

1.7. Voltage- gated calcium channels

Ca^{2+} ions influx into the cell is regulated by voltage- gated Ca^{2+} channels (VGCC). The presence of these channels was first described in the crustacean muscle fiber by Fatt and Katz in 1953.

The opening of VGCG is controlled by the membrane potential changes. Ca^{2+} entry through these channels occurs as a response to the action potentials or subthreshold depolarizing signals (Catterall, 2000; Meir, 2005). Ca^{2+} influx through VGCC is important for triggering of neurotransmitter release (Tsien et al., 1988; Dunlap et al., 1995; Catterall and Few, 2008; Augustine et al., 2003; McCue et al. 2010). Thus, an electrical signal of the depolarization is transduced with the entry of Ca^{2+} ions through VGCC to Ca^{2+} signaling. That provides synaptic transmission and therefore establishes the basis of cellular interactions in neuronal circuit.

1.8. Signaling in the apical tuft of L5 pyramidal neurons

Apical tuft of L5 pyramidal neurons presents an extensive pattern of branching of the apical dendrite located in L1. In the apical tuft through dendritic arbors L5 pyramidal neuron receives different synaptic inputs from distinct targets. Additionally, the extensive branching in the apical tuft of thick- tufted L5 pyramidal neurons can increase the receptive surface for comprehension of the synaptic inputs from distinct afferents (Rall, 1962).

An experimental inaccessibility of the fine apical tuft dendrites and spines for performing direct electrical recordings suggests future investigations of functional role of terminal processes and the examination of the integration of synaptic inputs in such tiny structures.

Several studies aiming to understand the interaction of the distal branches in the cortical circuit include biophysical- mathematical models. Based on the mathematical calculations and taking into consideration the biophysical properties of the biological membrane these models tried to explain and expand the functional applications of the extensive dendritic terminals. The basis of such model is cable theory that suggests the mechanism of the linear conductance along the dendritic membrane (Fig.1.10). This model was the subject of the mathematical calculations of several works starting in 1940 by Offner et al., continued by Rushton in 1946, Hodgkin and Huxley (1952), and developed by Rall (1957).

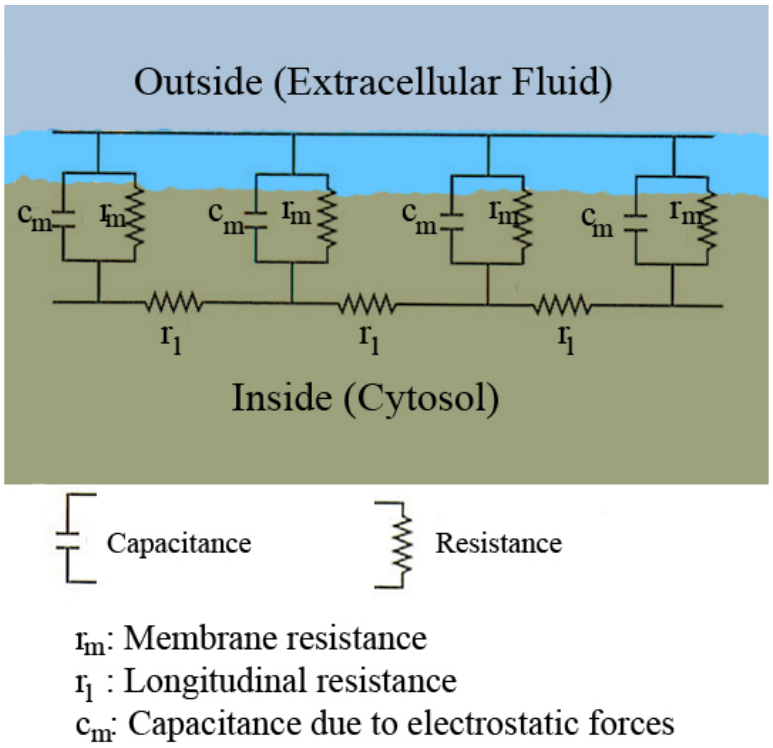

Figure 1.10 Cable theory scheme of the neuronal fiber (http://en.wikipedia.org/wiki/Cable_theory/).
The image shows the capacitance and resistance circuits along the parts of the passive neuronal fiber.

The classical cable theory predicts with the use of mathematical equations the flow of the current longitudinally in passive dendrites and axons. This theory considers dendrites as cylinder structures with membrane properties of capacitance and resistance. Referring to the calculations the current along the dendrite is dependent on the membrane properties, on the length of the branches, on the time required for change of the membrane potential. This dependence can be explained with the equation (Eq.1.1).

$$\lambda^2 \frac{\partial^2 V}{\partial x^2} = \tau \frac{\partial V}{\partial t} + V$$

Equation 1.1 Cable equation with length and time constants (http://en.wikipedia.org/wiki/Cable_theory/). V describes the voltage across the membrane, t is the time of the voltage change, x is the position along the length of the neuronal fiber, λ is the length, τ is the time constant on that voltage decays evoked by stimulation.

The passive dendrites act as low- pass filters, thus the synaptic potentials get attenuated with the spread from distal parts to the soma (Shepherd, 1998).

A computational model suggested by Rall (1964) investigated additionally synaptic inputs in the distal dendrites and described their importance. Rall (1959) suggested the equation for the branching pattern of the cellular morphology. He described in his works that if there is proportion of 3/2 regarding the diameter of parental and daughter dendritic branches, then it is possible to consider the voltage gradients along the branches as in the cable of the permanent diameter.

Thus, the computational models tried to predict experimental results with the organization of the electrical behavior of the distal branches to mathematical and biophysical laws. However, these models did not include properties that are present in the living cells, such as active dendritic conductances: voltage- gated ion channels (Stuart and Sakmann, 1994). Additionally, cable theory did not consider the diameter decrease of the branches in the distal parts of the dendritic tree.

1.9. Backpropagation in L5 pyramidal neurons

One of the properties of neocortical L5 pyramidal neurons is backpropagation of the action potential (bAP). The backpropagation is achieved due to the presence of active dendritic conductances such as voltage- activated Na^+, Ca^{2+}, K^+ channels (Connors abd Gutnick, 1993; Kim and Connors, 1993; Stuart and Sakmann, 1994; Spruston et al., 1995; Stuart et al., 1997). The previous works using computational models described dendrites as electrically inactive processes of the cell (Eccles, 1964; Rall, 1977). The finding of the voltage- gated channels in the dendritic membrane allowed examination of their role in the backpropagation of the action potential into the dendritic tree (Stuart and Sakmann, 1994; Spruston et al., 1995; Stuart et al., 1997). Though the non- homogeneous distribution of these voltage-activated channels in the somatic and dendritic membrane was described (Johnston et al., 1996). This finding suggests the possible spread of the regenerative potentials in defined parts of the dendritic tree (Larkum et al., 2001).

During active backpropagation neuronal activity travels in the retrograde direction. The following roles for this backpropagation were discussed. The important functional application of bAP was described in the induction of synaptic plasticity, especially in spike- timing- dependent plasticity (STDP) (Linden, 1999; Markram et al., 1997; Feldmann, 2000; Li et al., 2004). The precise timing of the synaptic input with the bAP and its sequence regulates the induction either of long-term potentiation (LTP) or long- term depression (LTD). Another essential function of

bAP was determined as the role in the development (Peinado et al., 1993), in synaptic interactions (Häusser et al., 2001), in the influence of the firing behavior of the cell (Larkum et al., 1999b; Larkum et al., 2001).

The site of the initiation of the action potential in pyramidal neurons is located approximately at 30-40μm from axon hillock distally (Colbert and Johnston, 1996b; Stuart et al., 1997; Palmer and Stuart, 2006). The evoked sodium action potential propagates actively to the axon and backwards into the dendritic tree (Stuart and Sakmann, 1994; Stuart et al., 1997; Buszáki and Kandel, 1998). bAP leads to an activation of dendritic Ca^{2+} channels and provides increase in intracellular Ca^{2+}.

The investigation of Ca^{2+} dynamics along the apical dendrite of L5 pyramidal neurons was performed in previous works in order to reveal the role of bAP in the synaptic interactions. The studies showed that bAP- evoked Ca^{2+} transients were attenuated in decremental way along the apical dendrite with increased distance from soma and were restricted to the distal dendrites of L5 pyramidal neurons in adult animals (4-week-old) (Schiller et al., 1997).

1.10. Basic mechanisms of synaptic transmission

Synaptic transmission is a main process of providing information transduction in neuronal circuit. The mechanism includes complex interactions of the signaling transfer through synaptic contacts. The basic unit that supplies communicative connections between neurons is the synapse.

The synaptic structure contains presynaptic and postsynaptic sites. The presynaptic button is represented by innervating part of the axon that provides target output to the postsynaptic button (Fig.1.12). The basic mechanism of the synaptic transmission in the excitatory cortical synapse is relayed on the ‘quantum release’ of the amino acid glutamate neurotransmitter into the synaptic cleft. The trigger for release of the neurotransmitter is Ca^{2+} ions flow, evoked with the depolarization through elicited action potential (Fig.1.12). Released neurotransmitter binds to the specific receptors on the postsynaptic site producing the excitatory postsynaptic potential.

In pyramidal neurons the main recipients of the excitatory inputs are dendritic protrusions- spines (Ishizuka et al., 1995) (Fig.1.13), considered as a part of the single glutamatergic synapse with postsynaptic density (Sabatini and Svoboda, 2002).

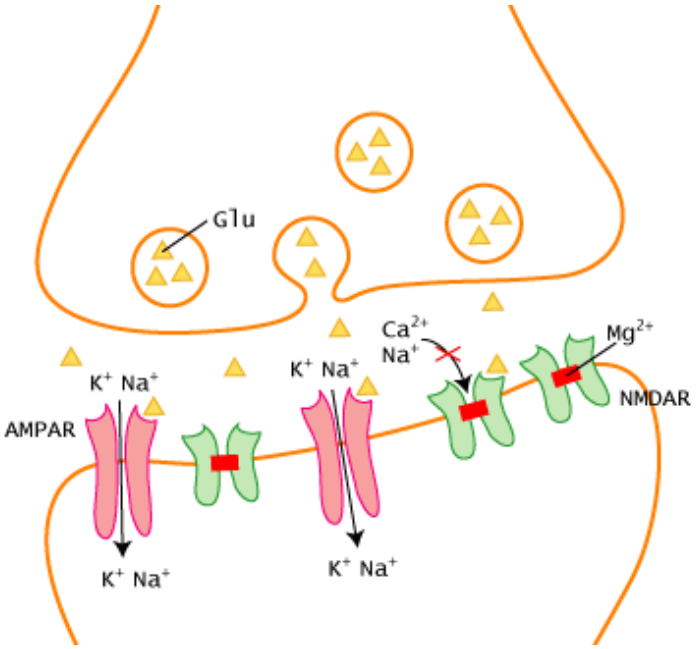

Figure 1.12. The scheme of the glutamatergic synapse (http://pubs.acs.org)

In previous studies spines were mentioned as 'multifunctional integrating unit' (Shepherd, 1996) relating to their significant involvement into various specific processes of signaling transfer. The spines play a role in synaptic plasticity (LTP, LTD), function as the receiving site of the synaptic input, increase dendritic surface area, perform as a coincidence detectors, represent the site of local Ca^{2+} increase and provide many other important implications in neuronal information flow (Shepherd, 1996). Impairment in the structure and function of spines play a role in numerous mental diseases such as schizophrenia (Glantz and Lewis, 2000), trisomy 21 (Down syndrome) (Marin- Padilla, 1976; Takashima et al., 1989) and several other brain disorders (Nimchinsky et al., 2002).

The size of the spine head varies dramatically from 0.001-1 μm^3 (Fig.1.13). The spine neck has negligible membrane area of less than 0.1 μm^2 (Nimchinsky et al., 2000). Considering electrical properties of the membrane protrusions, the synapses located on the spines have high resistance and small capacitance (Johnston and Wu, 1995), thus supplying local signaling. Therefore several suggestions were made considering the implications of the spine neck resistance in the regulation of the efficacy of the synaptic response (Rall, 1962; Koch and Poggio, 1983). The presence of the voltage- activated sodium and calcium channels located in the membrane of spines was also described (Denk et al., 1995).

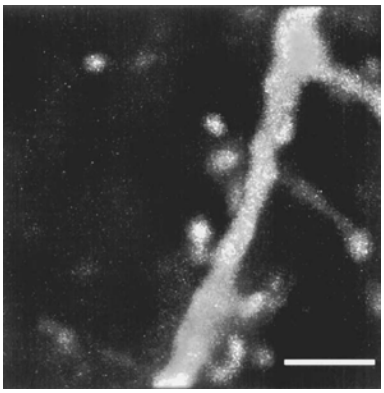

Figure1.13. Two- photon imaging of L5 pyramidal neuron loaded with Calcium Green-1 (Holthoff et al., 2002). Scale bar 5µm.

The functional application of individual synapse is defined by properties of receptors structure on the postsynaptic button. It was described that spines of pyramidal neurons contain NMDA and AMPA receptors (Kovalchuk, et al., 2000; Holthoff et al., 2004). AMPA- type glutamate receptors play a role in excitability: these receptors provide ion flow at resting membrane potentials (Sommer et al., 1992). NMDA- type glutamate receptors at hyperpolarized membrane potentials are blocked with Mg^{2+} that is removed upon depolarization providing Ca^{2+} entry (Mayer et al., 1984; Nowak et al., 1984; Genoux and Montgomery, 2007).

Thus, spines as synaptic structures play the basic role in neuronal interactions in the brain circuit. Therefore, the investigation of spine signaling is significant for understanding of the detailed mechanisms of the information transduction. Taking into consideration the tiny- size the examination of spines is complicated and requires application of the special techniques combined with high resolution imaging methods.

Chapter 2
Aim of the Study

The present study was aimed at describing the distinct properties of specific cell- types of L5 pyramidal neurons of the mouse somatosensory cortex. Such detailed investigations of genetically -defined cell classes of L5 pyramidal neurons are important for the extension of the role of these cells in order to understand the main output line of the cortex. For this purpose whole - cell recordings with biocytin filling and morphological reconstructions with camera Neurolucida were used.

Currently, there is no data available regarding the morphological and functional properties of the terminal dendritic branches and distal spines of L5 pyramidal neurons due to the experimental inaccessibility of such tiny structures. The investigation of the role of the distally located branches is essential in the extended understanding of the cortical circuitry. The signaling in the apical tuft presents the transduction of the information flow in L1 and thus can be considered to perform high- level integration of cortical signals.

The aim of the present study was to characterize morphological and functional properties of the distal dendrites and distal spines of L5 pyramidal neurons of mouse somatosensory cortex. In order to analyze the signaling in the apical tuft the method of whole- cell patch- clamp recordings was combined with voltage and Ca^{2+} imaging with the use of confocal and two- photon microscopy. In this study in order to investigate the synaptic transmission in distal dendrites and distal spines a new double- patch technique for fluorescent staining of the terminal branches was developed. For Ca^{2+} imaging from such small structures as spines and dendrites in the apical tuft of L5 pyramidal neurons a novel AOD- based two- photon scanning system was applied for the first time. Various hypotheses concerning functional implications of the tuft spines and distal dendrites are to be examined.

Chapter 3
Materials and methods

3.1 Animals

All experiments were performed according to institutional animal welfare guidelines and were approved by the government of Bavaria, Germany. BL/6 mice were used, aged between postnatal day 17 (P17) and 30 days old (P30) provided by the breeding facility of the Institute of Neuroscience, Technical University Munich (TUM). Mice were housed with 12 hours light/dark cycle. *Glt25d2* (*glt*) bacterial artificial chromosome (BAC) – EGFP transgenic mouse line (P17-P22) was received from the GENSAT project. The transgenic mice expressing thy-1–ChR2 (line 18) were between 12-28 days old and were kindly provided by Karl Deisseroth M.D., Ph.D., Stanford University, USA. AAV- ChR2- injected BL/6 mice were used at the age of P 26-32 and housed in the breeding facility of the Institute of Neuroscience, TUM.

3.2 Slice preparation

Brain slices offer certain advantages for the present work comparison to the experiments carried on the living animals. Slice preparation provides mechanically stable and long duration intracellular recordings due to the absence of the respiratory and heart beat pulsations. Such parameters as temperature, level of oxygenation can be maintained at the defined level. Additionally, the pharmacological agents can be applied in the desired concentrations intracellular or to the special region of interest in the slice (Wang and Kass, 1997). The direct visualization of the slice structure resolves the possibility to perform recordings from the different locations and on defined cell population.

For acute slice preparation the standard procedure was applied (Edwards *et al*. 1989, Konnerth, 1990; Edwards and Konnerth, 1992). Mice were deeply anesthetized by exposure to CO_2 and sacrificed by decapitation. The skull was opened along the sagittal suture, the brain removed and placed in ice-cold solution containing (in mM): 125 NaCl, 2.5 KCl, 0.5 $CaCl_2$, 6 $MgCl_2$, 1.25 NaH_2PO_4, 26 $NaHCO_3$, 20 glucose, saturated with 95% O_2 and 5% CO_2. The use of the low temperature of the slice cutting solution keeps the brain intact for the slicing and

slows down the metabolism activity of cells, allowing them to sustain the ischemic period during dissection (Wang and Kass. 1997).

The present study required the preparation of the acute thalamocortical slices of the vibrissal cortex. Thalamocortical slices preserve the pathways between thalamus and cortex and maintain the parallel orientation of the dendritic branches of the cortical neurons to the surface (Agmon and Connors, 1991). For the preparation of the thalamocortical slices the brain was placed on a 10 degree ramp made from glass (Fig.2.1A).

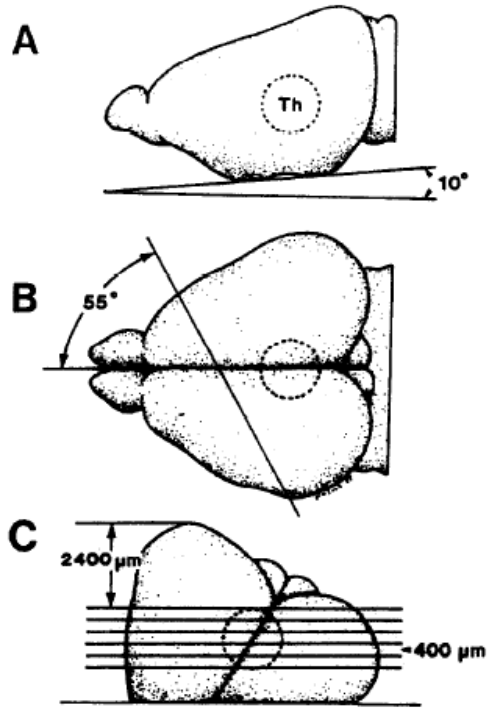

Figure 3.1 Procedure of the thalamocortical slice preparation (Agmon and Connors, 1991).
A.Brain on the 10 degree ramp
B.The angle and direction of the cut of the brain
C.The position of the brain glued to the vibratome stage

The vertical cut was made with the razor blade at an angle of 55 degrees to the right of the posterior- to- anterior axis of the brain. The remaining tissue of the brain was glued with Cyanoacrylat glue (Uhu GmbH, Bühl, Germany) with the cut surface down onto the stage of the vibratome (VT1200S, Leica, Wetzlar, Germany). The stage was placed on the tray of the vibratome with magnetic specimen holder. The tray contained ice-cold cutting solution, saturated with 95% O_2 and 5% CO_2.

The vertical deflection of the blade of the vibratome was adjusted to the minimal values to decrease the mechanical damage during the cutting procedure (Bischofberger et al., 2004). The acute slices of the vibrissal cortex 300µm thick were incubated at 36°C for 30 minutes in oxygenated standard solution containing (in mM): 125 NaCl, 2.5 KCl, 2 $CaCl_2$, 1 $MgCl_2$, 1.25 NaH_2PO_4, 26 $NaHCO_3$, 20 glucose, saturated with 95% O_2 and 5% CO_2 and then maintained at room temperature (25°C).

For recording the slice was transferred to the recording chamber and fixed mechanically with the grid. The recording chamber was continuously perfused with oxygenated standard solution. The perfusion solution was warmed to 32–34 °C.

3.3 Morphological reconstructions of cells

For the morphological characterization of the neurons biocytin (2 mg/ml; Sigma) was added to the intracellular solution. Biocytin has certain advantages to other intracellular markers including its high solubility in water, small molecular weight that allows intracellular applications (Horikawa and Armstrong, 1988).

After recording the slices were fixed in 100 mM phosphate buffered saline (PBS) containing 4% paraformaldehyde (PFA) for 24 hours at -4°C, stained using the diaminobenzidine (DAB) (Vectastain ABC kit, Vector Laboratories, CA) – horseradish peroxidase (HRP) protocol (Horikawa and Armstrong, 1988) and embedded in Mowiol (Kuraray Specialities Europe GmbH). Reconstructions of the dendritic morphology were made with camera Neurolucida (Microbrightfield, Colchester, VT) using a x100 (NA: 1.25, oil immersion) objective (Fig.3.2 A, B). All reconstructions were scaled and aligned to the pial surface (Fig.3.2 B).

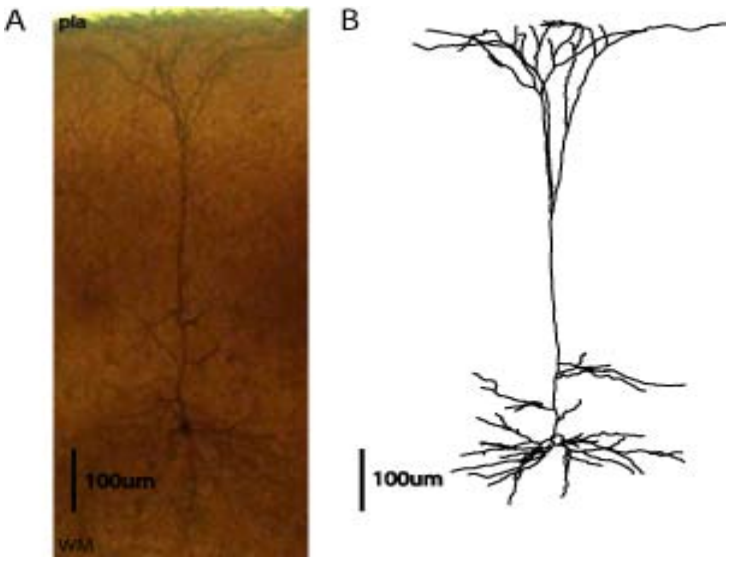

Figure 3.2 Morphology of L5 pyramidal neuron

A. Fragment of the DAB-stained slice with biocytin - labeled L5 pyramidal neuron

B. Example of the reconstructed L5 pyramidal neuron made with camera Neurolucida. The axon is removed.

DAB as a substrate of peroxidases (HRP) was used in the staining procedure for detection of the neuron loaded with biocytin in the slice. In the presence of hydrogen peroxide (H_2O_2) DAB is oxidized by the enzyme HRP, forming a brown precipitate, insoluble in water and organic solvents (Fig.3.3). This brown - colored product is concentrated at particular area labeled with HRP and can be detected by bright-field light microscopy (Fig.3.2 A) (Horikawa and Armstrong, 1988).

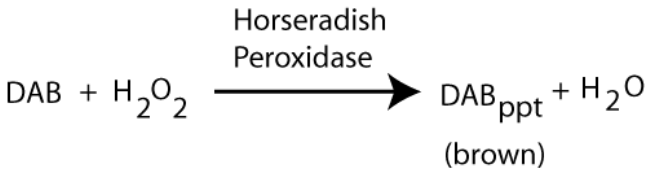

Figure 3.3 DAB reaction (http://course1.winona.edu/sberg/ILLUST/DABreaction.gif)

DAB reaction with H_2O_2 is catalyzed by HRP enzyme and resulted in insoluble brown-colored product and water (H_2O).

At the end of the staining procedure the labeled cells in the slices were detected with bright-field light microscopy and embedded in Mowiol (Kuraray Specialities Europe GmbH) for further reconstructions.

3.4. Patch-clamp recordings.

3.4.1 Patch-clamp recording technique

All experiments were performed on the L5 pyramidal neurons in acute cortical slices of the vibrissal cortex. The whole-cell recordings were performed according to the standard procedure (Edwards et al., 1989).

L5 pyramidal neurons were identified with infrared differential interference contrast (DIC) video- microscopy or using 63x objective (Plan Apochromat; NA 1, Zeiss, Germany). Patch- clamp recordings were done using EPC9/2, EPC10 Amplifier (HEKA, Lambrecht /Germany). Somatic whole- cell recording were obtained using glass electrodes of 4-6 MΩ resistance pulled with DMZ- Universal Puller (Zeitz- Instruments GmbH, Germany). The patch- clamp recordings were

performed with Pulse software (EPC9/2, HEKA) and Patch-Master software (EPC10, Version 2.53, HEKA).

The hyperpolarization to the holding resting potential of -70mV was applied and the capacitance of the pipette was compensated with C_{fast} built- in compensation circuit of the amplifier. The series resistance was measured and compensated with C_{slow} Pulse command based on the Ohm's Law: R=U/I.

The current clamp mode was used to observe voltage changes to the current injections; short depolarizing pulses with duration of 3-5 ms 500pA each were applied to evoke action potentials.

3.4.2 Morphological classification of *glt* pyramidal neurons

Acute coronal slices 300µm thick were obtained from *GLT25d2* BAC-EGFP transgenic mice aged from 17-to 22- day old. EGFP –labeled neurons were identified with Nipkow spinning disk system mounted onto the stationary stage upright microscope (Olympus BX51WI, Japan) with high-spatial resolution charge-coupled device (CCD) camera (PixelFly, QE, pco, Germany). The excitation light at 488nm was provided by 500mW Argon ion laser. 60x (60x/1.00 NA, Nikon, Japan) objective was used. After identification of somatas of EGFP- positive neurons (Fig.3.4) DIC video microscopy was used to establish whole-cell recordings for further dendritic morphological reconstructions. The neurons were loaded with biocytin for 15-20 minutes and after the filling of EGFP-positive neurons the slices were fixed in PBS with 4% PFA (Horikawa and Armstrong, 1998), embedded in Mowiol (Kuraray Specialities, Europe GmbH) and reconstructed with camera Neurolucida (Microbrightfield, Colchester, VT).

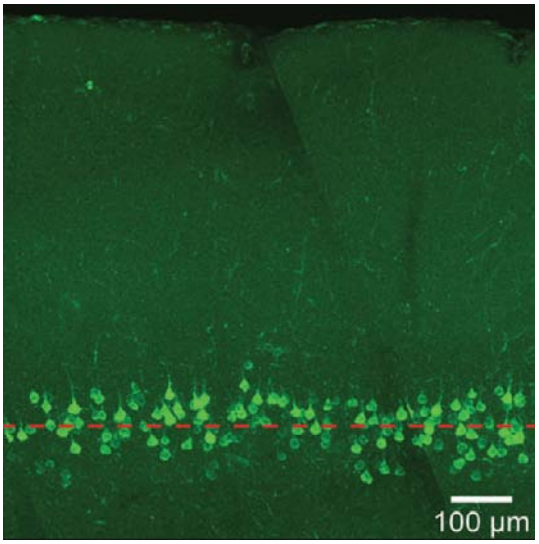

Figure 3.4 EGFP-positive glt- pyramidal neurons in the vibrissal cortex (Groh et al., 2010)

Image of the vibrissal cortex in the slice of GLT25d2 BAC-EGFP transgenic mice acquired with the confocal microscope. Red dotted line depicts the depth of the cell bodies from the pia.

3.4.3 Intracellular application of voltage-sensitive dye

The intracellular solution contained in (mM): 175 K-gluconate, 15 KCl, 5 NaCl, 5 Mg-ATP, 0.5 Na-GTP, 12.5 Hepes (pH 7.3) and 2 mg/ml biocytin (2 mg/ml; Sigma), 0.5-1 mM voltage- sensitive dye (VSD) JPW1114 (Invitrogen, Germany). The pulled glass electrodes were filled from the tip with clear intracellular solution (solution without indicator) by application of negative pressure for 10-30 seconds and then the pipette was filled with the intracellular solution containing voltage-sensitive dye (Fig.3.5).

This method of the loading allows the access of the voltage-sensitive dye molecules to the intracellular compartments of the cell. The staining was performed for 15-30 minutes. The patch electrode was pulled out to form an outside-out patch. The slice with the loaded cell was incubated for an additional 1 hour at room temperature to allow the diffusion of the voltage sensitive dye to the distal dendrites of the cell (Holthoff et al., 2010)..

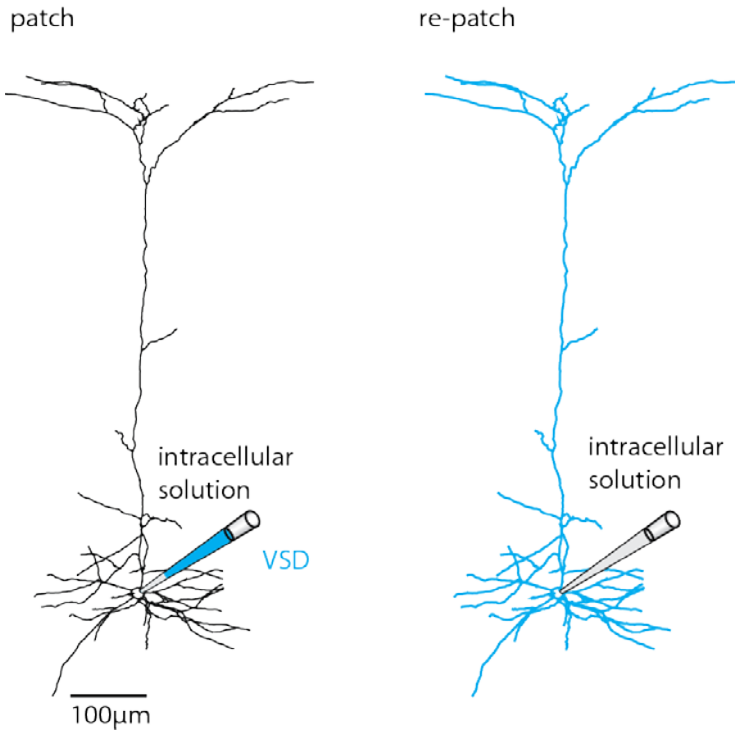

Figure 3.5 Schematic image of the technique for loading neurons with voltage-sensitive dye (VSD).
(Left) Neurolucida reconstruction of L5 pyramidal neuron. The patch pipette contains VSD and intracellular solution on the tip.
(Right) Reconstruction of the neuron filled with VSD after incubating for 1hour. The cell is re-patched with intracellular solution for further recordings.

To perform electrical recordings the stained cell was re-patched with clear intracellular solution and back-propagating action potentials were evoked in the current clamp mode by injected depolarizing current pulses through patch electrode of 3-5ms duration each. Back- propagating action potentials were also evoked by antidromic stimulation. The stimulation electrode with the resistance of 5-7MΩ connected to isolated pulse stimulator (Model 2100, GENEQ, Montreal, Canada) was placed 5-10 µm close to the axon hillock of the stained neuron. 1 to 2 pulses, each with the duration of 100µs with the frequency 50Hz at the amplitude of 4-8V were delivered via a stimulation electrode.

3.4. Development of a new method of intracellular application of fluorescent Ca^{2+} indicator dye for visualization of distant branches in L5 pyramidal neurons

The intracellular solution contained in (mM): 175 K-gluconate, 15 KCl, 5 NaCl, 5 Mg-ATP, 0.5 Na-GTP, 12.5 Hepes (pH 7.3) and 2 mg/ml biocytin (2 mg/ml; Sigma), 350µM Oregon Green Bapta-1 (OGB1) (488, hexapotassium salt, cell-impermeant, Invitrogen, Germany). The Bolus-loading technique was applied to obtain the sufficient concentration of the indicator in the distal processes of the stained neuron. The similar technique is used as multi-cell bolus loading method (MCBL) predominantly in vivo experiments (Stosiek et al., 2003; Kerr et al., 2005; Garaschuk et al., 2006).

In the present study the new method was developed and applied to enable the loading and further visualization of the micro-sized structures located in the distal parts of the dendritic tree. The glass patch electrode was filled with intracellular solution containing high concentration of the indicator (350µM OGB1), the cell was stained for 8- 10 minutes and afterwards the electrode was detached and outside-out patch formed. The stained cell was incubated for additional 20- 30 minutes for the diffusion of the indicator to the distal processes, then re- patched for electrical recordings with intracellular solution containing 100µM of the Ca^{2+} indicator OGB1.

3.5 Synaptic stimulation

Synaptic stimulation was performed using isolated pulse stimulator (Model 2100, A-M Systems, USA). Stimulation consisted of 1 or 2-3 pulses at 100 Hz with the duration of 100μs each. Short current injections were delivered via a stimulation pipette with the resistance of 5 to 8 MΩ (Zeitz Instruments, Germany). Stimulation pipette was fixed in the manipulator holder, connected to the stimulator and placed in layer 1 of the vibrissal cortex in the field of imaging plane 10 to 20 μm away from individual spine under the control and measurement of the piezo system (NV40/1 CL E, Piezosystem Jena, Germany).

3.6 Pharmacological agents used in the current experiments

In the series of the experiments the following receptor antagonists of glutamatergic transmission were applied extracellularly. 1, 2, 3, 4-Tetrahydro-6-nitro-2, 3-dioxo-benzo quinoxaline-7-sulfonamide disodium (NBQX) (Tocris, USA) at the concentration of 10μM was used to block glutamatergic transmission via AMPA receptors. NMDA receptor channel antagonist DL-2-amino-5-phosphopentanoic acid (DL-APV) (Sigma, Germany) at the concentration of 50μM was added to the bath.

3.7 Optical recordings

3.7.1 Voltage-sensitive dye

For the optical recordings of the submillisecond membrane potential changes in dendrites and neighboring spines the voltage-sensitive dye di- amino naphthyl ethenyl pyridinium (di -ANEPEQ or JPW1114) (Invitrogen, Germany) was applied. JPW1114 was chosen due to its higher solubility in water comparison to other voltage sensitive dyes and that allowed the intracellular application of this dye in the experiments (http:// products.invitrogen.com) (Fig.3.6). Additionally, the results from the previous studies show the high sensitivity, good signal- to- noise ratio (SNR) and sufficient spatial and temporal resolution, less photodynamic damage of JPW1114 in the fluorescent measurements (Antic and Zecevic, 1995). Intracellular injected voltage- sensitive dye provides the possibility for the detection of fast membrane potential changes (action potentials) simultaneously at different locations of the

dendritic tree and allows recordings from the fine structures where electrical recordings are not possible (Zochowski et al., 2000).

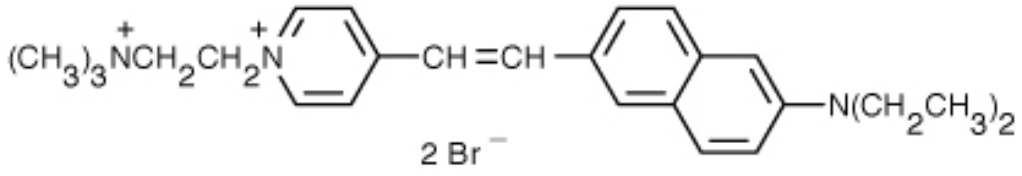

Figure 3.6 Chemical structure of JPW1114

(http:// products.invitrogen.com)

Spectral properties of the voltage- sensitive dye change in response to the changes of the membrane potential (Loew et al., 1985). Non- fluorescent voltage-sensitive dye starts to fluorescence after binding to the membrane (Fig.3.7).

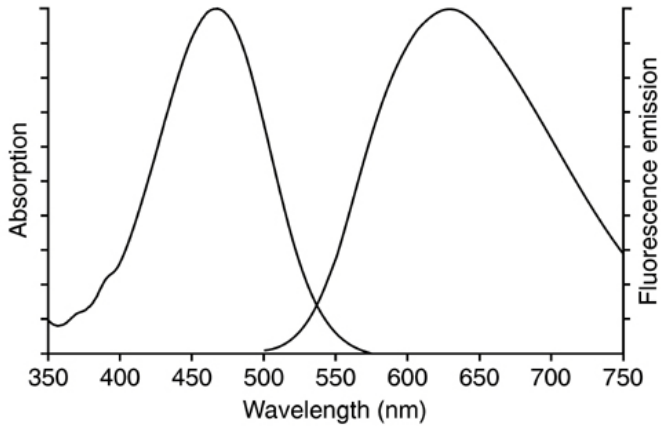

Figure 3.7 Absorption and fluorescence emission spectra of di -ANEPEQ bound to phospholipid bilayer membranes (http://products.invitrogen.com)

3.7.1.1 Optical recordings with voltage-sensitive-dye

Optical recordings for the experiments with the use of voltage-sensitive dye were performed using stationary stage upright microscope (Model BX51WI, Olympus Inc., Japan) and low noise rate CCD camera (Red- ShirtImaging LLC, Decatur, GA, USA) with low spatial resolution (80x80 pixels) (Fig.3.8). The source of

the excitation light was provided by a frequency- doubled 200 mW diode- pumped ND: YVO4 continuous wave laser emitting at 532nm (Newport- Spectra- Physics, Mountain View, CA, USA). The excitation light was reflected by a 560nm dichroic mirror and the fluorescence light passed through 610nm barrier filter. The microscope was supplied with spinning-disk confocal scanner for collecting z-stacks and 2 camera ports: a standard high spatial resolution CCD camera for infrared DIC and CCD camera with high spatial resolution (1024x1392 pixels).

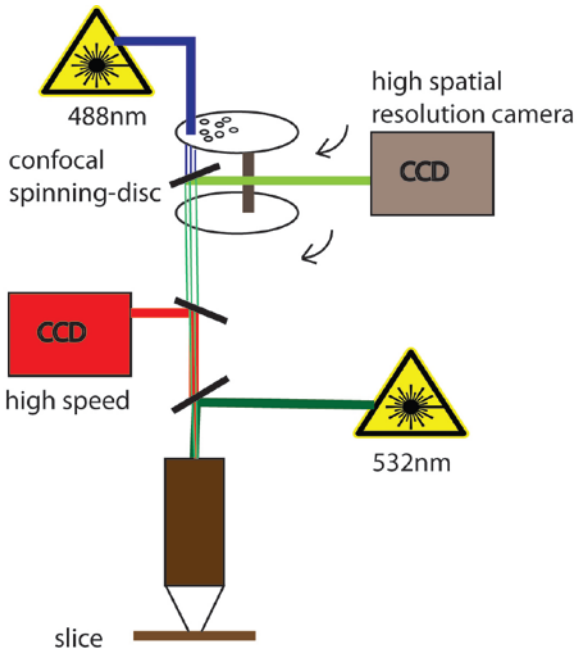

Figure 3.8 Scheme of experimental setup for voltage-sensitive dye imaging

Schematic drawing of the stationary stage upright microscope used for the imaging with voltage- sensitive dye.

The acquisition, display of the data was performed in Neuroplex software (RedShirtImaging, IDL, ITT Visual Information Solutions, Boulder, CO, USA). Fluorescent signals were recorded at 2KHz sampling frame rate in Neuroplex sofware program.

3.7.2 Ca^{2+} imaging

3.7.2.1 Fluorescent Ca^{2+} indicator

In the present study fluorescent Ca^{2+} indicator Oregon Green 488 BAPTA 1 (OGB1) was applied as an indicator of choice for detecting the dynamics of the intracellular Ca^{2+} concentration in the spines and neighboring dendrites in the apical tuft of L5 pyramidal neurons. OGB1 represents the Ca^{2+} indicator with high affinity with dissociation constant (K_d) of 170nM and allows the measurement of small changes in Ca^{2+} close to the resting values (Paredes et al., 2008) with less phototoxicity (Svoboda et al., 1997).

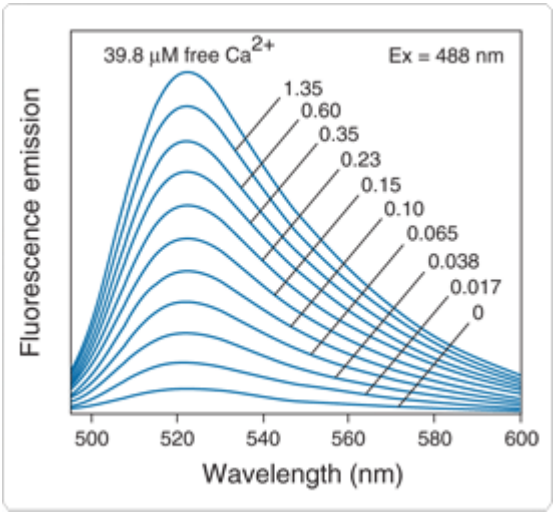

Figure 3.9 Emission spectra of OGB1 (http:// products.invitrogen.com)

The one-photon excitation maximum of OGB1 is close to 488 (Brain and Bennett, 1997; Digregorio and Vergara, 1997) and can be excited by argon laser and for two- photon (2-photon) excitation the maximum is in the range of 800-810nm (Haugland et al., 2005). The emission spectrum is reliant to the free Ca^{2+} and the wavelength.

3.7.2.2 Ca^{2+} imaging with Nipkow disk- based confocal microscope

The recordings of the dynamics in the intracellular Ca^{2+} were performed on the same experimental setup described in chapter 3.7.1.1 (see the Fig.3.8). The

advantage of Ca^{2+} imaging with this system was the use of the spinning Nipkow disk (QLC 100; VTi; UK) and CCD-camera (NeuroCCD, RedShirt Imaging, USA) as detector. The spinning Nipkow disk method provided high resolution, high sensitivity and high speed of the obtained recordings in the apical dendrites of L5 pyramidal neurons (Nakano, 2002).

The synchronization of the Nipkow disk with CCD-camera was provided by function generator (TG1010A; TTi; UK). Excitation light 488 nm was supplied by 500 mW Argon ion laser. The data was recorded at frequency of 40Hz with the use of Neuroplex program (RedShirt Imaging, USA).

The spinning Nipkow disk method is based on the use of the spinning disk with multiple pinholes (Fig.3.10). Another spinning disk with the microlens developed by The Yokogawa Electric Corporation provides the projection of the laser beams to the pinholes (Nakano, 2002). The speed of the spinning disk rotation reaches up to 1800-5000 rpm allowing scanning at high frequencies (Ichihara et al., 1996; Inoue and Inoue, 2002).

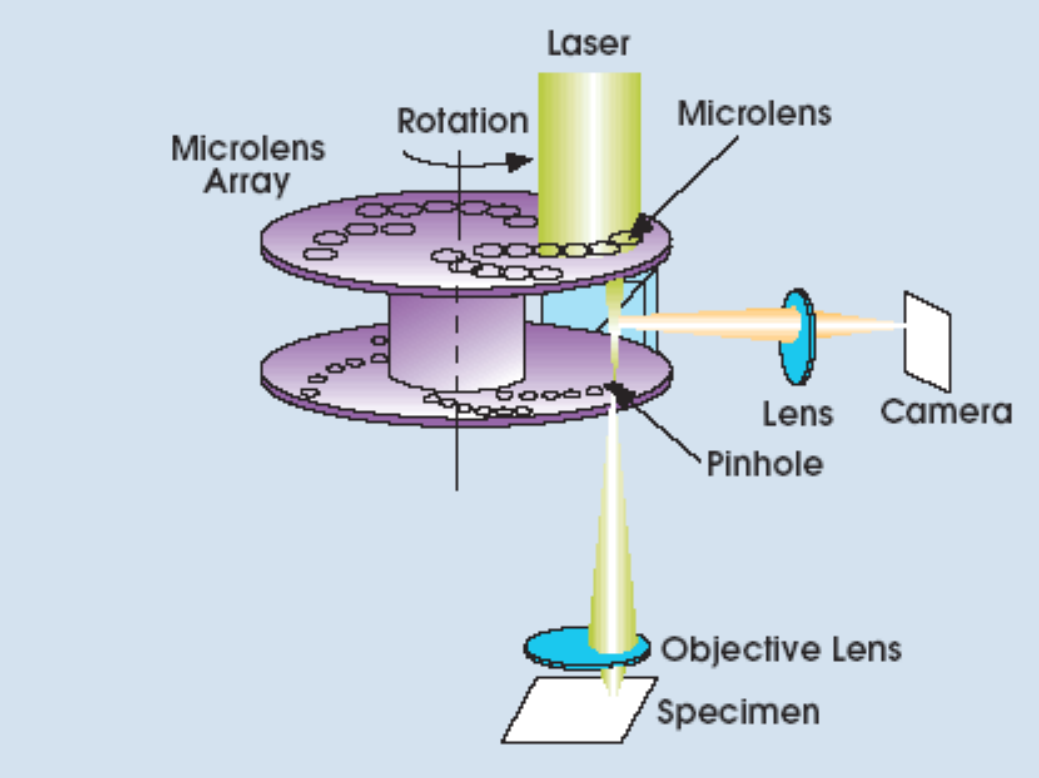

Figure 3.10 Schematic overview of Nipkow disk system (http://www.hi.helsinki.fi/amu/AMUCf_tut/). The scanning point goes across the specimen gathering fluorescence through the pinhole (Takahashi et al., 1999). Out- of- focus fluorescence is left of and that provides an advantage for obtaining high resolution images (Diliberto et al., 1994).

Acute coronal/thalamocortical slices of somatosensory cortex were used to perform Ca^{2+} recordings along the apical dendrite. L5 pyramidal neurons were visualized with infrared DIC microscopy. Whole- cell recordings were established for filling the neuron with Ca^{2+} fluorescent indicator 100µM OGB1. After 15- 30 minutes of loading the level of the fluorescence was estimated with CCD- camera. Brief current injections through the patch- pipette evoked Ca^{2+} transients recorded along the apical dendrite at different distances from soma.

In other series of experiments ChR2- thy1 promotor transgenic mice were used to record Ca^{2+} dynamics along the apical dendrite of L5 pyramidal neurons into response to *in vivo*- like stimulation. ChR2- expressing L5 pyramidal neurons in acute thalamocortical slices of somatosensory cortex were identified from EGFP fluorescent soma and fluorescent dendrites with the use of CCD-camera and Nipkow scanning disk system. The excitation light was provided at 488nm at lowest light intensity in order to avoid activation of ChR2. By establishing of whole- cell recordings L5 neurons were loaded with low affinity fluorescent Ca^{2+} indicator 300µM of OGB6F. The higher concentrations of the indicator were required in order to be able to visualize distal dendrites and to acquire good signal- to- noise ratio (SNR) of Ca^{2+} transients. Brief current injections were delivered to the soma through patch- pipette. The stimulus injected repeated the sequence of the activity of L5B-ChR2 pyramidal neuron recorded *in vivo* by Dr. A.Groh containing different frequencies of the spiking behavior. Ca^{2+} transients were recorded into the response of bAP along the apical dendrite starting with the proximal part towards distal dendritic branches.

3.7.2.3 Ca^{2+} imaging with AOD-based two-photon microscopy

The present study required the use of two –photon (2- photon) laser scanning microscopy that represents considerable advantages comparison to current available techniques of microscopy. 2-photon laser scanning fluorescence microscopy allows deeper penetration (600 µm) into the slice, especially taking into consideration the 3-dimensional (3D) orientation of dendritic processes in the slice (300µm) (Denk et al., 1990). Additionally the admission of less photodamage makes possible to perform recordings in the slice for longer period of time without any destruction to the living tissue (Potter, 1996, Denk and Svoboda, 1997).

The experimental setup for Ca^{2+} imaging in the dendritic spines consisted of custom- built 2-photon laser scanning microscope (upright microscope (BX50WI, Olympus)) (Leischner, 2011) supplied with Photomultiplier, 2 acousto- optical deflectors (AOD) (Fig.3.11), beam compressor (pre- chirper). 2-photon excitation light was provided by pulsed Titanium- Sapphire laser (Chameleon Ultra; Coherent, USA) at 800nm with 140fs pulse length and with 80MHz pulse repetition rate. The localized excitation was detected with 63x objective (Plan Apochromat; NA 1; Zeiss; Germany). AOD1 (4150; Crystal Technology; USA) controlled the angle of a laser beam in x- direction. Y-direction scanning was operated by the galvanic mirror (6215H; Cambridge technology; USA). The second AOD (AOD2) (4150; Crystal Technology; USA) was installed for balancing of the chromatic dispersion from scanning of AOD1. The emission light was divided from the excitation light with the dichroic mirror (HC 735 LP; AHF Analysentechnik AG; Germany). For the control of the optical dispersion a pulse compressor (pre-chirper) (FemptoControl; APE; Germany) was used and it has optimized the width of femtosecond pulses of the laser and sustained the peak intensity.

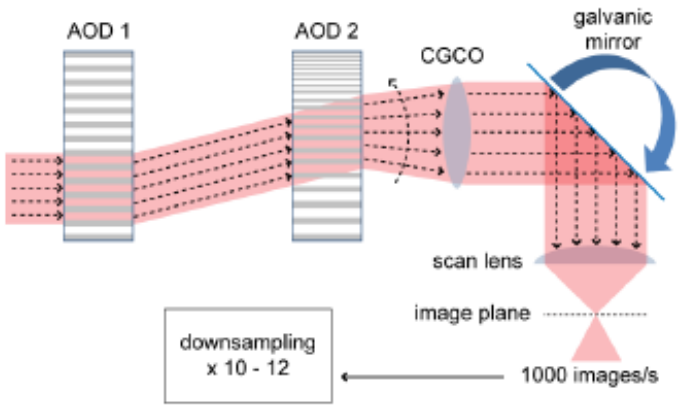

Figure 3.11 Schematic of the AOD- based 2- photon microscope (Chen et al., 2011)
AOD- based 2-photon microscope contains of 2 acousto- optical deflectors (AOD). The setup provides scanning at high speed. The high spatial resolution of the acquired images is provided by the application of the frequency- dependent chirped grating compensation optics (CGCO).

This system has provided optimal detection of Ca^{2+} dynamics in such small structures as spines and distal dendrites in the acute slices. The detailed description of the advantages of the recently developed system and its construction is depicted in study of Leischner, 2011 (Fig.3.12).

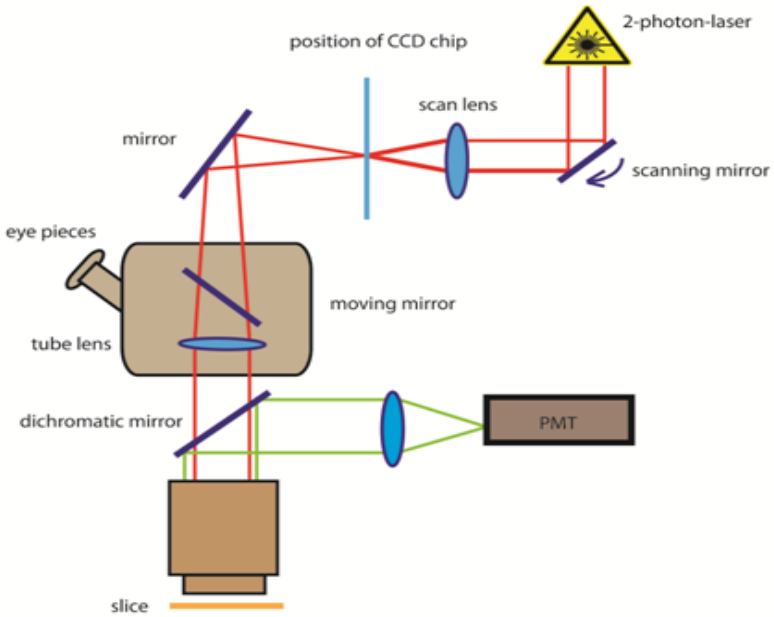

Figure 3.12 Basics of the setup for Ca^{2+}imaging with 2-photon laser scanning microscope (Leischner, 2011).

The presented scheme represents the pathway of 2-photon- laser light. The excitation light (red line) is detected with the objective and the emission light (green line) is sighted to PMT.

The acquisition of the data was performed using LABVIEW- based custom written software package (Leischner, 2011) (National Instruments, Austin, Texas, USA). High-speed Ca^{2+} imaging recordings were obtained at 240x240x320 (the parameters of the obtained image have the size of 25x25µm at this certain frequency recording) or at 640 frame rate. The display of the recording data at 40Hz was performed automatically in the online mode of the LABVIEW program. The z-stack of the recorded region of interest was obtained subsequently after performed recording using LABVIEW-based custom written software package at 240x240x320 frame rate.

3.8 Optogenetics

Optogenetics represents the complex of optical and genetic methods. The optical method with the use of the light- activated cation channel from the green *algae Chlamydomonas reinhardtii* channelrhodopsin2 (ChR2) allows control of the neural activity with the precise time scale of milliseconds (Boyden et al., 2005). The genetic method provides targeting of the specific cell- types in the defined area of the brain. The targeting in optogenetics is achieved with the use of the viruses with specific promoters that restrict the expression of ChR2 to the defined cell population (Zhang et al., 2007). The use of adeno- associated (AAV) vectors permits injections into the living brain to deliver ChR2 to special neuronal types (Zhang et al., 2010). Thus, the optogenetics method allows the studies in mapping of the neuronal circuits between specific cell- types and defined brain areas and their functional characterization.

3.8.1 Characterization of ChR2- positive neurons in transgenic thy1- ChR2 mice

Acute slices were obtained from 18- to 24- day- old (n=15) and 12 days old (n=2) thy1- ChR2 mice (thy1- promoter). The standard procedure of the slice preparation (see Chapter 3.2) and standard solutions were used. EYFP- labeled neurons were identified using a CCD camera (PixelFly QE, pco, Germany) with high- spatial resolution (1392x1024 pixels) mounted on a spinning- disk confocal scanner attached to the stationary stage upright microscope (Olympus BX51WI, Japan). The source of the excitation light was 500mW Argon laser at 488nm. A water immersion objective (40X/0.8 NA, Nikon, Japan) was used. After ChR2-positive neurons were visualized by their EYFP- fluorescence whole-cell recordings were performed using infrared DIC microscopy. The neurons were filled with biocytin for 15-30 minutes for further morphological characterization. Detailed description of the methods applied in this study can be found in the recent publication of Groh et al., 2011.

3.8.2 Use of optogenetics for identification of the thalamic inputs to L5 pyramidal neurons

To target thalamocortical pathway adeno- associated virus (AAV) with the genes for ChR2 with mcherry fluorescence was injected to thalamic nucleus (POm) of BL/6 mice *in vivo*.

Mice were injected at the postnatal day between P16-P19. *In vivo* injections to POm were performed by Dr. Albrecht Stroh, Charlotta Rühlmann. BL/6 mice at the certain age were anesthetized by injecting intraperitoneally (200µl) ketamine (0,53mg/ml) in mixture with xylazine (5,6mg/ml). For the craniotomy the mouse head was fixed in stereotaxic frame, the following coordinates were applied: posterior to bregma 1.5mm, lateral to the midline 1mm, dorsal ventral 2.8mm. Cre-encoding AAV (GENEDETECT, NZ) and floxed ChR2- encoding AAV (AAV- DIO- ChR2-mCherry plasmid, Deisseroth, K.) construct was produced in the laboratory facility of the Institute of Neuroscience, Technical University Munich (TUM) by Sarah Bechthold (Cardin et al., 2009). The delivery of AAV construct to POm was performed through durotomy with the use of a glass pipette (outer tip diameter 45µm, inner diameter 15µm). 50nl of the viral constructs were injected through the glass pipette. The incision place was covered with the adhesive at the end of the procedure (Vetbond, 3M Animal care Products, MN). 0.1mg Lidocain was used as analgetics in the post- operative period (Stroh et al., 2011).

10 to 14 days were permitted for the expression of ChR2. After the preparation of the acute thalamocortical slices (300µm) the expression level of ChR2 with mcherry fluorescence in Pom and vibrissal cortex was determined under the fluorescent lamp.

To perform optical stimulation of the thalamocortical pathway whole- cell recordings from L5 pyramidal neurons were established. The optical fiber 50, 100µm in diameter (Thorlabs, Grönberg, Germany) was fixed in the pipette holder and connected to the laser with the excitation light of 488nm (10mW solid state sapphire laser) (Coherent, Dieborg, Germany). Light pulses of defined duration (2, 5, 20ms, the train of 10 pulses at 10 Hz) were delivered by the control of the custom written Labview software package (Andreas Fohr, TUM) (National Instruments, Austin, Texas, USA). The optical fiber was placed on the surface of L5 of the vibrissal cortex.

The measurements were obtained in the current clamp mode of Patch Master software (EPC 10, Version 2.53, HEKA). The intracellular solution contained (mM): 175 K-gluconate, 15 KCl, 5 NaCl, 5 Mg-ATP, 0.5 Na-GTP, 12.5 Hepes (pH 7.3) and

2 mg/ml biocytin (2 mg/ml; Sigma), 100µM Oregon Green Bapta-1 (OGB1) (488, hexapotassium salt, cell- impermeant, Invitrogen, Germany).

The electrical responses of the stimulation of the thalamocortical afferents were recorded in the current clamp mode. Evoked EPSPs were evoked to the application of light flashes on the level of the basal dendrites of the patched L5 pyramidal neuron.

3.9 Data analysis and statistics

3.9.1 Data analysis

Online analyses were used for rough examination of the fluorescence intensity of the cellular compartments and the presence of the signaling to the evoked stimulus.

Quantitative data analyses were performed offline.

Data obtained for voltage-sensitive dye imaging and for Ca^{2+} imaging with Nipkow disk- based confocal microscope in Neuroplex (RedShirtImaging, IDL, ITT Visual Information Solutions, Boulder, CO, USA) was analyzed by exporting data with drawn region of interest in Igor Pro software (Wavemetrics, Lake Oswego, Oregon, USA).

Recorded data with AOD- based 2- photon microscopy for Ca^{2+} imaging with 320Hz or with 640Hz was downsampled by factor of 8 or 16 respectively to the frequency of 40Hz to optimize SNR using a LABVIEW-based custom written software package (Leischner, 2011) (National Instruments, Austin, Texas, USA). The advantages of this method called low- power temporal oversampling (LOTOS) are described in detail in Cheng et al., 2011.

ImageJ (http://rsb.info.nih.gov/ij/) and Igor Pro software were used for image analyses. The electrical recordings in current clamp mode obtained with Pulse/ Patch Master software were analyzed in Igor Pro macro Patch Power Tools (PPT, http://wavemetrics.com/).

By drawing regions of interest (ROIs) in ImageJ software the neuronal Ca^{2+} transients were measured from individual spines and adjacent part of the dendrite in the apical tuft. The baseline fluorescence was measured as subtraction from the non- fluorescent region of interest. $\Delta F/F=(F0-F1)/F0$

Three dimension (3D) reconstructions of the region of interest (ROI) for further detailed 3D morphology were obtained by conversion of z- stack in Labview and loaded into Amira program (version 5.3, Visage Imaging GmbH, Berlin, Germany).

The final definiteness of the morphological spine and dendrite structure was increased by sharpening the z- stack projection image using deconvolution software (Huygens, Scientific Volume Imaging, Hilversum, The Netherlands).

3.9.2 Statistical analysis

Statistical analysis was made using SPSS (Chicago, USA) and Excel (Microsoft Office Word 2007) software. Measured values were calculated as mean values with the standard error of the mean (SEM).

For the documentation and display of the data the following Adobe programs were used: Adobe Illustrator, Adobe Photoshop (Adobe Systems, USA).

Chapter 4

Results

Morphological and functional analysis of L5 pyramidal neurons

4.1 Characterization of thick- tufted L5B pyramidal neurons in the mouse vibrissal cortex

L5 pyramidal neurons are the output neurons in the cortex providing projections to the subcortical structures of the brain (Reichova and Sherman., 2004). L5 pyramidal neurons of the vibrissal cortex are the part of the thalamocortical pathway that transmits sensorymotor information about mouse whisker movements and tactile exploration (Lu and Lin, 1993; Yu et al., 2006). Therefore the detailed investigation of cortical L5 pyramids properties will extend the functional role of these neurons in the signaling transfer between cortex and thalamus and broaden the information of the synaptic mechanisms of sensorymotor transduction in the mammalian brain.

Figure 4.1 Morphological characteristics of thick- tufted L5B pyramidal neurons

Dendritic reconstructions of biocytin- filled L5B pyramidal neurons in the mouse vibrissal cortex. The apical tufts are aligned to pial surface from somata depth in the slice.

In the present study a method of choice for morphological analyses of subpopulation of L5B pyramidal neurons was biocytin loading with the use of patch-clamp technique *in vitro* and further reconstructions with camera Neurolucida. L5B thick- tufted pyramidal neurons were identified in the bright- field microscopy from the large pyramidal shaped soma and location in deep parts of L5 (Fig. 4.2).

The present morphological analysis of L5B pyramidal neurons of the mouse vibrissal cortex revealed the unique morphology of this specific cell- type. The apical dendrite originates from soma and directs towards pia matter with oblique dendrites processing laterally. The apical dendrite has the prominent bifurcation and terminates in L1 forming the extended branching of the dendrites (Fig.4.1). The dendrites with the distance from soma decrease in diameter reaching 1µm in the terminals adjacent to pia.

			distance (µm)				dendritic length (µm)		
cell	age	slice	pia-WM	cell-pia	L4-pia	midline	apical	basal	total
1	P20	thalamocortical	988	589	466	2929	4347	2173	6521
2	P20	thalamocortical	1125	723	565	3082	5365	1982	7347
3	P21	thalamocortical	1110	628	476	3169	3484	1794	4278
4	P23	thalamocortical	969	639	526	2749	3212	1279	4491
5	P23	thalamocortical	1135	887	520	2531	3203		
6	P23	thalamocortical	1132	748	561	2461	3804		
7	P19	thalamocortical	1088	660	501	2752	4324	1914	6238
8	P21	thalamocortical	1047	659	506	1100	3962	3421	7383
9	P22	thalamocortical	1021	611	433	2854	3969	3081	7050
10	P23	thalamocortical	1031	663	483	2359	3513	1599	5113
11	P21	thalamocortical	937	556	395	3000	5845	2032	7878
12	P20	thalamocortical	922	590	428	2783	3189	1222	4411
13	P20	thalamocortical	1190	813	560	3048	4172	331	4503
14	P23	thalamocortical	890	550	386	3200	3719	2662	5841
15	P23	thalamocortical	933	597	390	2688	4405		
16	P24	thalamocortical	948	579	420	2886	3309	2285	5594
		mean	1029,1	655,75	476	2724,44	3989	1982,7	5896
		STD	92,271	94,384	61,999	496,809	761,5	809,11	1275,71
		STE	23,068	23,596	15,5	124,202	190,4	224,41	353,817

Figure 4.2 Summary of the morphological properties of thick- tufted L5B pyramidal neurons

The table determines the dendritic length of the apical and basal dendrites of thick- tufted L5B pyramidal neurons (n=16) in mouse vibrissal cortex. The soma depth in L5 was defined from the distances from pia. The measurements were performed with camera Neurolucida.

In this study the intrinsic membrane properties were additionally examined. The electrophysiological analysis revealed different patterns of the firing to response to the current injection. The brief stimulus evoked two or three spikes of high frequency (Fig.4.3B *left*). To the long duration stimulus L5B pyramidal neurons responded with two firing patterns: bursts of spikes at high frequency and high frequent spikes. The recordings were obtained in the current clamp mode (Fig.4.3B *right*).

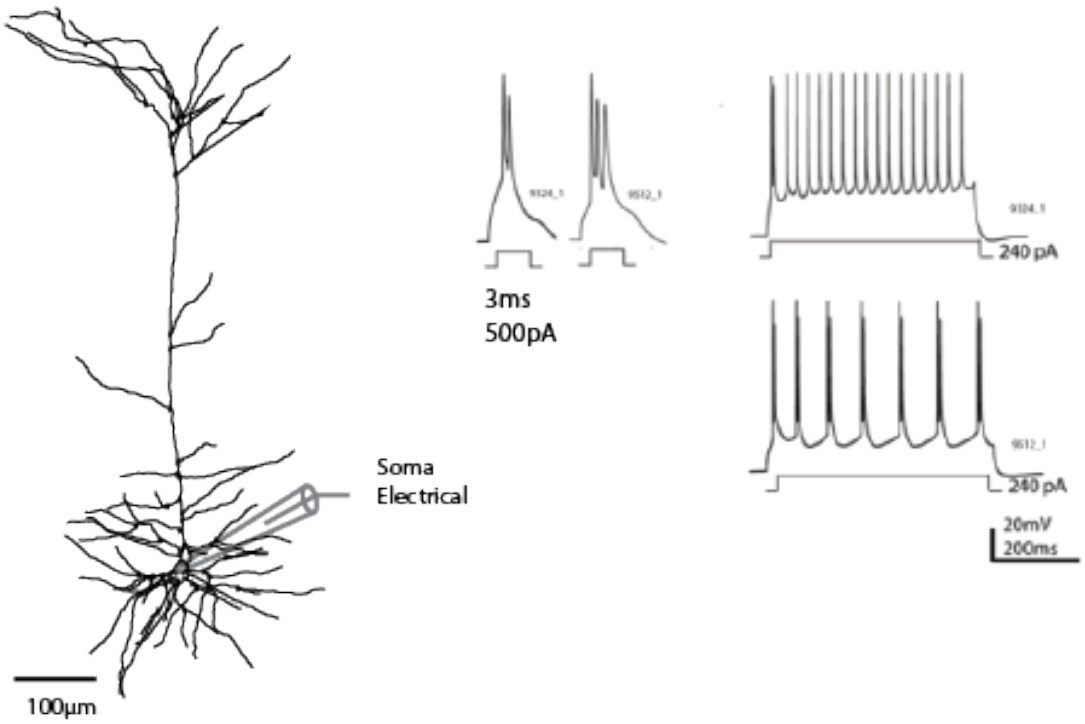

Figure 4.3 Electrophysiological properties of thick- tufted L5B pyramidal neurons.

A.Dendritic reconstruction of biocytin- filled thick- tufted L5B pyramidal neuron in the vibrissal cortex
B.Electrophysiological properties of thick- tufted L5B pyramidal neurons represent distinct firing patterns into response to brief (left) and prolonged (right) current injection.

4.2 Characterization of *Glt25d2-* L5 pyramidal neurons

Next, genetically defined cell- type in L5 of somatosensory cortex from transgenic *Glt25d2* (*glt*) bacterial artificial chromosome (BAC) - EGFP (promoter for glycosyltransferase) mouse was characterized.

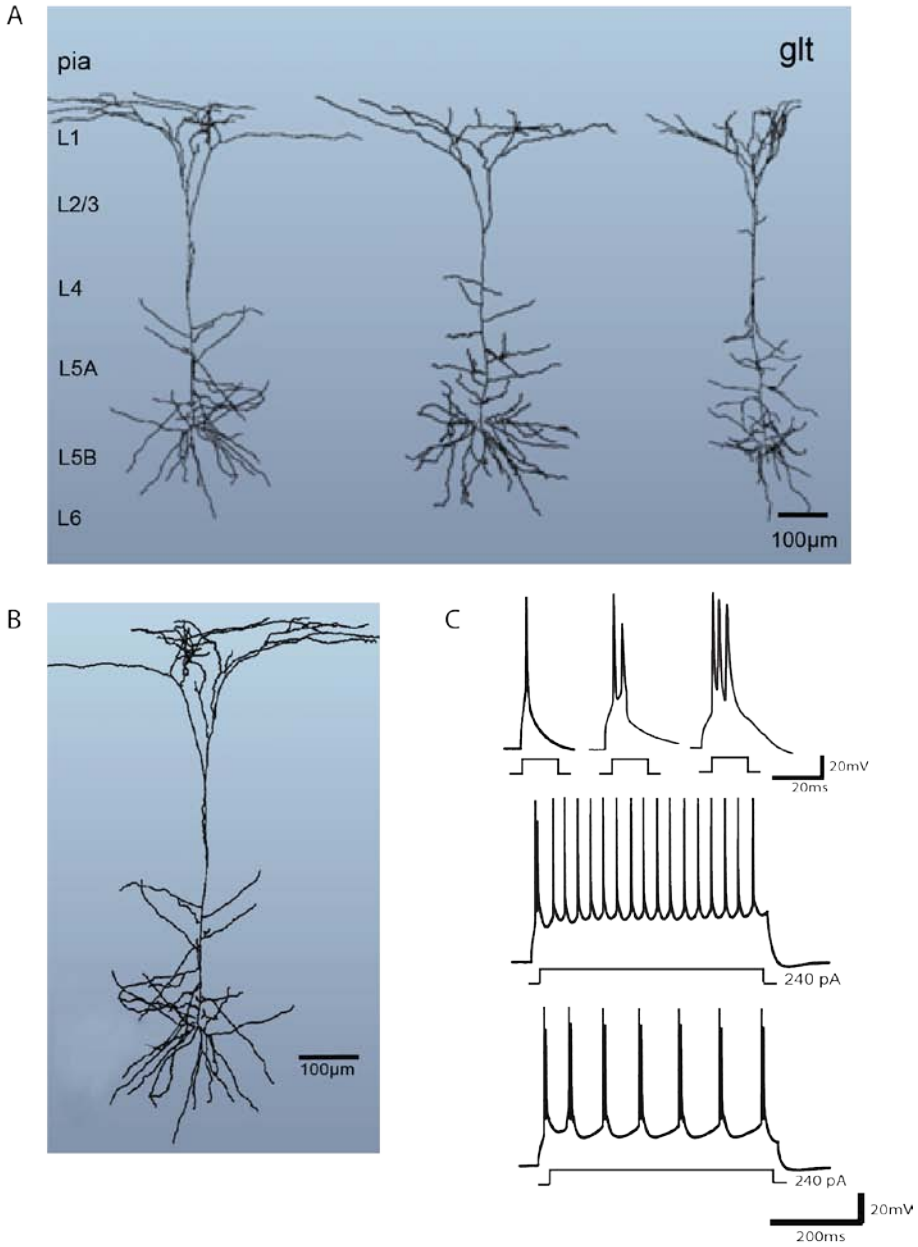

Figure 4.4 Morphological and electrophysiological properties of glt L5 pyramidal neurons.

A.3D display of biocytin- filled glt EGFP-positive neurons reconstructed with camera Neurolucida, shown with Amira program for 3D morphology. The apical tufts are aligned to pial surface. The soma of glt- pyramidal neurons are found in L5B in the mouse vibrissal cortex.
B.3D reconstruction image of biocytin- filled glt- pyramidal neuron
C.Electrophysiological properties of glt- pyramidal neurons

For morphological analysis in the present study *glt*- pyramidal neurons were identified by EGFP fluorescence and filled with biocytin for further reconstructions with camera Neurolucida. The dendritic reconstructions of *glt*- L5 pyramidal neurons (Fig.4.4A) revealed the properties of thick- tufted L5 pyramidal neurons (Fig 4.1) with the extended dendritic branching pattern in L1, therefore long apical dendrite (4102±565µm, n=6) and location in the deep levels of L5 (soma depth 619±21µm, n=6) relating to L5B pyramidal neurons (Fig.4.2).

			distance(µm)			dendritic length (µm)		
cell	age	slice	pia-WM	cell-pia	L4-pia	apical	basal	total
1	20	coronal	1050	600	548	4326	5504	9830
2	21	coronal	1134	665	532	4107		
3	22	coronal	1180	680	566	6262	4165	10427
4	17	coronal	880	542	475	4645	3908	8553
5	20	coronal	980	587	520	3026	2815	5841
6	17	coronal	1045	645	440	2248	1048	3296
		mean	1044,83	619,83	513,5	4102	3488	7589,4
		STD	107,351	52,579	47,36	1386	1666	2978,7
		STE	43,8257	21,465	19,34	565,9	680,2	1216,1

Figure 4.5 Dendritic database table of glt- pyramidal neurons

Glt pyramidal neurons (n=6) in the mouse vibrissal cortex were estimated from the length of the apical and basal dendrites. The soma depth was evaluated from the distance from pial surface. The measurements were acquired with camera Neurolucida.

For the analysis of the intrinsic membrane properties of *glt*- pyramidal neurons the current injections of short and prolonged durations were applied (Fig.4.4C). The electrophysiological properties of this specific cell class depict firing patterns of fast-spiking and intrinsically bursting neurons. This spiking behavior is similar to the population of thick- tufted L5 pyramidal neurons in the wild type mouse (Fig.4.3).

Thus, the morphological and functional correspondence of genetically- defined *glt*- neurons refers this defined cell- type to the subpopulation of thick- tufted L5B pyramidal neurons of the mouse vibrissal cortex.

4.3 Characterization of ChR2 thy1-promoter positive neurons

ChR2- positive neurons in the transgenic mouse line thy1- ChR2 (line 18) in the vibrissal cortex were characterized. The detailed analysis of these neurons was performed in order to classify ChR2- positive neurons to the specific cell population and for further investigation with the use of ChR2 activation the specific corticothalamic projection targets of these neurons *in vivo* conditions.

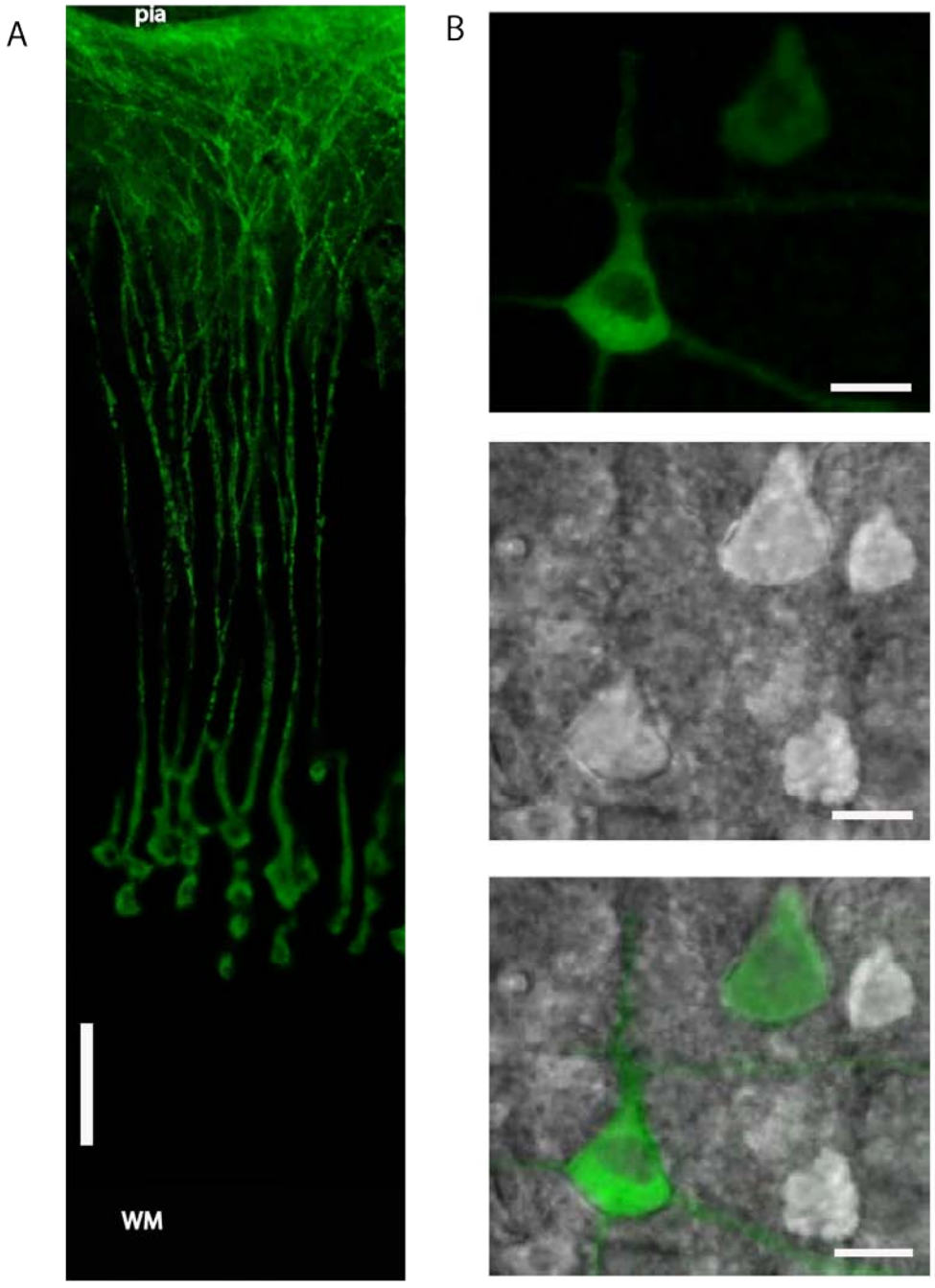

scale bar 100µm

Figure 4.6.Identification of ChR2 thy1- promoter positive neurons

A. ChR2 positive neurons were visualized in the acute thalamocortical slices with the confocal Nipkow disk system by their EYFP fluorescent soma and fluorescent dendrites. The fluorescent image depicts the area of the mouse vibrissal cortex with ChR2 positive neurons. B. The soma of ChR2 positive neuron was first identified from EYFP fluorescence and then with DIC optics for further whole- cell recordings and biocytin loading. The top image depicts soma of two ChR2 – positive EYFP- fluorescent neurons. The middle image shows the visualization of ChR2 – positive neurons with DIC. The bottom image is the overlay of the fluorescent and DIC images.

ChR2- positive neurons were fused with EYFP in this transgenic mouse line. ChR2- expressing neurons were detected with the confocal spinning disk system from EYFP- fluorescent cell body and fluorescent extending apical dendrite with terminals ending in L1 (Fig.4.6A). The fluorescence signal intensity prevailed in the apical branches located adjacent to pia. ChR2- positive neurons were found in the cortical slice in deep layers, in L5 and conterminous to L6 (soma depth 783±60µm, n=17) that corresponds to L5B pyramidal neurons (Fig.4.2).

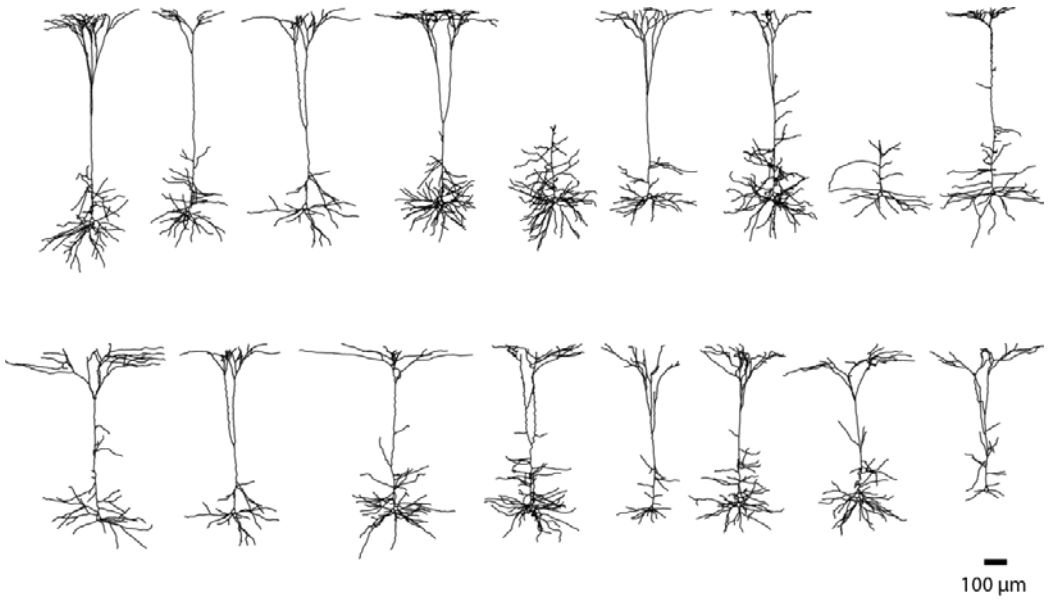

Figure 4.7 Morphological classification of ChR2 thy1- promoter positive neurons

3D display of EYFP- positive neurons filled with biocytin and reconstructed with Neurolucida. 15 neurons show the morphological properties of thick- tufted L5B pyramidal neurons, 1 short- tufted L5 neuron, 1 L6 neuron. Apical tufts are aligned to pia.

The identified ChR2- positive neurons were filled with biocytin for detailed morphological classification. The dendritic morphology of ChR2-positive neurons (Fig.4.7) depicts the similarities with the group of L5B pyramidal neurons (Fig.4.1) in the wild type mouse from the location in the cortex, extended branching pattern of the terminal tuft, long apical dendrite (5041±1796µm). Described above morphological properties refer ChR2 thy1- promoter positive neurons to the group of thick- tufted L5B pyramidal neurons with certain anatomical, functional properties and projection targets.

4.4 Selective stimulation of POm afferents reveals specific connection between thalamus and L5A basal dendrites in the vibrissal cortex

To selectively map the thalamocortical connections between POm and its inputs to the specific cortical cell layers AAV- ChR2 injection in the present study was applied. This allowed the stimulation of the specific thalamocortical axonal arbors selectively from POm without involvement of the activation of the other thalamocortical pathways.

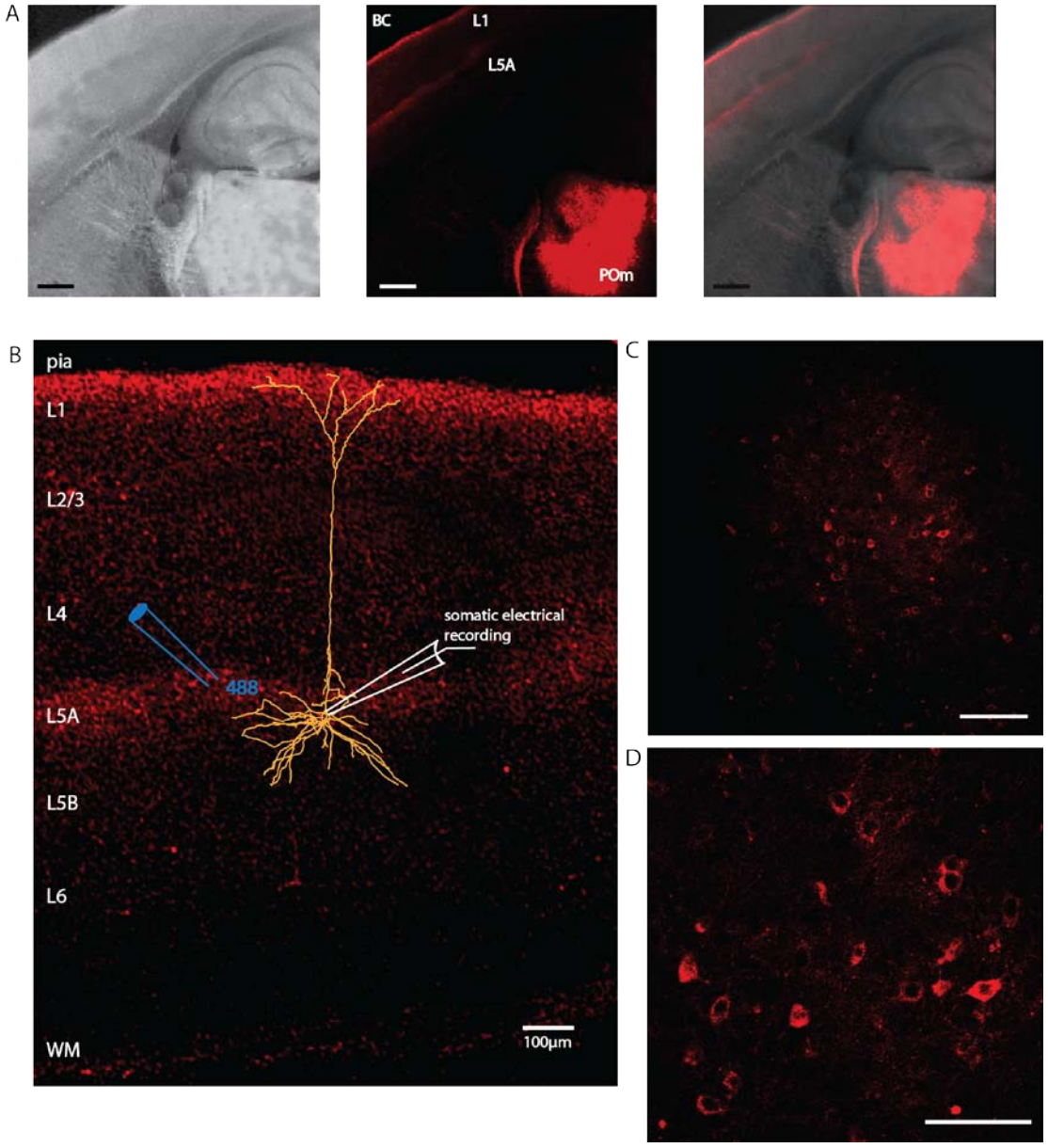

Figure 4.8 AVV-ChR2 injections into POm of the thalamus result in ChR2/mCherry expression in thalamocortical afferent fibers and in POm neurons

A. (left). Transmitted light image of the thalamocortical slice. Scale bar 500µm.
(middle). ChR2-mcherry expression in POm and anterograde labeling of thalamocortical fibers in L1 and L5A of mouse vibrissal cortex. Fluorescence is of higher intensity at the site of injection (in POm). Scale bar 500µm.
(right). Overlay of transmitted light image and fluorescent image. Scale bar 500µm
B. Overlay of the reconstructed L5A pyramidal neuron and fluorescent confocal image of ChR2- mcherry expression in thalamocortical fibers. The blue pipette indicates the side of the laser stimulation with the excitation light of 488nm.
C. Expression of ChR2-mcherry in POm. The image shows the fluorescent somas of POm neurons. Scale bar 100µm
D. Higher magnification delineates membrane bound expression of ChR2 in POm neurons. Scale bar 50µm

AAV- ChR2 injection was applied into POm following the defined coordinates *in vivo*. ChR2/mCherry expression was detected at the side of the injection in POm (Fig.4.8 C; D) and sparse labeling of ChR2/mCherry fluorescent axonal arbors was present in all layers of the vibrissal cortex with the fluorescence signal prevailing in L1 and in L5A (Fig.4.8 A). Thus, confocal images of anterograde labeling of thalamocortical axonal fibers indicate POm innervating L5A and L1 of the vibrissal cortex. To investigate the functional connectivity the light activation with the optical fiber (diameter 50, 100µm) (Thorlabs, Grönberg, Germany) of ChR2- expressing thalamocortical axonal arbors in L5 was performed in this study. Acute thalamocortical slices were prepared in order to retain the thalamocortical pathway and preserve parallel orientation of the dendritic tree to the surface of the slice.

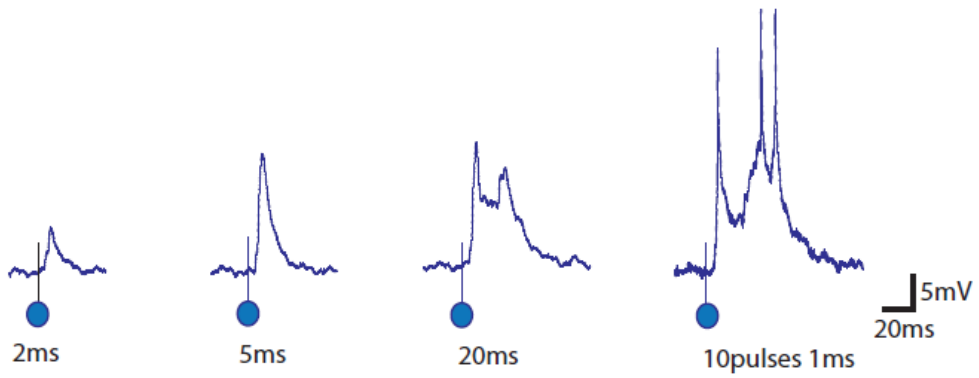

Figure 4.9 Light evoked responses of ChR2-expressing thalamocortical axons at the basal dendrites reveal synaptic excitation in L5A pyramidal neurons.

Spikes recorded in the Current Clamp mode (CC mode) from L5A pyramidal neuron to the response of the laser stimulation of the thalamocortical arbors on the level of the basal dendrites.

To investigate thalamocortical input from POm to L5A the light activation of ChR2- expressing axonal fibers was applied to the basal dendrites (Fig.4.8 B). Whole -cell recordings were established in order to record the synaptic responses to the light stimulus and for biocytin filling for further dendritic reconstructions.

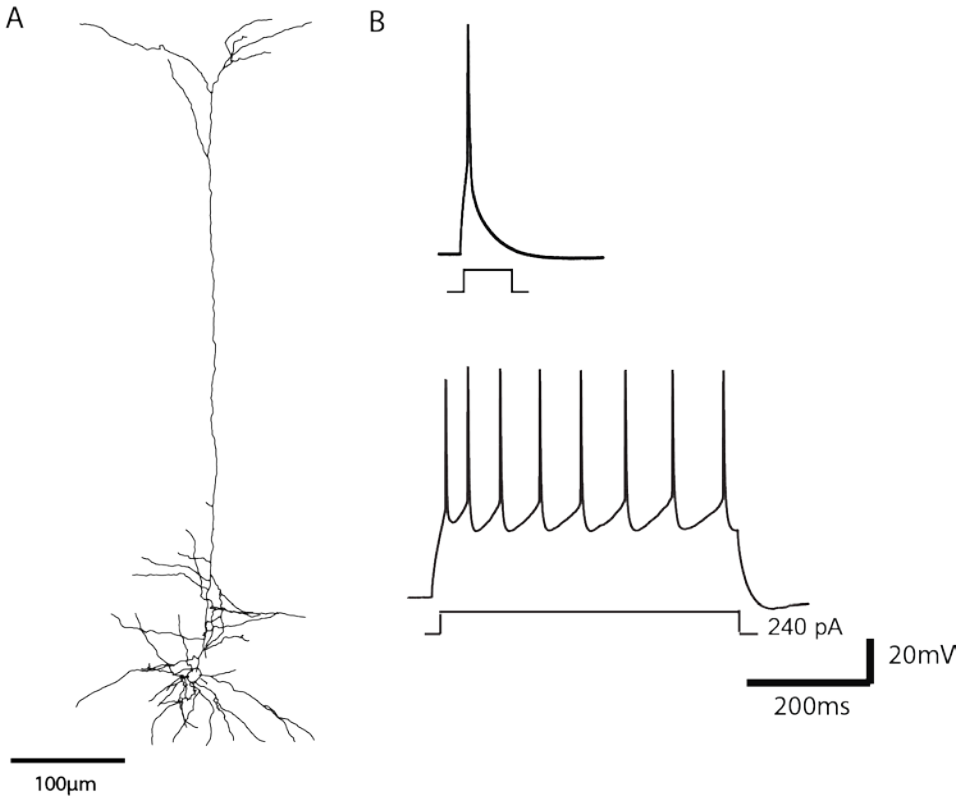

Figure 4.10 Functional properties of L5A slender- tufted pyramidal neuron

A. Biocytin- filled Neurolucida reconstruction of L5A pyramidal neuron.
B. Spiking pattern of the neuron in (A) reveals properties of L5A pyramidal neuron. To brief current injection neuron fires single spike. To the prolonged stimulation neuron responses with the low- frequency spiking pattern.

Light flashes of brief (2ms, 5ms) to prolonged duration (20ms) and 10 light flashes each of duration 1ms evoked robust postsynaptic responses in L5A

pyramidal neurons (Fig.4.9). The synaptic responses induced by light activation of ChR2- expressing axonal arbors showed 2-3 ms delay of the response (Fig.4.9).

The recorded pyramidal neurons showing synaptic responses to the optical stimulation depicted the characteristics of L5A pyramidal neurons: morphology of slender- tufted L5 pyramidal neurons (Fig.4.10 A) and regular spiking pattern to the prolonged current injection (Fig.4.10 B).

Therefore, the present results described that the specific activation of the thalamocortical pathway revealed synaptic connections between POm and basal dendrites of L5A pyramidal neurons.

Voltage and Ca^{2+} imaging in dendrites and spines of L5 pyramidal neurons

4.5 Time course of bAP in the dendrites and spines in the apical tuft of L5 pyramidal neurons corresponds to the time course of somatic response

Recordings of membrane potentials from distal dendrites and spines of L5 pyramidal neurons is hampered by the small size of these structures and it is often impossible to perform direct electrical recordings from these fine dendrites.

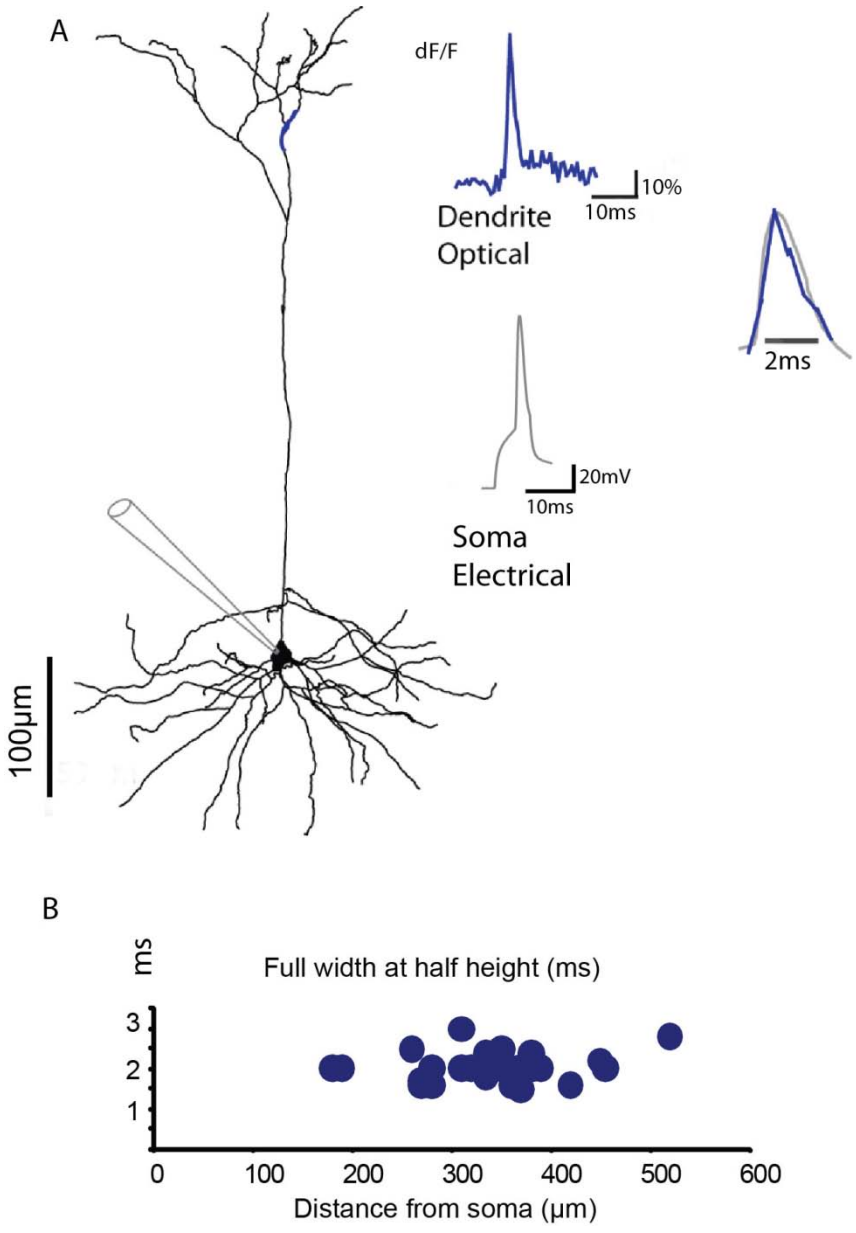

Figure 4.11 Time course of the back- propagating action potential in the apical tuft and in soma of L5 pyramidal neuron

A. (left) Image of reconstructed L5 pyramidal neuron loaded with JPW1114. (Top Right) the optical dendritic signal in the apical tuft evoked by single bAP by current injection to the soma. (Bottom right) Overlay of the somatic electrical response with the optical signaling in the apical tuft.
B. The summary of the time course of the optical signal from the apical dendrite recorded at different distances from soma evoked by single bAP.

In order to study the dynamics of backpropagation of the action potential to the distal branches and spines the use of voltage- sensitive dye (VSD) with the tailored loading technique was applied in the present study. The voltage- imaging has allowed performing of the recordings of the membrane potential changes in the distal dendrites and neighboring spines of L5 pyramidal neurons without use of the patch electrodes.

Single bAPs were evoked at the area of the axon hillock, the region responsible for action potential (AP) initiation (Fuortes et al., 1957; Palmer and Stuart, 2006). The backpropagation in the series of the experiments was elicited antidromically by placing the stimulation pipette to the region of the AP initiation zone or by injection of the depolarizing current to the soma through the patch-pipette. The antidromic stimulation allowed the determination of the kinetics of membrane potential changes in the intact cell without the need of electrical recordings. The dynamics of bAPs were examined in dendrites and spines of L5 pyramidal neurons along the apical dendrite located at different distances from soma.

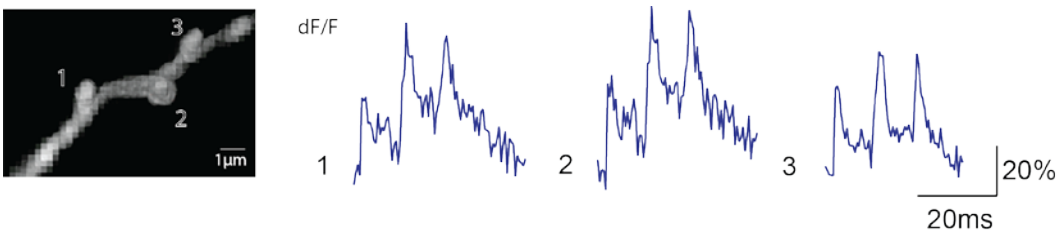

Figure 4.12. Time course of the spine signaling in the apical tuft of L5 pyramidal neuron

(Left). The fluorescent image of the spiny dendritic branch in the apical tuft of L5 pyramidal neuron filled with JPW1114. (Right).Corresponding optical signals from individual spines evoked antidromically by triplet of backpropagating action potentials

The kinetics of the membrane potential changes recorded optically in the distal dendritic branches were compared to the electrical signal obtained in the soma and to the optical signals from other parts of the apical dendrites. The recordings revealed the fast time course of the fluorescently detected membrane potential changes in the apical tuft similar to the rapid time course of the somatic action potential (Fig. 4.11 A). Hence, the fast time course of the dendritic bAPs was independent of the distance from soma. The half width duration of the optical signal was 2 to 3 ms and did not reveal any dependence on the location of the recording in the apical dendrite (Fig. 4.11 B). The bAPs evoked from individual spines also showed the rapid rise time in the apical tuft dendrites of L5 pyramidal neurons (Fig. 4.12.).

4.6 Attenuation of Ca^{2+} signal along the apical dendrite of L5 pyramidal neuron

In order to examine Ca^{2+} dynamics along the apical dendrite of L5 pyramidal neurons into the response to single bAPs and thus to study the role of the dendritic backpropagation in the synaptic plasticity, confocal Ca^{2+} imaging was performed in the following experiments.

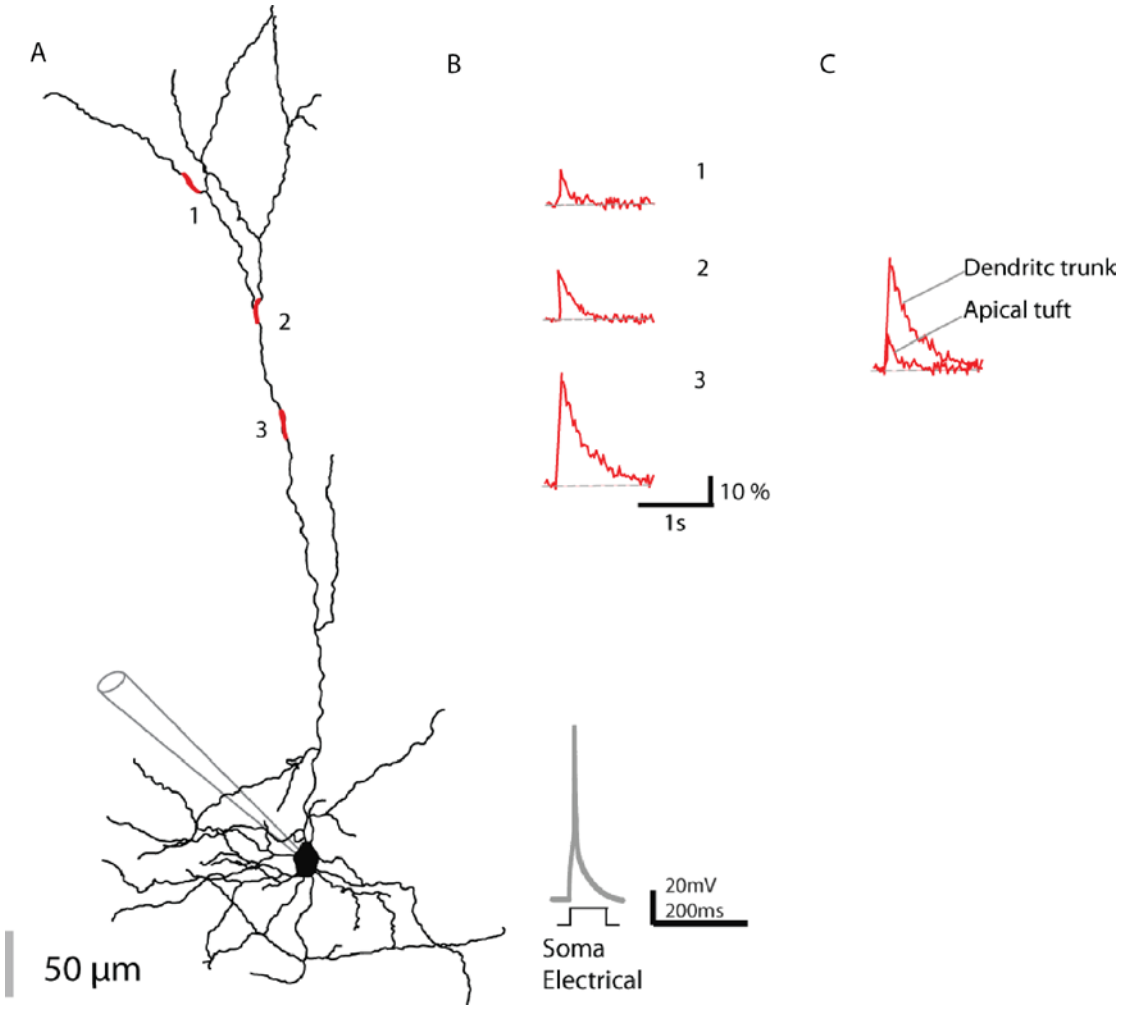

Figure 4.13 Attenuation of Ca^{2+} signal along the apical dendrite as the factor of distance from soma

A.Reconstructed L5 pyramidal neuron with indications of the recorded regions.
B.Ca^{2+} transients from distinct parts of the dendritic tree located at different distances from soma evoked by single bAPs elicited by current injection through the patch-pipette in the Current Clamp mode and recorded with CCD camera (Red Shirt) with Neuroplex program at 40Hz.

C. The superposition of Ca^{2+} transients obtained in the dendritic trunk close to the soma and in the apical tuft.

Whole- cell recordings in L5 pyramidal neurons in mice aged P15-P17 were combined with the loading of the cell with 100μM OGB1 for Ca^{2+} imaging and with biocytin for further dendritic reconstructions. Ca^{2+} imaging was performed at different dendritic regions along the apical dendrite, from proximal part to the distal processes. Single bAPs elicited by depolarizing current injection through the patch-pipette evoked Ca^{2+} fluorescent transients in the dendrites of L5 pyramidal neurons (Fig.4.13B). The investigation of Ca^{2+} signaling revealed the attenuation of Ca^{2+} fluorescent transient along the apical dendrite. With the increase of the distance from soma dF/F of bAP- evoked Ca^{2+} fluorescent transient decreased in the amplitude revealing low detectable Ca^{2+} signal in the apical tuft (Fig. 4.13C). These results indicate that single bAPs does not influence Ca^{2+} signaling in the tuft of L5 pyramidal neurons.

The decrement attenuation of Ca^{2+} fluorescent transients in the distal parts of the dendritic tree is not entirely understood and raises an important question about the mechanisms of the integration of the backpropagation in the distal processes of L5 pyramidal neurons, its involvement into the synaptic plasticity and the activity patterns that manage to backpropagate successfully into the tuft.

4.7 *In vivo*- like patterns of stimulation contain effective frequencies of back propagation into the apical tuft

We applied *in vivo*- like stimulation to investigate the patterns of bAPs that invade the distal tufts of L5 pyramidal neurons. In *in vivo* conditions neurons integrate trains of spikes at different frequencies. In order to simulate the impact of the physiological behavior in the distal dendrites, bAPs were evoked containing sequence of the frequencies recorded *in vivo*.

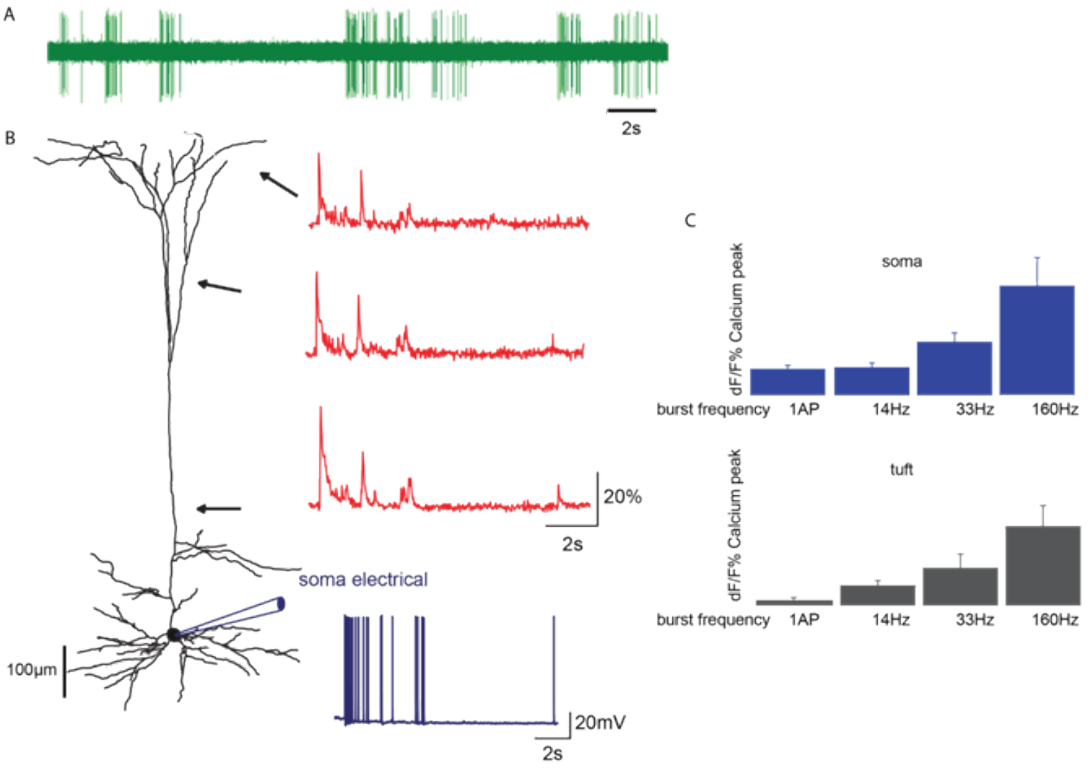

Figure 4.14 Effectiveness of the bAP in the tuft is dependent on the frequency of applied stimulus.

A.Spontaneous activity of L5B ChR2 pyramidal neuron in vivo. Recording obtained from ChR2- thy1 transgenic mouse by Dr. A.Groh.
B.(Left) Reconstruction of L5B ChR2- positive neuron. (Right) In vivo- like train of bAPs was applied in vitro by current injection through patch- pipette (blue). Ca^{2+} transients recorded from the dendrites (red) located proximally and in the distal parts of the apical dendrite.
C.The summary of frequency- dependence of Ca^{2+} transients in soma and tuft.

To obtain action potentials spiking patterns from L5 pyramidal neurons thy1-ChR2 (line 18) mouse line with EGFP-positive ChR2- expression in the population of thick- tufted L5B pyramidal neurons (Groh et al., 2011) was used. *In vivo* spontaneous spiking behavior was recorded by Dr. A. Groh identified as ChR2-

expressing L5 neuron in the somatosensory cortex from the light- activated response (Fig.4.14 A). *In vivo* obtained sequence of spikes was applied *in vitro* conditions. EGFP- positive ChR2- expressing L5B pyramidal neurons were identified from the fluorescent soma and dendrites with the confocal spinning disk system and with the use of low intensity laser light with the excitation wavelength at 488nm. With the application of the DIC- optics whole- cell recordings were established for Ca^{2+} imaging with low affinity Ca^{2+} indicator (300µM OGB6F). For morphological reconstructions the intracellular solution contained biocytin. *In vivo* pattern containing defined sequence of the spiking behavior was evoked by current injections at distinct frequencies through the patch pipette. bAP- evoked Ca^{2+} fluorescent transients were acquired along the apical dendrite (Fig.4.14 B). The recordings revealed the attenuation or failure of Ca^{2+} transient evoked by bAPs at low frequencies in the distal apical branches and invasion of the apical tuft with the stimulus applied at high frequencies (Fig.4.14 C).

Thus, the bAP in the distal dendrites is frequency dependent and the physiological train of spikes contains the patterns of stimuli that invade the apical tuft.

4.8 Development of a new special double- patch procedure for staining of distant terminal branches and distant spines

The standard intracellular loading technique has several restrictions for studies performed in the distant branches and distant spines of L5 pyramidal neurons. The limitations that complicate to acquire the data from thin dendritic terminals are related to the length of the apical dendrite in L5 pyramidal neurons that reaches over 3989µm and location in deep cortical layers (soma depth over 600µm) (Fig.4.2). Hence, the distribution of the fluorescent indicator is restricted to the proximal processes of the cell and does not reach branches located in L1 in the concentration level sufficient to visualize distant terminals and distant spines. Due to access limitations the detailed morphological properties and functional applications of the distantly located processes and distal spines has not been investigated yet.

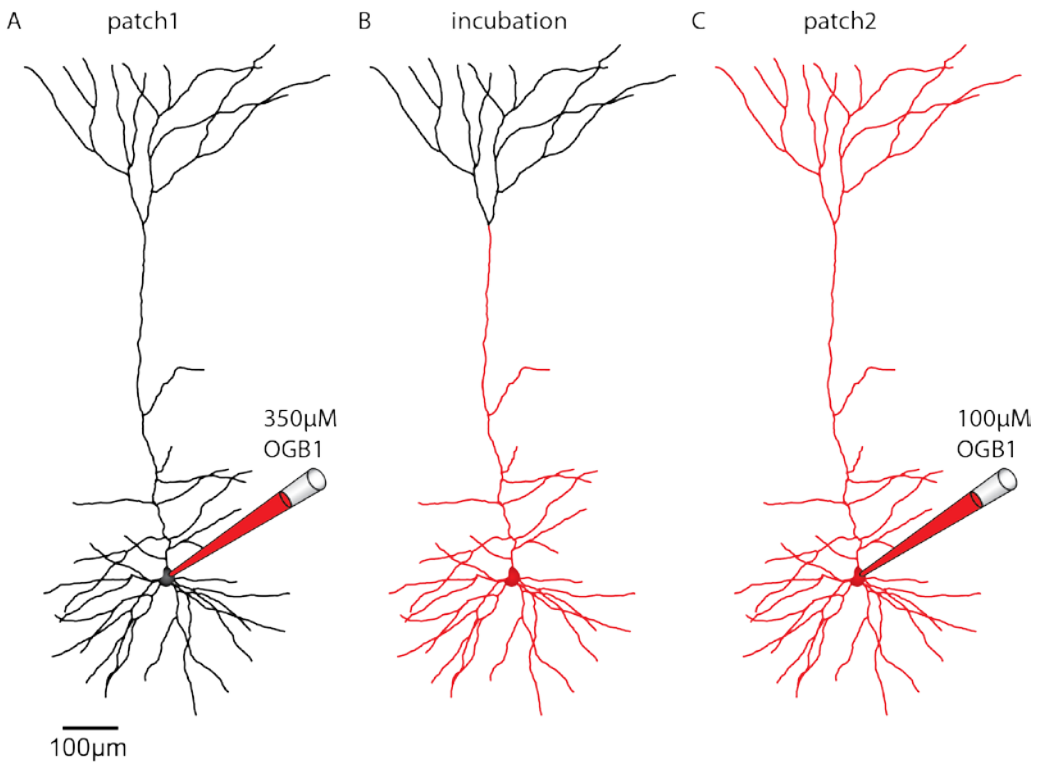

Figure 4.15 Schematic depiction of a new loading technique applied for staining of distant branches. Reconstruction of biocytin- filled thick- tufted L5 pyramidal neuron. The images show the level of the indicator distribution in the dendritic tree (red). The technique consists of three consecutive steps.

A.First step includes the establishment of whole- cell recording in order to fill the cell with the high concentration of the indicator.
B.Incubation in the recording chamber for 30 minutes is applied for redistribution of the indicator from the proximal branches to the distant terminals.
C.Re- patching of the neuron with 100µM OGB1 for further recordings.

In the present study to obtain recordings from the apical tuft of L5 pyramidal neurons I developed new special loading technique. This newly developed method directing for the fluorescent staining of the distantly located branches allowed the distribution of the fluorescent indicator at the sufficient level to the apical tuft to visualize dendritic branches located distantly from soma and terminal spines and to acquire Ca^{2+} recordings with optimized SNR. To retain the distal branches of L5 pyramidal neurons from deterioration during cutting slice preparation procedure the thalamocortical slices were used. That allowed preserve the branches of the apical tuft due to the parallel orientation of the dendritic tree of L5 pyramidal neurons in the vibrissal cortex.

The newly developed method includes several consecutive steps. The first step consists of the establishment of whole-cell recording with a high concentration of Ca^{2+} fluorescent indicator included in the patch pipette (350μM OGB1) (Fig.4.15A). After filling the cell for 8 to 10 minutes the patch pipette is pulled away. The level of Ca^{2+} indicator is estimated from the fluorescence level. At the time point of pipette withdrawal L5 neurons contain detectable level of Ca^{2+} dye up to the main dendritic bifurcation (Fig.4.15B). During the next 20- 30 minutes Ca^{2+} dye will distribute between soma and dendrites. Therefore, the incubation in the recording chamber was applied in order to obtain the equal diffusion of the fluorescent indicator to the terminal branches. The re- patch with 100μM of Ca^{2+} indicator in the pipette permitted to acquire Ca^{2+} recordings from the stained dendritic terminals and distant spines in L1.

4.9 Reconstruction of the spines in the apical tuft of thick-tufted L5 pyramidal neurons

The newly developed double- patch technique (Fig.4.15) application permitted to obtain reconstructions of the spiny dendritic branches in the apical tuft from thick-tufted L5 pyramidal neurons. The morphological description of the distant spines was obtained by acquirement of the z- stack and use of the deconvolution method to sharpen the image (Fig.4.16 B). 3D reconstructions of the distal spiny dendritic branches were accomplished with the use of Amira program and permitted the visualization of the complexity of the spine structures (Fig.4.16 C; D) at different angles.

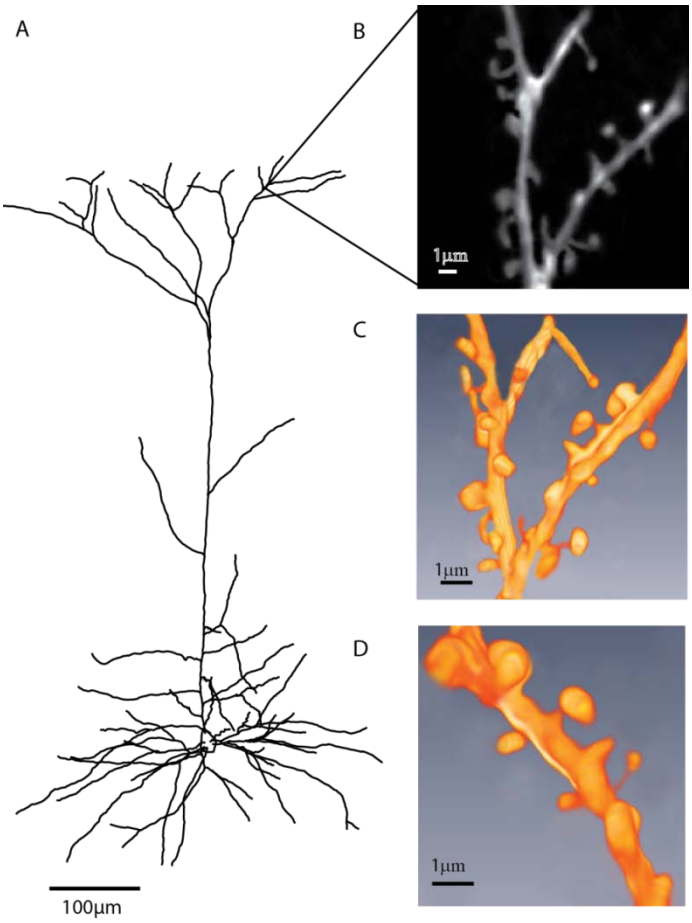

Figure 4.16 Characterization of the spines in the apical tuft of thick- tufted L5 pyramidal neurons

A.Biocytin- filled reconstruction of thick- tufted L5 pyramidal neuron.
B.Z- stack of 2- photon- image of the spiny dendritic branch in the apical tuft after deconvolution.
C.3D Amira reconstruction of spiny dendritic branch as in B. The image was obtained as z-stack with custom- written Labview software.
D.3D Amira reconstruction of the part of the dendritic branch in the apical tuft at high magnification.

The images of the dendritic reconstructions (Fig.4.16C) depict the fragments of the distal dendrites with large diversity of the spines various in shape, in length of the spine head and length of the spine neck. The size of the spines varies in the apical tuft in size with some of the membrane protrusions reaching up to 1µm.

4.10 Ca^{2+} imaging using LOTOS from individual spines in the apical tuft

To obtain high- sensitive recordings with good SNR of the signal and to reduce phototoxic influence during Ca^{2+} imaging from single spines in the apical tuft of L5 pyramidal neurons the method of low- power temporal oversampling (LOTOS) was implemented in the present study. LOTOS- imaging involves high- sampling rate of the acquired images, low intensity of the required excitation light and short pixel dwell- times (Chen et al., 2011).

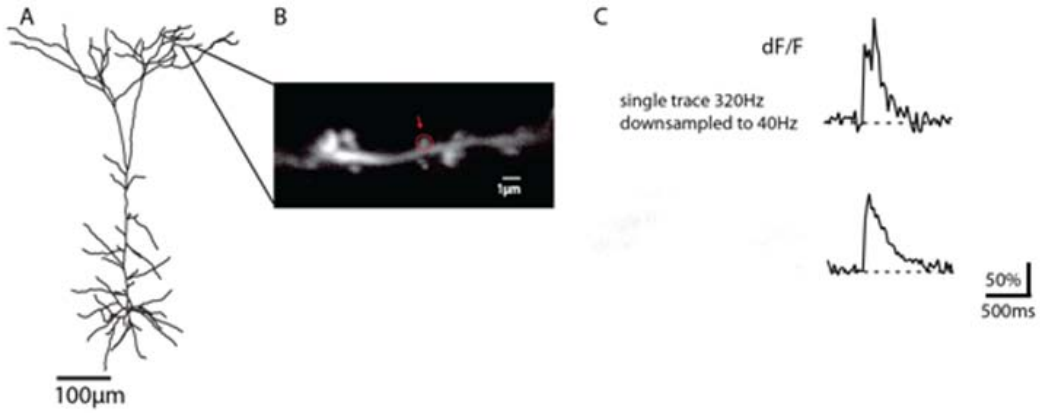

Figure 4.17 Ca^{2+} imaging method principle from the individual spine in the apical tuft

A.Reconstruction of biocytin- filled thick- tufted L5 pyramidal neuron.
B.2-photon image of the spiny dendritic branch in the apical tuft. Arrow indicates an active spine from which Ca^{2+} transient in C was recorded.
C.Single traces. (Top) Ca^{2+} transient from the individual spine in response to the single synaptic stimulation in the apical tuft acquired at 320Hz and downsampled to 40Hz. (Bottom) Ca^{2+} *transient evoked synaptically recorded at 640Hz with downsampling to 40Hz.*

Ca^{2+} signals from individual spines in this series of experiments were recorded with the use of high- speed AOD- based 2- photon microscopy (Fig.4.17 B). The images of the spiny dendritic branches in the apical tuft were obtained at frame rate of 320Hz and at 640Hz. The downsampling of the images recorded at high-frequency was performed offline by factor of 8 or 16 to the frequency of 40 Hz. This procedure optimized SNR and demonstrated robust Ca^{2+} signals from individual spines (Fig.4.17 C).

Hence, the implementation of LOTOS- based imaging combined with high-speed AOD- based 2- photon microscopy has improved the quality of the obtained Ca^{2+} imaging recordings.

4.11 Ca^{2+} kinetics in spines in the apical tuft

To characterize the synaptic transmission in the apical tuft of thick- tufted L5 pyramidal neurons Ca^{2+} dynamics from individual spines was analyzed in the present study.

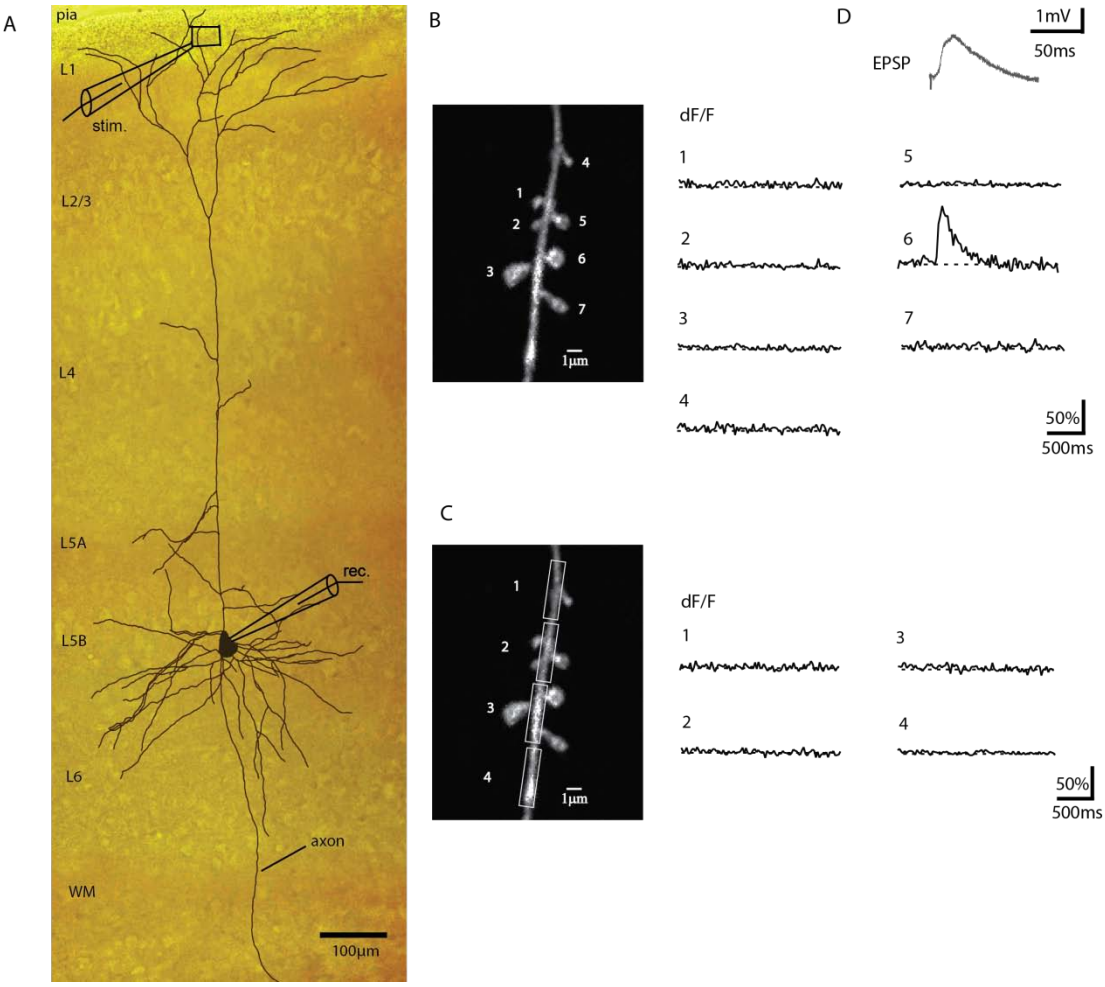

Figure 4.18 Ca^{2+} signaling in the individual spines in the apical tuft of thick- tufted L5 pyramidal neurons

A.Neurolucida reconstruction of biocytin- filled thick- tufted L5 pyramidal neuron superimposed with the image of area in the vibrissal cortex in acute thalamocortical slice. The pipettes indicate the recording and the stimulation sites.
B.(Left) 2- photon image of the spiny dendritic branch in the apical tuft with enumerated spines. (Right) Ca^{2+} transient from an individual spine evoked synaptically.
C.(Left) 2- photon image of the spiny dendritic branch with the enumerated portions of the dendritic shaft. (Right) Ca^{2+} imaging in the dendritic shaft in the apical tuft as in B.
D.Single EPSP recorded at the soma in a response to synaptic stimulation of the afferent fibers in the apical tuft applied at 7V.

Whole- cell recordings were established with the use of the new double- patch technique. After the single spines in the apical tuft were resolved with the use of high- speed AOD- based 2- photon microscopy the focal stimulation was applied. The stimulation pipette of high resistance was placed near the spine of choice located on the distant dendritic branch in the upper part of L1 (10- 40µm from pia surface), its location was adjusted during the experiment (Fig.4.18 A). The region of interest containing spiny dendritic branch in the apical tuft was imaged (Fig.4.18 B left). Single shock stimulation delivered through stimulation pipette evoked local Ca^{2+} signal restricted to the spine of choice (Fig.4.18 B right). The evoked Ca^{2+} transients had mean of rise time (10-90%) 37±4ms (n=9). The mean of decay time course was 207±19ms (n=9). EPSP of amplitude of 2mV with delay of 2- 3 ms from the start of the stimulus was recorded at the soma into response of the applied stimulus (Fig.4.18 D).

4.12 Quantification of release probability rate in the apical tuft

The characterization of the synaptic efficacy of the synapses located in the apical tuft is of great physiological importance. The quantification rate of the release probability in the distal synapses defines the strength of the synapse (Maass and Zador, 1999) receiving determined input in L1 and therefore providing the basis of the neuronal interactions in the upper layers of the cortex. The determination of the release probability in the previous studies was described as a vesicle fusion and transmitter release in the presynaptic site in response to an action potential (Del Castillo and Katz, 1954; Branco et al., 2008).

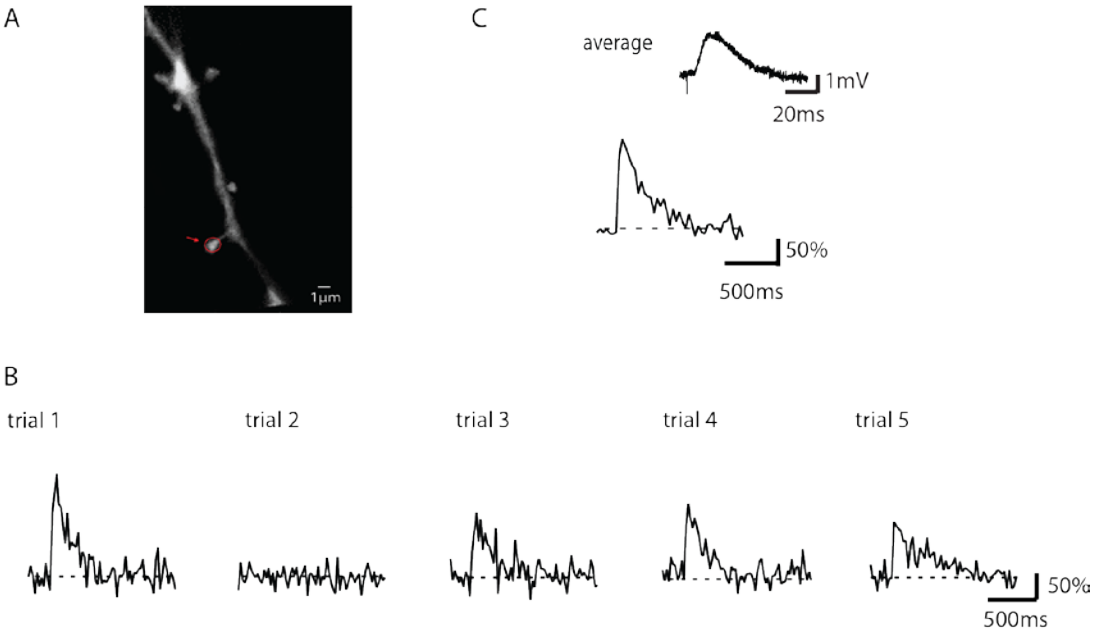

Figure 4.19 The synaptic response probability in the apical tuft of thick- tufted L5 pyramidal neurons in the vibrissal cortex.
A. 2- photon image of the spiny dendritic branch in the apical tuft. The arrow shows an active spine.
B. Ca^{2+} transients from individual spine in the apical tuft evoked by single synaptic stimulation in L1. The image shows single traces of Ca^{2+} transients evoked in consecutive trials at low frequency between stimuli.
C. (Top) EPSP recorded at the soma into the response to the single synaptic stimulation in the apical tuft.
(Bottom) Average of Ca^{2+} transients in 5 consecutive trials

Thus, in the present study the analysis of the release probability in the distal synapses was quantified in the dynamics of Ca^{2+} transients from spines recorded as

the sequence of 5 to 10 consecutive trials into response to the focal single- shock stimulation. The intervals between trials were recorded at low frequency range. For obtaining of Ca^2 signals from the terminal spines in the apical tuft with the use of the double- patch technique whole- cell recordings were established. That allowed to obtain somatic EPSP response into the synaptic stimulation (Fig.4.19 C) and fill L5 thick- tufted pyramidal neuron with biocytin for dendritic reconstructions (Fig.4.19 A).

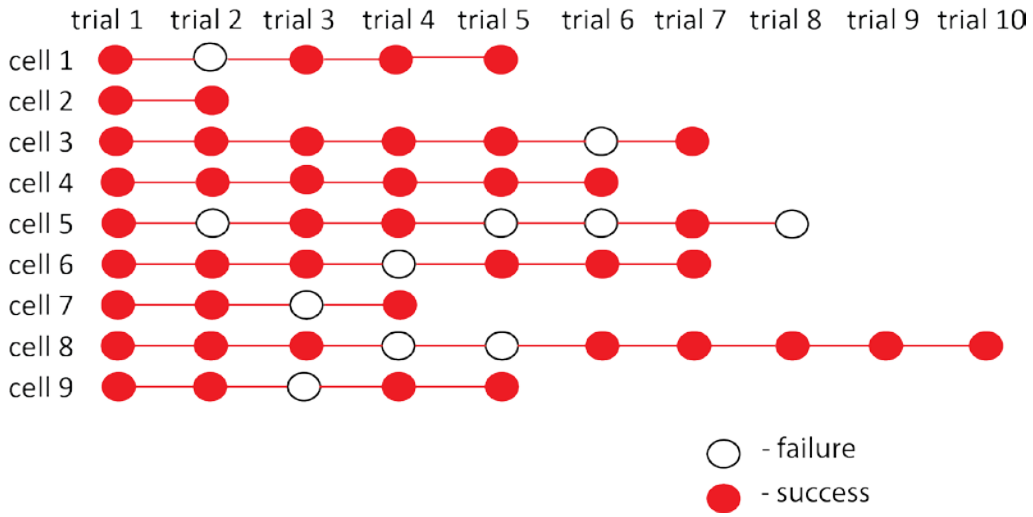

Figure 4.20 Summary of release probability in the apical tuft in the series of the sequential trials.

The table shows data from 9 thick-tufted L5 pyramidal neurons and depicts the reliable probability to evoke Ca^{2+} transients in the synapses in the apical tuft from trial to trial.

The stimulation pipette was placed in the upper L1 in the vicinity of the dendritic spine of interest. Single pulse current stimulation evoked robust Ca^{2+} - transient from individual spine (Fig.4.19 B). Consecutive trials of the single- shock stimulation in the apical tuft revealed low failure rate of the recorded Ca^{2+} signals. The results of the Ca^{2+} transients dynamics recordings determine the success rate of 82% of release probability (n=9) in the synapses found in the apical tuft of L5 thick- tufted pyramidal neurons (Fig.4.20).

4.13 Ca^{2+} signaling in spines of the apical tuft is NMDAR and AMPAR dependent

In order to investigate the mechanism of synaptically- evoked Ca^{2+} transients from the spines in the apical tuft of thick- tufted L5 pyramidal neurons I examined the contribution of the NMDA and AMPA receptors.

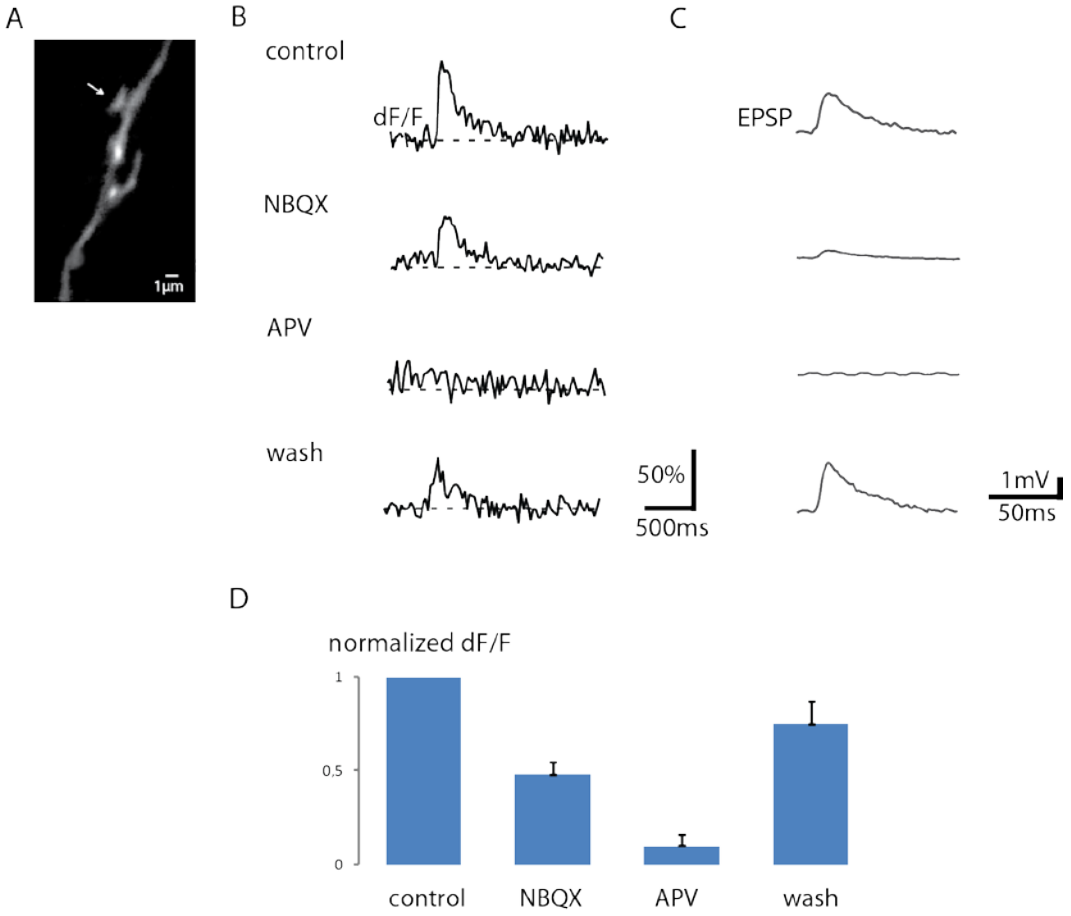

Figure 4.21 Ca^{2+} signaling in spines of the apical tuft requires activation of AMPARs and NMDARs (n=5).

A.2-photon image of the dendritic spiny branch in the apical tuft. The arrow indicates the activated spine.
B.Ca^{2+} signals (dF/F) from the spine in A evoked by single stimulus at 7V in control conditions, bath- applied NBQX (10µM), APV (50µM) and after wash.
C.EPSP recorded at the soma to the response of the synaptic stimulation in B in control conditions, after application of NBQX, APV and after wash out of the antagonists.
D.Summary presents the effects of NBQX and APV on Ca^{2+} signaling from the individual spines.

After the application of the double- patch procedure, establishment of whole-cell recording the stimulation pipette with the fine tip opening was placed in the vicinity of the dendritic spine of choice. The brief current pulse elicited Ca^{2+} transient in individual spine and EPSP recorded at the soma in the current clamp mode (Fig.4.21B, C). Bath- applied antagonist of AMPA receptor 10µM NBQX reduced dF/F amplitude of the spine Ca^{2+} transients (Fig.4.21 B) evoked at resting membrane potential of -70mV. Associated EPSP recorded at the soma was significantly decreased in the amplitude, showing low detectable signal. With the application of NMDA receptor channel antagonist in the bath no Ca^{2+} transient and EPSP were detected (Fig.4.21 B, C).

The blocking of the synaptic transmission was reversible: with the remove of the antagonists and recording in the control conditions Ca^{2+} transients and somatic EPSP were restored in the amplitude.

Thus, synaptically evoked spine Ca^{2+} signals in the apical tuft in thick- tufted L5 pyramidal neurons are primarily dependent on Ca^{2+} ions entry through NMDA receptor channels. The involvement of AMPARs in the synaptic transmission in the distant branches is not excluded.

4.14 Cooperativity in Ca^{2+} spine signaling in the apical tuft

To investigate the impact of high frequency and high intensity stimulation to the distal synapses of thick- tufted L5 pyramidal neurons Ca^{2+} imaging from individual spines and dendritic shafts in the apical tuft was conducted. After the application of the double– patch clamp technique whole- cell recordings were established.

First, single- shock stimulation at minimal intensity was performed that evoked Ca^{2+} transient from one single spine in the region of interest (Fig.4.22). Ca^{2+} imaging from the segments of the dendritic shaft did not detect any Ca^{2+} signaling in the field of view to the response of the single- shock stimulation of the afferent fibers in L1 (Fig. 4.22B).

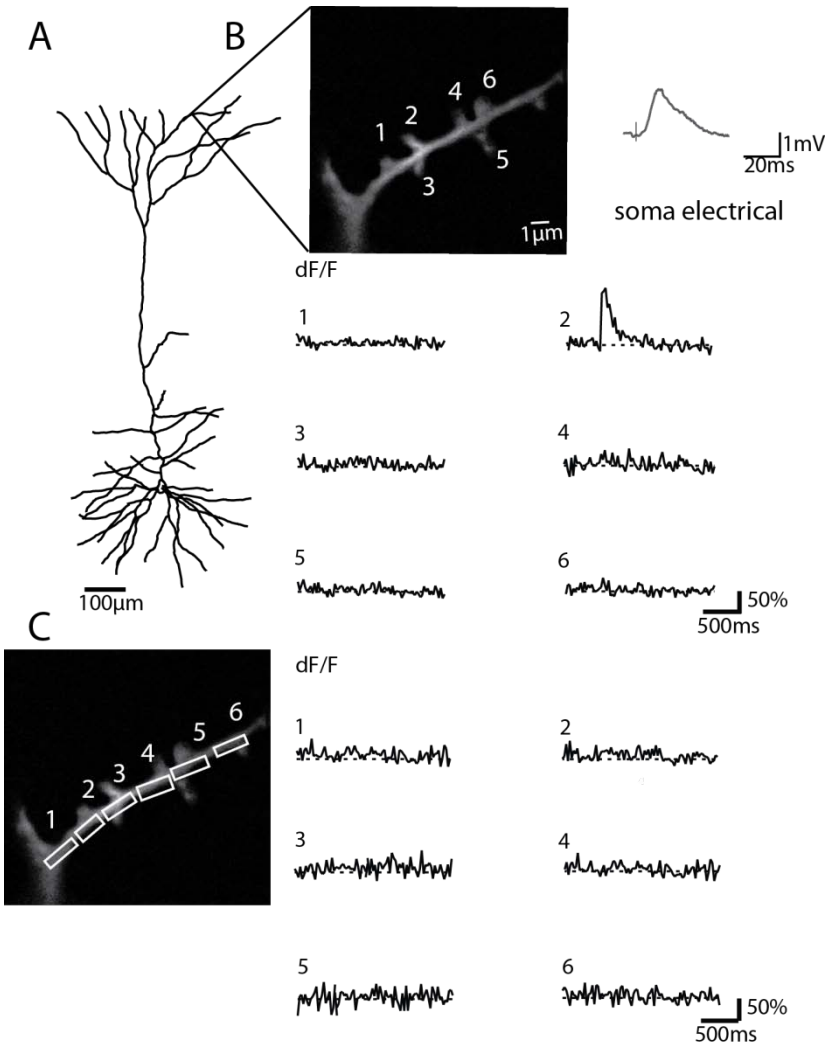

Figure 4.22 Spine- signaling in the apical tuft of L5 pyramidal neuron

Ca^{2+} transients from single spines in the apical tuft evoked by stimulation of the afferent fibers in L1 of the cortex show localized response in the spine.

A.Biocytin- filled reconstructed thick- tufted L5 pyramidal neuron.
B.2- photon image of the spiny dendritic branch in the apical tuft with spines (1-6). EPSP recorded at the soma. Ca^{2+} transients from single spines to the single- shock stimulation at 7V.
C.2- photon image of the distal spiny branch with enumerated parts of the dendritic shaft.

The stimulation intensity was afterwards increased to the level when Ca^{2+} transient was elicited from the neighboring spine (Fig.4.23A) and the parent dendrite (Fig.4.23C). The peak amplitude of Ca^{2+} signaling in the dendritic shaft was highest at the site of the active spines.

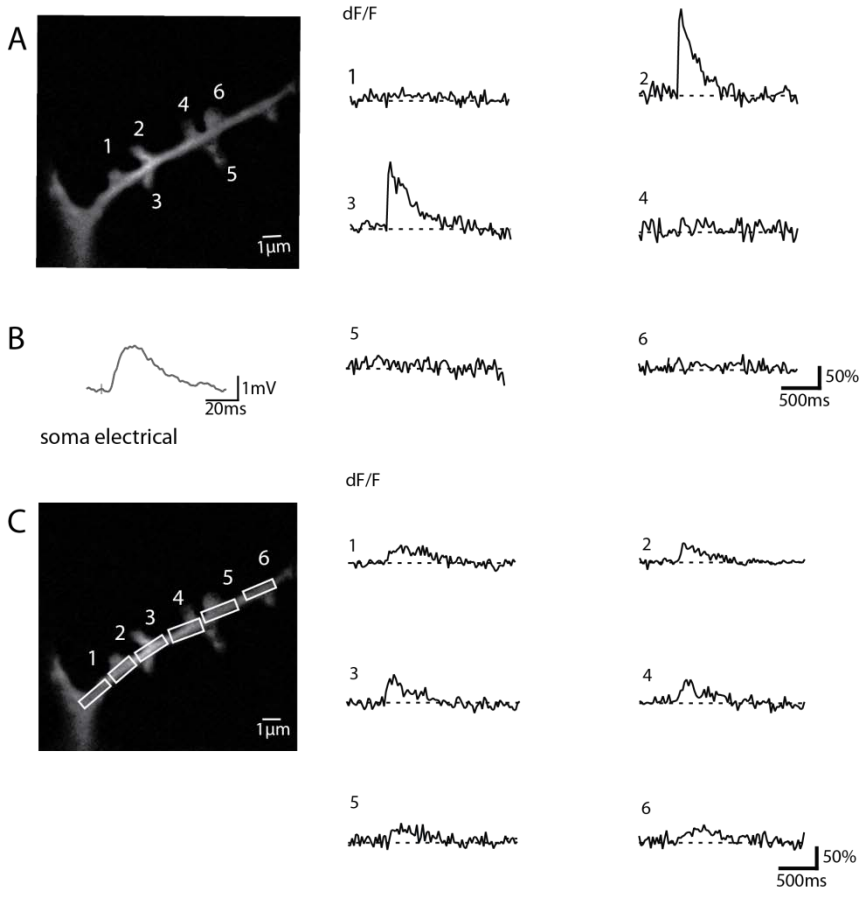

Figure 4.23 Cooperativity in Ca^{2+} spine signaling in the apical tuft of thick- tufted L5 pyramidal neurons. Increase of the synaptic stimulation intensity.

A.(Left) 2- photon image of the spiny dendritic branch in the apical tuft with enumerated spines. (Right) Ca^{2+} transients from individual spines as a response to the increased intensity of the single- shock stimulation from 7 to 10V.
B.EPSP at the soma evoked by stimulation protocol
C.(Left) 2- photon image of the distal dendritic branch as in A with the enumerated dendritic sections. (Right) Ca^{2+} transients recorded from dendritic shaft in the apical tuft as a response to the synaptic stimulation as in A.

Ca^{2+} transients were evoked in several spines and in the parental dendritic shaft upon high frequency stimulation of the afferent fibers leading to the similar impact as with increase of the stimulation intensity (Fig.4.24). The stimulation was performed at 100Hz delivered through a stimulation pipette: 2 stimuli at 7V. The EPSP recorded somatically showed summation with increase in amplitude (Fig.4.23B).

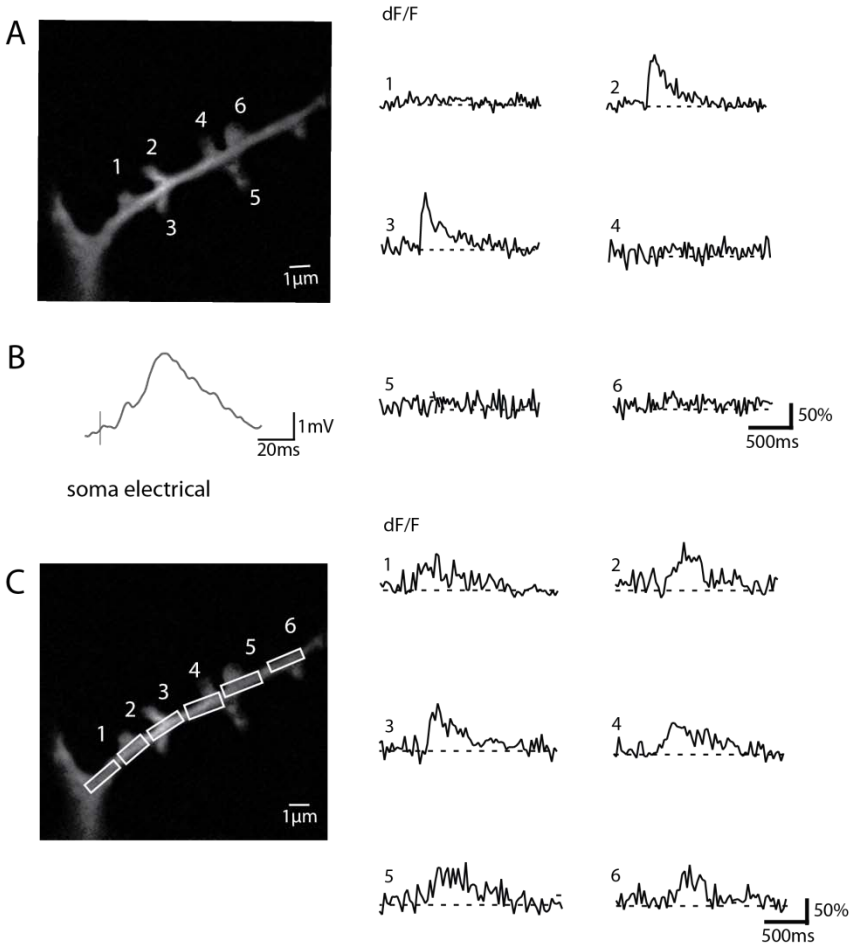

Figure 4.24 Cooperativity in Ca^{2+} spine signaling in the apical tuft of thick- tufted L5 pyramidal neurons. Synaptic stimulation at high frequency.

A.(Left) 2- photon image of the distal spiny dendritic branch with spines (1-6).(Right) Ca^{2+} transients from individual spines as response to synaptic stimulation at 100Hz.
B.EPSP recorded at the soma
C.(Left) 2- photon image of the terminal branch as in A with the enumerated parts of the dendrite. (Right) Ca^{2+} transients from the corresponding parts of the dendrite evoked by two synaptic stimuli at 100Hz at 7V.

Thus, the involvement of the dendritic conductance in the synaptic responses in the apical tuft raises the questions of the possible mechanisms and the purpose of the shaft impact to the spine signaling in the distal branches.

Chapter 5

Discussion

5.1 Morphological and functional analysis of L5 pyramidal neurons

5.1.1Characterization of genetically- defined L5 pyramidal neurons

This study reports the characterization of the morphological and functional properties of genetically- defined cell- types of L5 pyramidal neurons in the vibrissal cortex of two transgenic mouse lines.

Thus, the investigation of the properties of genetically- defined population of L5 pyramidal neurons from transgenic GLT25d2 (*glt*) BAC- EGFP mouse revealed the morphological and electrophysiological similarities with thick- tufted L5B pyramidal neurons in the vibrissal cortex. These results are in line with the previous work by Groh et al., 2010 showing the analogous characteristics of these genetically- labeled neurons in the visual and vibrissal cortices. L5 pyramidal neurons expressing EGFP promoter for glycosyltransferase are found in deep cortical L5 and have extensive dendritic arborization in L1. Electrophysiological recordings show the firing modes of intrinsically bursting neurons and fast- spiking neurons into response to the prolonged current injection.

This investigation of this specific cell population of *glt* L5 pyramidal neurons can be regarded as the basis for the further functional examinations in the context of Ca^{2+} imaging in this defined cell- type. Additionally, the characterization of specific neuronal populations regarding gene expression can extend the classification of the distinct cellular populations in the cortex. Hence, future considerations of the studies carried out on genetically- defined neuronal classes can sort the large diversity of the cortical cellular populations to the distinct cell groups with the defined histological and physiological properties.

Another genetically- targeted group of L5 pyramidal neurons expressing EYFP- ChR2 in the vibrissal cortex was additionally characterized in the present study using another transgenic mouse thy-1 ChR2 (line 18). The results described that ChR2- positive neurons share the morphological and physiological properties of thick- tufted L5B pyramidal neurons. The dendritic reconstructions revealed the pyramidal neurons located in deep parts of L5 with large dendritic branching pattern in L1. Prolonged stimulus applied to this type of neurons elicited patterns of fast-spiking or intrinsically bursting neurons.

The fusion protein EYFP ChR2 expressed in L5 pyramidal neurons analyzed in this work showed the prevailing fluorescent signal in the apical tuft. This can be of advantage for using of this mouse line *in vivo* conditions for the optical stimulation of the extensive apical tufts to examine the functional role of this cell- type.

Previous studies reported the thalamocortical inputs to L5 pyramidal neurons *in vitro* and with the use of the anatomical tracing methods (Agmon et al., 1993; Brecht, 2007; Petreanu et al., 2007; Petreanu et al., 2009, Meyer, Wimmer et al., 2010). Whereas the projection targets of these neurons were shown in the specific thalamic nucleus (POm) *in vitro* and from tracing data (Deschenes et al., 1998; Veinante et al., 2000; Markram, 2006; Groh et al., 2010).

How the corticothalamic connections of L5B pyramidal neurons to the subcortical structures are arranged *in vivo* conditions was not yet detailed investigated. The classification of ChR2- positive neurons in the present study allowed the use of this transgenic mouse line to examine thalamocortical connectivity *in vivo* with the optical stimulation of the apical tufts of these neurons.

Thus, the results of *in vivo* investigation described that the signaling in the thalamocortical pathway has the back- forward direction with the information flow from cortical L5B pyramidal neurons to POm thalamic nucleus (Groh et al., 2011). The future examinations of this connectivity can include the properties and integration purpose in the neuronal transduction of this reverse pathway signaling. The hypothesis regarding such bidirectional thalamocortical connections can also be that cortex in the hierarchy of the neuronal network regulates the activity of the subcortical structures.

5.1.2 POm inputs to the basals of L5A pyramidal neurons in the somatosensory cortex

The results in this thesis with the use of ChR2 for the precise mapping of the thalamocortical connections describe the inputs from specific thalamic nucleus POm to the basal dendrites of L5A pyramidal neurons. The light activation of ChR2-expressing axonal arbors with the optical fiber produced postsynaptic response in L5A pyramidal neurons. The dendritic reconstructions of L5 pyramidal neurons that responded to the light activation showed the morphology of slender- tufted L5 neurons and the behavior of regular- spiking L5A pyramidal neuron found in the upper parts of L5 in the cortex.

These results are in accordance with the previous studies describing the histological evidence (Meyer, Wimmer et al., 2010) and functional connections between POm and this specific cell- type (Petreanu et al., 2009; Meyer, Wimmer et

al., 2010). The distinct morphological and electrophysiological properties of L5A pyramidal neurons similar to the present results were described in the previous works (Chagnac- Amitai et al., 1990; Larkman and Mason, 1990; Wang and McCormick, 1993; Kasper et al., 1994)

The results of the present study show the new approach of the optical stimulation of tiny ChR2- expressing axonal arbors with the use of an optical fiber and possibility to record light produced postsynaptic responses.

The future works conducted for mapping of the specific thalamocortical inputs to the distinct processes of L5 pyramidal neurons described in detail with the use of the optogenetic tools can provide the simplified and clear knowledge of the organizational structure of the large amount and complexity of the diverse inputs in the cortex. Another issue to be examined is Ca^{2+} imaging from individual spines into response to the optical stimulation of the defined axonal arbors for determination of the specificity of the activated inputs.

5.2 Voltage and Ca^{2+} imaging in dendrites and spines of L5 pyramidal neurons

Signaling in distal dendrites and spines of L5 pyramidal neurons

The results of this thesis describe the signaling in the apical tuft of L5 pyramidal neurons in the vibrissal cortex. The present study investigated morphological properties of the distal dendrites and distal spines and characterized the membrane potential changes and Ca^{2+} signaling in the terminal branches of L5 pyramidal neurons. Additionally a new loading technique was developed and applied for Ca^{2+} imaging from individual spines and tiny distal dendrites in the apical tuft.

5.2.1Rapid kinetics of bAP in the apical tuft of L5 pyramidal neurons

The present study demonstrates the rapid time scale of backpropagating action potential (bAP) in the distal spines and distal dendrites of L5 pyramidal neurons of the mouse vibrissal cortex corresponding to the fast time course of the somatic response. Additionally, bAP was not attenuated along the apical dendrite, with the half width duration of 2-3ms of the optical signal. This finding is in line with the recent work performed with the use of voltage- sensitive dye (VSD) showing fast kinetics of bAPs along the apical dendrite elicited by somatic current injection in L5 pyramidal neurons of the mouse visual cortex.

In the present study time course was investigated not only in the conditions with bAP evoked by somatic current injection, but additionally with antidromic stimulation. This condition allowed examine membrane potential changes in the intact cell without the use of the electrodes. bAP evoked antidromically also showed fast time course of the optical signal independent on the distance from soma.

My results surprisingly are not in accordance with the previous works characterizing electrical signaling in the distal dendrites with the use of the multiple patch- clamping technique. The results of the past studies described distance-dependent attenuation of the membrane potential changes in amplitude decrement and increase of the half width of the AP in the terminal branches (Stuart et al., 1997; Larkum et al., 2001). This alteration of the electrical signal in the distal dendrites can be related to the disadvantages of the performed dendritic recordings with the high-resistance electrodes (Stuart et al., 1993; Stuart et al., 1997) such as an access resistance and the electrode capacitance that can influence the shape of the bAPs (Waters et al., 2005).

Thus, the finding of the rapid time course of bAP along the apical dendrite of L5 pyramidal neurons, especially in the distal dendritic branches can be important for the cellular integration in the neuronal circuit and play defined role in the synaptic plasticity. The future investigations can be directed to the examination of the membrane potential changes in STDP in the postsynaptic and presynaptic sites, also *in vivo* conditions.

5.2.2 bAP- evoked Ca^{2+} transients in the apical tuft of L5 pyramidal neurons

The present study also investigated Ca^{2+} dynamics of bAPs in the apical dendrites of L5 pyramidal neurons of the somatosensory cortex. The results describe the attenuation of Ca^{2+} transient evoked by single bAPs in the distal branches in the decremental manner, whereas the high frequency stimulation produced relevant backpropagation of Ca^{2+} transient in the apical tuft.

These results are in accordance with the previously performed studies investigated bAP properties of L5 pyramidal neurons. The past works characterized the decrease of the amplitude of Ca^{2+} transient elicited by single AP with the distance from soma (Stuart et al., 1997; Schiller et al., 1997). The application of high frequency protocol defined the efficacy of such stimulation in the tuft (Williams and Stuart, 2000; Gulledge and Stuart, 2003; de Kock and Sakmann, 2008). The mechanisms for the faithfully backpropagation of the high frequency stimulation to the apical tuft was described due to the supralinear temporal summation with the

participation of terminal dendritic sodium and Ca^{2+} channels (Williams and Stuart, 2000).

My results additionally describe that spiking activity of ChR2- L5B pyramidal neuron recorded *in vivo* contains the patterns of frequencies that backpropagate effectively into the distal branches. Thus, the intact neuron in the living brain can interact with the defined spiking activity that provides effective transduction of the signaling and therefore supplying mechanisms for the information flow.

Attenuation of the bAP in the apical tuft in the decremental manner provides questions of how L5 pyramidal neuron with its long apical dendrite integrates synaptic inputs in the terminals. For this purpose the investigation on the level of the individual spines can resume the mechanisms and functions of the signaling in the distal branches of L5 pyramidal neurons.

5.2.3 A newly developed double- patch loading technique for the investigation of the distal spines

The work presented in this thesis resolves the problem of the obtaining of the experimental data from the distant dendrites and distant spines of L5 pyramidal neurons. The development of a new double- patch procedure in this thesis allowed access to the terminal branches and therefore perform morphological characterization combined with Ca^{2+} imaging recordings from the distal dendritic branches and spines in the apical tuft, not possible up to now.

An inaccessibility of the terminal dendrites of L5 pyramidal neurons to the direct investigation due to their fine size and due to the somata location in the deep cortical layers restricted the examination of these structures to the proximal branches with the use of the available loading techniques *in vitro*. The previous works aiming at characterizing Ca^{2+} signaling from individual spines and parental dendrites of pyramidal neurons were carried out on the basal dendrites (Polsky et al., 2004) or on the proximal part of the apical dendrite (Holthoff et al., 2002) lacking recordings from the apical tuft in L1.

The description of the signaling in the apical tuft was limited to prediction of the experimental data with the computational models. Though these models based on the mathematical and biophysical equations (Eccles, 1964; Rall, 1977) did not consider the properties of the neuron in the experimental conditions. The presence of the active voltage conductances in the dendrites (Kim and Connors, 1993; Stuart and Sakmann, 1994; Stuart et al., 1997) and in spines (Denk et al., 1995) contradicts the passive current flow described in the mathematical models. Additionally, the dendritic diameter diminishes with the distance from soma with

terminal dendrites reaching 1 µm in size that was also out of consideration in the cable theory.

Although, the recent studies tried to establish *in vivo* approach for Ca^{2+} imaging in deep cortical layers with the use of regenerative amplification multiphoton microscopy (RAMM) (Mitmann et al., 2011). This method allowed recordings from soma and populations of apical dendrites, still there are improvements to be done for providing *in vivo* examinations from the level of individual spines and tiny distal dendritic branches.

Hence, the new loading technique developed in the present study provides possibility for the investigation of the functional role of the distant spines and dendrites.

5.2.4 Characterization of the synaptic responses in the distal spines and distal dendrites of thick- tufted L5 pyramidal neurons

First, in the present study the morphological and functional properties of thick-tufted L5 pyramidal neurons of mouse vibrissal cortex were characterized as the basis of the functional study. The dendritic reconstructions show distinct morphology of this specific cell- type with the location in deep parts of L5. Another property of L5B cell population is the long apical dendrite, oblique branches with lateral orientation and extensive dendritic arborization in L1. These specific morphological characteristics define also the intrinsic membrane properties revealing two patterns of spiking as response to a prolonged stimulus: fast- spiking and intrinsically-bursting firing modes.

Previous works on characterization of thick- tufted L5 pyramidal neurons are in line with the present study providing similar descriptive results of the morphological and physiological properties of this specific cell- type (Larkman and Mason, 1990; Connors and Gutnick, 1990; Wang and McCormick, 1993; Kasper, et al., 1994; Angulo et al., 2003; Groh et al., 2010).

The future detailed studies of the electrophysiological properties can extend the role of L5 pyramidal neurons as the output neurons of the cortex (Reichova and Sherman, 2004). Additionally, the distinct dendritic architecture of this cell population with the extensive branching in L1 provides the interest for further investigations of the functional applications of such morphology in the synaptic transduction in the high- level cortical signaling mechanisms.

Next, Ca^{2+} signaling from individual spines and parent dendrites in the distal branches was analyzed. In this work the single- shock stimulation of the afferent

fibers in L1 evoked large Ca^{2+} transients from a single spine, whereas synaptic stimulation at high frequency elicited recruitment of the neighboring spines and additionally evoked Ca^{2+} transients in the parent dendrite. Also, an increase in the amplitude of the single- shock stimulus evolved Ca^{2+} transient in several spines with Ca^{2+} influx in the dendritic tree. The possible mechanisms for such cooperativity can be the activation of VGCC or previously described NMDA- spike (Larkum and Nevian, 2008; Larkum et al., 2009). The further examinations with the use of the antagonists are to be implemented in order to investigate the mechanisms involved.

My results additionally describe that Ca^{2+} signaling in the dendritic spines in the apical tuft is NMDAR- dependent. Ca^{2+} transients were reversibly blocked with the application of the NMDAR antagonist APV, showing that the major entry of Ca^{2+} in the apical tuft is through NMDARs. The application of AMPAR antagonist NBQX caused the reduction of the amplitude of Ca^{2+} transient, although the role of AMPARs in Ca^{2+} influx is not excluded.

In previous study the similar results were found in different brain regions: Kovalchuk et al., 2000 described the role of NMDAR and AMPAR in the synapses of the hippocampal neurons. Additionally, in rat hippocampal pyramidal neurons it was described that AMPAR channels have low Ca^{2+} permeability, thus indicating the other sources providing significant Ca^{2+} influx (Jonas and Sakmann, 1992). Holthoff et al., 2004 showed similar with the present study results from individual spines in the apical and basal dendrites of L5 pyramidal neurons of the mouse visual cortex.

The release probability (p_r) investigated in the present study showed the efficacy of the apical tuft synapses quantified as 80%. That differs from previous studies indicating the stochastic nature of the process and high variability of the release probability in different synapses (Branco et al., 2008; Branco and Staras, 2009). The past works determined average p_r value of 0.5 in the synapses and low values investigated *in vivo* (Borst, 2010).

Thus, the presence of large Ca^{2+} transients elicited into response of single-shock stimulation in the apical tuft and high p_r at the distal synapses can provide several hypotheses of its mechanism and possible functional applications in the neuronal information transduction. Does the high p_r presents the particular property of thick- tufted L5 pyramidal neurons due to their distinct dendritic morphology and therefore increased surface of the received synaptic input (Rall, 1962)? Or due to the specific innervation sources provided to the distal branches located in the upper parts of L1 adjacent to pia from the determined input target? Another hypothesis supports the idea that the apical tuft can function as an independent part of the cell with its particular physiological properties. Thus, the previous work described the

three functional compartments model of thick- tufted L5 pyramidal neuron with proximal apical dendrites and obliques, basal dendrites and axonal initiation zone, tuft dendrites and distal apical initiation zone (Larkum et al., 2001).

It is also possible, that the apical tuft supports the synaptic democracy mechanism (Häusser, 2001; Roth and London, 2004; Rumsey and Abbott, 2006) with the synaptic scaling for the compensation of the fine- size of the dendritic branches supplying equilibrium of the terminal processes with the proximal parts of the neuron.

The apical tuft can be referred in the hierarchy of the brain architecture as the source of integration of the high- level cortical signals. This is particular important in the study of L5B pyramidal neurons due to their specific morphological architecture of the extensive dendritic arborization pattern in L1 and considering the function of this specific cell- type as driving output neurons of the cortex (Reichova and Sherman., 2004.).

I would propose for future studies to include the functional examination of the apical tuft of L5 pyramidal neurons with regards to the synaptic plasticity and most importantly the investigation of the functional properties of the distal dendrites and distal spines *in vivo*.

Chapter 6

Acknowledgments

This work was conducted under the supervision of Prof. Dr. Arthur Konnerth.

I am grateful to Prof. Dr. Arthur Konnerth for providing me the opportunity to take part in the PhD program ‘Medical Life Science and Technology’ and to have a chance to learn and apply new methods and techniques in the present studies. I would like to thank Prof. Dr. Konnerth for his scientific supervision of my work, valuable practical advices and support.

I appreciate the fruitful collaboration with Prof. Dr. Bert Sakmann and members of his lab, especially with Dr. Alexander Groh. I have extended my knowledge in the cellular morphology and mastered the technique of cell labeling and reconstructions.

Thanks to Prof. Dr. Knut Holthoff, from whom I had a chance to learn the basics of patch- clamp technique. I would also like to thank Prof. Dr. Helmuth Adelsberger for his support and advices concerning the PhD program. Thanks to Dr. Katrin Offe for solving the organizational questions.

Thanks to Ulrich Leischner, PhD for development and setting the AOD-based two- photon system that allowed me to perform series of the imaging experiments in thin structures such as spines and distal dendrites. Thanks to Dr. Albrecht Stroh for his comments and together with Charlotta Rühlmann for the viral injections. Thanks to Dr. Jana Hartmann for the guidance of the neuroscience scientific seminar. Thanks to Jia Lou for her help with the Illustrator programs. Thanks to Christine Karrer for technical assist.

Thanks to all the colleagues for their support, advices and time spent together through all these years. Personal thanks to Andreas Fohr for his friendship and support.

I also would like to thank my family and my friends for their constant believe in me and tremendous support.

Chapter 7

Bibliography/ References

Adamantis, A.R., Zhang, F., Aravanis, A.M., Deisseroth, K. and Lecea, L. (2007). Neural substrates of awakening probed with optogenetic control of hypocretin neurons. *Nature* 450(7168):420-424

Agmon, A., Connors, B.W. (1991). Thalamocortical responses of mouse somatosensory (barrel) cortex in vitro. *Neurosci.* 41(2-3):365-379.

Agmon, A., Yang, L.T., O'Dowd, D.K., Jones, E.G. (1993). Organized growth of thalamocortical axons from the deep tier of terminations into layer IV of developing mouse barrel correx. *J Neurosci*.13(12):5365-5382

Angulo, M.C., Staiger, J.F., Rossier, J., Audinat, E. (2003). Distinct local circuits between neocortical pyramidal cells and fast- spiking interneurons in young adult rats. *J Neurophysiol.* 89(2):943-953

Antic, S., Zecevic, D. (1995). Optical signals from neurons with internally applied voltage-sensitive dyes. *J Neurosci* 15(2):1392-1405

Arlotta, P., Molyneaux, B.J., Chen, J., Kominami, R., Macklis, J.D. (2005). Neuronal subtype- specific genes that control corticospinal motor neuron development in vivo. *Neuron*. 45 (2):207-221

Augustine, G.J., Santamaria, F., Tanaka, K. (2003). Local calcium signaling in neurons. *Neuron.* 40(2):331-346

Bailey, C.H., Kandel, E.R., Si, K. (2004). The persistence of long-term memory: a molecular approach to self- sustaining changes in learning- induced synaptic growth. *Neuron.* 44(1):49-57

Bischoberger, J., Engel, D., Li, L., Geiger, J.R., Jonas P. (2006). Patch-clamp recording from mossy fiber terminals in hippocampal slices. *Nat Protoc*. 1(4):2075-2081.

Borst, J.G.G. (2010). The low synaptic release probability *in vivo*. *Trends in Neurosciences*. 33(6):259-266

Boyden, E.S., Zhang, F., Bamberg, E., Nagel, G. and Deisseroth, K. (2005). Millisecond timescale, genetically targeted optical control of neural activity. *Nat Neurosci.* 8(9):1263-1268

Brain, K.L., Bennett, M.R. (1997). Calcium in sympathetic varicosities of mouse vas deferens during facilitation, augmentation and autoinhibition. *J Physiol (London).* 502:521-536

Branco, T., Staras, K., Darcy, K.J. and Goda, Y. (2008). Local dendritic activity sets release probability at hippocampal synapses. *Neuron.* 59(3):475-485

Branco, T. and Staras, K. (2009). The probability of neurotransmitter release: variability and feedback control at single synapses. *Nat. Rev.* 10(5):373-383

Braunewell, K.- H. (2005). The darker side of Ca^{2+} - signaling by neuronal Ca^{2+} - sensor proteins: From Alzheimer's disease to cancer. *Trends Pharmacol. Sci.* 26(7):345-351

Brecht, M. (2007). Barrel cortex and whisker- mediated behaviors. *Current Opinion in Neurobiology*. 17(4):408-416

Brown, E., M. (2008). Calcium signaling and disease. *Subcell. BIochem*. 45:139-167

Buzsáki, G. and Kandel, A. (1998). Somatodendritic backpropagation of action potebntials in cortical pyramidal cells of the awake rat. *J Neurophysiol*. 79(3):1587-1591

Cajal, S.R. (1911). Histologie du systeme Nerveux de l'Homme et des Vertebres. Vol.II. (translated by S.Azoulay). Paris

Cardin, J.A., Carlén, M., Meletis, K., Knoblich, U., Zhang, F., Deisseroth, K., Tsai, L. and Moore, C.I. (2009). Driving fast-spiking cells induces gamma rhythm and controls sensory responses. *Nature.* 459(7247):663-667

Catterall, W.A. (2000). Structure and regulation of voltage- gated Ca^{2+} channels. *Annu. Rev. Cell Dev. Biol.* 16:521-525

Catterall, W.A., Few, A.P. (2008). Calcium channel regulation and presynaptic plasticity. *Neuron.* 59(6):882-901

Caterall, W.A. (2011). Voltage- gated calcium channels. *Cold Spring Harb Perspect Biol.* 3(8):1-23

Chagnac-Amitai, Y., Luhmann, H. J., Prince, D.A. (1990). Burst generating and regular spiking layer 5 pyramidal neurons of rat neocortex have different morphological features. *J Comp Neurol*. 296(4):598-613

Chen, X., Leischner, U., Rochefort, N.L., Nelken, I. and Konnerth, A. (2011). Functional mapping of single spines in cortical neurons *in vivo*. *Nature.* Doi:10.1038/nature10193

Christophe, E., Doerflinger, N., Lavery, D.J., Molnar, Z., Charpak, S., Audinat, E. (2005). Two populations of layer V pyramidal cells of the mouse neocortex: development and sensitivity to anesthetics. *Neurophysiol*. 94(5):3357–3367

Colbert, C.M. and Johnston, D. (1996b). The site of action potential initiation an Na^{+} channel densities in the initial segment and soma of subicular pyramidal neurons. *J Neurosci.* 16:6676-6687

Connors, B.W., Gutnick., M.J. (1990). Intrinsic firing properties of diverse neocortical neurons. *Trends Neurosci*. 13(3):99-104

Cruikshank, S.J., Urabe, H., Nurmikko, A.V. and Connors, B.W. (2009). Pathway-specific feedforward circuits between thalamus and neocortex revealed by selective optical stimulation of axons. *Neuron.* 65(2):230-245

DeFelipe, J. and Farinas, I. (1992). The pyramidal neuron of the cerebral cortex : morphological and chemical characteristics of the synaptic inputs. *Prog Neurobiol.* 39(6):563-607

Del Castill, J. and Katz, B. (1954). Quantal components of the end- plate potential. *J. Physiol.* 124(3):560-573

de Kock, C.P.J. and Sakmann, B. (2008). High frequency action potential bursts (≥100Hz) in L2/3 and L5B thick tufted neurons in anaesthetized and awake rat primary somatosensory cortex. *J Physiol.* 586(14):3353-364

Denk, W., Strickler, J.H, Webb, W.W. (1990). Two- photon laser scanning fluorescence microscopy. *Science.* 248 (4951):73-76

Denk, W., Sugimori, M. and Llinas, R. (1995). Two types of calcium response limited to single spines in cerebellar Purkinje cells. *Proc. Natl. Acad. Sci* USA 92(18): 8279-8282

Denk, W., Svoboda, K. (1997). Photon up manship: why multiphoton imaging is more than a gimmick. *Neuron*. 18(3):351-357

Deschenes, M., Veinante, P., Zhang, Z.W. (1998). The organization of corticothalamic projections: reciprocity versus parity*. Brain Res Rev*. 28(3):286-308

Diamond, M.E., Armstrong-James, M., Ebner, F.F. (1992). Somatic sensory responses in the rostral sector of the posterior group (POm) and in the ventral posterior medial nucleus (VPM) of the rat thalamus. *J Comp Neurol* . 318(4):462-476

Digregorio, D. A., Vergara, J. L. (1997). Localized detection of action potential-induced presynaptic calcium transients at a *Xenopus* neuromuscular junction. *J Physiol (London)* 505(Pt.3):585-592

Diliberto, P. A., Wang, X. F and Herman B. (1994). Confocal imaging of calcium in cells. *Methods Cell Biol*. 40:243-262.

Dunlap, K., Luebke, J.I., Turner, T.J. (1995). Exocytotic calcium channels in mammalian central neurons. *Trends Neurosci* 18(2):89-98

Eccles, J.C. (1964). The Physiology of synapses. *Springer Verlag, Berlin*.

Edwards, F. A., Konnerth, A., Sakmann, B. and Takahashi, T. (1989). A thin slice preparation for patch clamp recordings from neurones of the mammalian central nervous system. *Pflugers Arch (Eur. J. Physiol.)* 414(5):600–612

Edwards, F.A. and Konnerth, A. (1992). Patch-clamping cells in sliced tissue preparations. *Methods Enzymol.* 207:208–222

Fatt, P. and Katz, B (1953). The effects of inhibitory nerve impulses on a crustacean muscle fiber. *J Physiol.* 121(2):374-389

Fee, M.S., Mitra, P.P., Kleinfeld, D. (1997). Central versus peripheral determinants of patterned spike activity in rat vibrissa cortex during whisking. *J Neurophysiol*. 78(2):1144-1149

Feldman, D.E. (2000). Timing- based LTP and LTD at vertical inputs to layer II/III pyramidal cells in rat barrel cortex. *Neuron.* 27(1):45-56

Feng, G., Mellor, R.H., Bernstein, M., Keller-Peck, C., Nguyen, Q.T., Wallace, M., Nerbonne, J.M., Lichtman, J.W., Sanes, J.R. (2000). Imaging neuronal subsets in transgenic mice expressing multiple spectral variants of GFP. *Neuron.* 28(1):219-222

Fenno, L., Yizhar, O. and Deisseroth, K. (2011). The development and application of optogenetics. *Annu.Rev.Neurosci.* 34:389-412

Fluhler, E., Burnham, V.G., Loew, L.M. (1985). Spectra, membrane binding and potentiometric responses of new charge shif probes. *Biochemistry*. 24 (21):5749-5755

Fuortes, M.G.F., Frank, K., Becker; M.C. (1957). Steps in the production of motoneurons spikes. *J Gen Physiol.* 40(5):735-752

Garaschuk, O., Milos, R.I., Grienberger, C., Marandi, N., Adelsberger, H., Konnerth, A. (2006). Optical monitoring of brain function *in vivo*: from neurons to networks. *Pflugers Arch*. 453(3):385-396

Genoux, D. and Montgomery, J.M. (2007). Glutamate receptor plasticity at excitatory synapses in the brain. *Clinical and experimental Pharmacology and Physiology*. 34(10):1058-1063

Golgi, C. (1886). Recherches sur l'histologie des centres nerveux. *Archives italiennes de Biologie 3*:285-317

Gradinaru, V., Mogri, M., Thompson, K.R., Henderson, J.M. and Deisseroth, K. (2009). Optical deconstruction of Parkinsonian neural circuitry. *Science.* 324(5925):354-359

Groh, A., de Kock, C.P., Wimmer, V.C., Sakmann, B. and Kuner, T. (2008). Driver or coincidence detector: modal switch of a corticothalamic giant synapse controlled by spontaneous activity and short- time depression. *J. Neurosci.* 28(39):9652-9663

Groh, A., Meyer, H.S., Schmidt, E.F., Heintz, N., Sakmann, B., Krieger, P. (2010). Cell-type specific properties of pyramidal neurons in neocortex underlying a layout that is modifable depending on the cortical area. *Cereb Cortex*. 20(4):826-836

Grynkiewicz, G., Poenie, M. and Tsien, R.Y. (1985). A new generation of Ca^{2+} indicators with greatly improved fluorescence properties. *J.Biol.Chem.* 260(6):3440-3450

Gulledge, A.T. and Stuart, G.J. (2003). Action potential initiation and propagation in layer 5 pyramidal neurons of the rat prefrontal cortex: absence of dopamine modulation. *J Neurosci.* 23(36):11363-11372

Hattox, A.M., Nelson, S.B. (2007). Layer V neurons in mouse cortex projecting to different targets have distinct physiological properties. *J Neurophysiol.* 98(6): 3330- 3340

Hawkin, R.D., Kandel, E.R., Bailey, C.H. (2006). Molecular mechanisms of memory storage in Aplysia. *Biol.Bull.* 210(3):171-191

Haugland, R.P., Spence, M.T.Z., Johnson, I.D., Basey, A. (2005). Handbook. A guide to fluorescent probes and labeling techniques. Section 19.1 (*http:// invitrogen.com*)

Helmchen, F., Svoboda, K., Denk, W. and Tank, D.W. (1999). *In vivo* dendritic calcium dynamics in deep- layer cortical pyramidal neurons. *Nat.Neurosci*. 2(11):989-996

Holthoff, K., Kovalchuk, Y, Yuste, R., Konnerth, A. (2004). Single- shock LTD by local dendritic spikes in pyramidal neurons of mouse visual cortex. *J. Physiol.* 560(1):27-36

Holthoff, K., Tsay, D. and Yuste, R. (2002). Calcium dynamics of spines depend on their dendritic location. *Neuron.* 33(3):425-437

Holthoff, K., Zecevic, D., Konnerth, A. (2010). Rapid time course of action potentials in spines and remote dendrites of mouse visual cortex neurons. *J Physiol*. 588(7):1085-1096

Hodgkin, A. L. and Huxley, A.F. (1952). A quantitative description of membrane current and its application to conduction and excitation in nerve. *J. Physiol.* 117(4): 500-544

Hodgkin, A.L. and Rushton, W.A.H. (1946). The electrical constants of a crustacean nerve fibre. *Proc. R. Soc. London B.* 134(873):444-479

Horikawa, K., Armstrong, W.E. (1988) A versatile means of intracellular labeling injection of biocytin and its detection with avidin conjugates. *J. Neurosci Methods*. 25(1):1-11.

Hovnanian, A. (2008). Calcium signaling and disease. *Subcell. Biochem.* 45:337-363

Häusser, M., Major, G., Stuart, G.J. (2001). Differential shunting of EPSPs by action potentials. *Science*. 291(5501):138-141

Häusser, M. (2001). Synaptic function: Dendritic democracy. *Curr. Biol.* 11(1):10-12

Ichihara, A., Tanaami, T., Isozaki, K., Sugiyama, Y., Kosugi, Y., Mikuriya, K., Abe, M. and Uemura, I. (1996). High-speed confocal fluorescence microscopy using a Nipkow scanner with microlenses. For 3-D imaging of fluorescent molecule in real time. *Bioimages* 4:57-62

Inoue, S, and Inoue, T. (2002). Direct view high- speed confocal scanner. The CSU-10. Cell Biological Applications of Confocal Microscopy. *2nd Edition (methods in Cell Biology, Vol.70). Academic Press.*70:87-127

Johnston, D., Magee, J.C., Colbert, C.M. and Chrisitie, B.R. (1996). Active properties of neuronal dendrites. *Annu.Rev.Neurosci.* 19:165-186

Johnston, D. and Wu, S.M.-S. (1995). Foundations of cellular neurophysiology. *Cambridge, MA. MIT Press.*

Jonas, P. and Sakmann, B. (1992).Glutamate receptor channels in isolated patches from CA1 and CA3 pyramidal cells of rat hippocampal slices. J.Physiol. 455:143-171

Jones, E.G. (1984). Laminar distribution of cortical efferent cells. In: Cellular components of the cerebral cortex. *New York: Plenum Press.* 1:521–554.

Kasper, E.M., Larkman, A.U., Lübke, J., Blakemore, C. (1994). Pyramidal neurons in layer 5 of the rat visual cortex. I. Correlation among cell morphology, intrinsic electrophysiological propertirs, and axon targets*. J Comp Neurol*. 339 (4):459-474

Kasper, E.M., Larkman, A.U., Lübke, J., Blakemore, C. (1994). Pyramidal neurons in layer 5 of the rat visual cortex. II. Development of electrophysiological properties. *Comp Neurol*. 339(4):475-94

Kasper, E.M., Lübke, J., Larkman, A.U., Blakemore, C. (1994). Pyramidal neurons in layer 5 of the rat visual cortex. III. Differential maturation of axon

targeting, dendritic morphology, and electrophysiological properties. *J Comp Neurol*. 339(4):495-518

Kerr, N.D., Greenberg, D., Helmchen, F. (2005). Imaging input and output of neocortical networks in vivo. *PNAS*. 102(39):14063-14068

Koch, C., Poggio, T. (1983). A theoretical analysis of electrical properties of spines. *Proc. R. Soc. London Ser*. B 218(1213):455-477

Konnerth, A. (1990). Patch- clamping in slices of mammalian CNS. *TINS* 13(8):321–323

Kovalchuk, Y., Eilers, J., Lisman, J. and Konnerth, A. (2000). NMDA receptor-mediated subthreshold Ca^{2+} signals in spines of hippocampal neurons. *J Neurosci.* 20(5):1791-1799

Kravitz, A.V., Freeze, B.S., Parker, P.R.L., Kay, K., Thwin, M.T., Deisseroth, K. and Kreitzer, A.C. (2010). Regulation of parkinsonian motor behaviours by optogenetic control of basal ganglia circuitry. *Nature.* 466(7306):633-639

Larkman, A., Mason, A. (1990). Correlations between morphology and electrophysiology of pyramidal neurons in slices of rat visual cortex. I. Establishment of cell classes*. J Neurosci*. 10(5):1407-1414

Larkum, M.E., Zhu, J.J., Sakmann, B. (1999b). A new cellular mechanism for coupling inputs arriving at different cortical layers. *Nature.* 398(6725):338-341

Larkum, M.E., Zhu, J.J. and Sakmann, B.J. (2001). Dendritic mechanisms underlying the coupling of the dendritic with the axonal action potential initiation zone of adult rat layer 5 pyramidal neurons. *J. Physiol* 553(Pt 2):447-466

Larkum, M.E., Nevian, T. (2008). Synaptic clustering by dendritic signaling mechanisms. *Curr. Opin. Neurobiol.* 18(3):321-331

Larkum. M.E., Nevian, T., Sandler, M., Polsky, A., Schiller, J. (2009). Synaptic integration in tuft dendrites of layer 5 pyramidal neurons: a new unifying principle. *Science.* 325(5941):756-760

Leischner, U. (2011). Ultra- fast two- photon microscopy for in vivo brain imaging. Institute of Neuroscience, Faculty of Medicine (Munich, Technische Universität München (TUM)), 90-97.

Li; C.-Y., Lu, J.-T., Wu, C.-P., Duan, S.-M., Poo, M.-M. (2004). Bidirectional modification of presynaptic neuronal excitability accompanying spike timing-dependent synaptic plasticity. *Neuron.* 41(2):257-268

Linden, D.J. (1999). The return of the spike: postsynaptic action potentials and the induction of LTP and LTD. *Neuron*. 22(4):661-666

Loew, L.M., Cohen, L.B., Salzberg, B.M., Obaid, A.L., Bezanilla, F. (1985). Charge- shift probes of membrane potential. Characterization of aminostyrylpyridinium dyes on the squid giant axon. *Biophys J*. 47(1):71-77

Lu, S.M., Lin, R.C. (1993). Thalamic afferents of the rat barrel cortex: a light- and electron-microscopic study using *Phaseolus vulgaris* leucoagglutinin as an anterograde tracer. *Somatosens Motor Res*. 10(1):1-16

Lübke, J., Feldmeyer, D. (2007). Excitatory signal flow and connectivity in a cortical column: focus on barrel cortex. *Brain Struct Funct.* 212(1):3-17

Maass, W. and Zador, A. (1999). Dynamic stochastic synapses as computational units. *Neural Comput.* 11(4):903-917

Marin- Padilla, M. (1976). Pyramidal cell abnormalities in the motor cortex of a child with Down's syndrome. A Golgi study. *J. Comp. Neurol.* 167(1):63-81

McCue, H.V., Haynes, L.P. and Burgoyne, R.D. (2010). The diversity of calcium sensor proteins in the regulation of neuronal function. *Cold Spring Harb Perspect Biol.* 2(8):1-20

Markram, H., Lübke, J., Frotscher, M., Sakmann, B. (1997). Regulation of synaptic efficacy by coincidence of postsynaptic APs and EPSPs. *Science.* 275(5297): 213-215

Mayer, M.L., Westbrook, G.L., Guthrie, P.B. (1984). Voltage- dependent block by Mg^{2+} of NMDA responses in spinal cord neurons. *Nature.* 309(5965):261-263

Meir, A. (2005). Voltage dependent Ca^{2+} (Ca_v) channels. *Modulator.* 20:2-6

Minta, A., Kao, J.P. and Tsirn, R.Y. (1989). Fluorescent indicators for cytosolic calcium based on rhodamine and fluorescein chromophores. *J.Biol.Chem.* 264(14):8171-8178

Meyer, H.S., Wimmer, V.C., Hemberger, M., Bruno, R.M., de Kock, C.P., Frick, A., Sakmann, B., Helmstaedter, M. (2010). Cell type-specific innervations in a column of rat vibrissal cortex. *Cereb Cortex*. 20(10):2287-2303

Meyer, H.S., Wimmer, V.C., Oberlaender, M., de Kock, C.P., Sakmann, B., Helmstaedter, M. (2010). Number and laminar distribution of neurons in a thalamocortical projection column of rat vibrissal cortex. *Cereb Cortex*. 20(10):2277-2286

Mitchell, B.D., Macklis, J.D. (2005). Large- scale maintenance of dual projections by callosal and frontal cortical projection neurons in adult mice. *J Comp Neurol*. 482(1):17-32

Mitmann, W., Wallace, D.J., Czubayko, U., Herb, J.T., Schaefer, A.T., Looger, L. L., Denk, W. and Kerr, J.N.D. (2011). Two- photon calcium imaging of evoked activity from L5 somatosensory neurons *in vivo*. *Nat. Neurosci.* 14(8):1089-1094

Molnar, Z., Cheung, A.F.P. (2006). Towards the classification of subpopulations of layer V pyramidal projection neurons. *Neurosci. Res.*. 55(2):105–115

Mountcastle, V.B., Talbot, W.H., Sakata, H., Hyvärinen, J. (1969). Cortical neuronal mechanisms in flutter- vibration studied in unanesthetized monkeys. Neuronal periodicity and frequency discrimination. *J Neurophysiol.* 32(3):452-484

Nagel, G., Ollig, D., Fuhrmann, M., Kateriya, S., Musti, A.M., Bamberg, E., Hegemann, P. (2002). Channelrhodopsin-1: a light- gated proton channel in green algae. *Science.* 296(5577):2395-2398

Nagel, G., Szellas, T., Huhn, W., Kateriya, S., Adeishvili, N., Berthold, P., Ollig, D., Hegemann, P., Bamberg, E. (2003). Channelrhodopsin-2, a directly light-

gated cation- selective membrane channel. *Proc Natl Acad Sci U S A.* 100(24): 13940-13945

Nakano, A. (2002). Spinning-disk confocal microscopy- a cutting edge tool for imaging of membrane traffic. *Cell structure and function*. 27(5):349-355

Nimchinsky, E.A., Sabatini, B.L. and Svoboda,K. (2002). Structure and function of dendritic spines. *Annu. Rev. Physiol.* 64:313-353

Nowak, L., Bregestovski, P., Ascher, P., Herbet, A., Prochiantz, A. (1984). Magnesium gates glutamate- activated channels in mouse central neurones. *Nature.* 307(5950):462-465

Offner, F., Weinberg, A. and Young, G. (1940). Nerve conduction theory: some mathematical consequence of Bernstein's model. *Bull. Math. Biophys.* 2:89-103

Palmer, L.M. and Stuart, G.J. (2006). Site of action potential initiation in layer 5 pyramidal neurons. *J Neurosci.* 26(6):1854-1863

Paredes, R.M., Etzler, J.C., Watts, L.T., Zheng, W., Lechleiter, J.D. (2008). Chemical calcium indicators. *Methods*. 46(3):143-151

Peinado, A., Yuste, R., Katz, L.C. (1993). Gap junctional communication and the development of local circuits in neocortex. *Cereb. Cortex.* 3(5):488-498

Petersen, C.C.H. (2003). The barrel cortex- integrating molecular, cellular and systems physiology. *Pflugers Arch.* 447(2):126-134

Petreanu, L., Huber, D., Sobczyk, A., Svoboda, K. (2007). Channelrhodopsin-2-assisted circuit mapping of long- range callosal projections. *Nat Neurosci.* 10(5):663-668

Petreanu, L., Mao, T., Sternson, S. M., Svoboda, K. (2009). The subcellular organization of neocortical excitatory connections. *Nature*. 457(7233):1142-1145

Polsky, A., Mel, B.W. and Schiller, J. (2004). Computational subunits in thin dendrites of pyramidal cells. *Nat Neurosci.* 7(6):621-626

Potter, S.M. (1996). Vital imaging: two photons are better than one. *Curr Biol*. 6 (12):1595-1598

Rall, W. (1957). Membrane time constant of motoneurons. *Science.* 126:454

Rall, W. (1959a). Dendritic current distribution and whole neuron properties. *Naval Med. Res. Inst. Res. Report* NM 01-05-00.01.01

Rall, W. (1959b). Branching dendritic trees and motoneuron membrane resistivity. *Exp. Neurol.* 1:491-527

Rall, W. (1962). Electrophysiology of a dendritic neuron model. *Biophys J.* 2(2): 145-167

Rall, W. (1964). Theoretical significance of dendritic trees for neuronal input-output relations. *In Neural Theory and Modeling, ed. R.F.reiss. Stanford Univ. Press.*

Rall, W. (1977). The nervous system. *Handbook of Physiology*. Physiol. Soc., Bethesda, Maryland.

Reichova, I. and Sherman, S.M. (2004). *J Neuropsyiol* 92(4):2185-2197

Roth, A. and London, M. (2004). Rebuilding dendritic democracy. Focus on 'Equalization of synaptic efficacy by activity- and timing- dependent synaptic palsticity'. *J. Neurophysiol.* 91(5):1941-1942

Rumsey, C.C. and Abbott, L.F. (2006). Synaptic democracy in active dendrites. *J. Neurophysiol.* 96(5):2307-2318

Shepherd, G.M. (1996). The dendritic spine: A multifunctional integrative unit. *J. Neurophysiol.* 75(6):2197-2210

Shepherd, G.M. (1998). The synaptic organization of the brain. *Fourth edition. Oxford University Press.*

Schiller, J., Schiller, Y., Stuart, G. and Sakmann, B. (1997). Calcium action potentials restricted to distal apical dendrites of rat neocortical pyramidal neurons. *J Physiol.* 505(3):605-616

Sommer, B., Monyer, H., Wisden, W., Verdoorn, T.A., Burnashev, N., Sprengel, R., Sakmann, B., Seeburg, P.H. (1992). Glutamate- gated ion channels in the brain. Genetic mechanism for generating molecular and functional diversity. *Arzneimittelforschung.* 42(2A):209-210

Spruston, N., Schiller, Y., Stuart, G. and Sakmann, B. (1995). Activity- dependent action potential invasion and calcium influx into hippocampal CA1 dendrites. *Science.* 268(5208):297-300

Stanfield, B.B., Jacobowitz, D.M. (1990). Antibody to a soluble protein purified from brain selectively labels layer V corticofugal projection neurons in rat neocortex. *Brain Res*. 531(1-2):219-224

Stosiek, C., Garaschuk, O., Holthoff, K., Konnerth, A. (2003) In vivo two-photon calcium imaging of neuronal networks. *Proc Natl Acad Sci U S A*. 100(12):7319-7324

Stroh, A., Adelsberger, H., Rühlmann, C., Fischer, S., Schierloch, A., Deisseroth, K., Konnerth, A. (2011). Making waves: initiation and propagation of slow oscillation- associated cortical calcium waves *in vivo*. *Submitted.*

Stroh, A., Tsai, H.C., Wang, L.P., Zhang, F., Kressel, J., Aravanis, A., Santhanam, N., Deisseroth, K., Konnerth, A., Schneider, M.B. (2011). *Stem cells.* 29(1):78-88

Stuart, G.J., Dodt, H.-U., Sakmann, B. (1993). Patch- clamp recordings from the soma and dendrites of neurons in brain slices using infrared video microscopy. *Pflügers Arch*. 423(5-6):511-518

Stuart. G.J., Sakmann, B. (1994). Ative propagation of somatic action potentials into neocortical pyramidal cell dendrites. *Nature.* 367(6458):69-72

Stuart, G., Schiller, J., Sakmann, B. (1997). Action potential initiation and backpropagation in rat neocortical pyramidal neurons. *J.Physiol*. 505(3):617-632

Svoboda, K., Denk, W., Kleinfeld, D., Tank, D.W. (1997). *In vivo* dendritic calcium dynamics in neocortical pyramidal neurons. *Nature* 385(6612):161-165

Suzuki, T., Yamasaki, K., Fujita, S., Oda, K., Iseki, M., Yoshida, K., Watanabe, M., Daiyasu, H., Toh, H., Asamizu, E., Tabata, S., Miura, K., Fukuzawa, H., Nakamura, S., Takahashi, T. (2003). Archaeal- type rhodopsins in Clamydomonas: model structure and intracellular localization. *Biochem Biophys Res Commun*. 301(3):711-717

Takahashi, A., Camacho, P., Lechleiter, J.D. and Herman, B. (1999). Measurement of intracellular calcium. *Physiological Reviews*. 79(4):1089-1123

Takashima, S., Ieshima, A., Nakamura, H., Becker, L.E. (1989). Dendrites, dementia and the Down syndrome. *Brain Dev*. 11(2):131-133

Theyel, B.B., Llano, D.A., Sherman, S.M. (2010). *Nat Neurosci* 13(1):84-88

Tsien, R.W., Lipscombe, D., Madison, D.V., Bley, K.R., Fox, A.P. (1988). Multiple types of neuronal calcium channels and their selective modulation. *Trends Neurosci* 11(10):431-438

Van der Loos, H., Woolsey, T.A. (1973). Somatosensory cortex: structural alterations following early injury to sense organs. *Science*. 179(71):395-398

Veinante, P., Lavallee, P. and Deschenes, M. (2000). Corticothalamic projections from layer 5 of the vibrissal cortex in the rat*. J.Comp.Neurol.* 424(2):197-204

Wang, Z., McCormick, D.A. (1993). Control of firing mode of corticotectal and corticopontine layer V burst- generating neurons by norepinephrine, acetylcholine, and 1S, 3R- ACPD. *J Neurosci.* 13(5):199-216

Wise, S.P., Jones, E.G. (1978). Dvelopmental studies of thalamocortical and commissural connections in the rat somatic sensory cortex. *J Comp Neurol*. 178(2):187-208

Wang, T., Kass, I.S. (1997). Preparation of brain slices. *Methods Mol. Biol.* 72:1-14

Waters, J., Schaefer, A., Sakmann, B. (2005). Backpropagating action potentials in neurones: measurement, mechanisms and potential functions. *Progress in Biophysics & Molecular Biology.* 87(1):145-170

Williams, S.R. and Stuart, G.J. (2000). Backpropagation of physiological spike trains in neocortical pyramidal neurons: implications for temporal coding in dendrites. *J Neurosci*. 20(22):8238-8246

Woolsey, T.A., Van der Loos, H. (1970). The structural organization of layer IV in the somatosensory region (SI) of mouse cerebral cortex. The description of a cortical field composed of discrete cytoarchitectonic units. *Brain Res*. 17(2):205-242

Yang, S.N., Tang, Y.G., Zucker, R.S. (1999). Selective induction of LTP and LTD by postsynaptic [Ca^{2+}]i elevation. *J Neurophysiol.* 81(2):781-787

Yu, C., Haidar Liu, S., Ahissar, E. (2006). Parallel thalamic pathways for whisking and touch signals in the rat. *PLoS Biol*. 4(5):e124

Zhang, F., Gradinaru, V., Adamantidis, A.R., Durand, R., Airan, R.D., de Lecea, L., Deisseroth, K. (2010). Optogenetic interrogation of neural circuits: technology for probing mammalian brain structures. *Nat Protoc* 5(3):439-456

Zhang, F., Wang, L- P., Boyden, E.S. and Deisseroth, K. (2006). Channelrhodopsin-2 and optical control of excitable cells. *Nat Methods.* 3(10): 785-792

Zhang, F., Wang, L.P., Brauner, M., Liewald, J.F., Kay, K., Watzke, N., Wood, P.G., Bamberg; E., Nagel, G., Gottschalk, A., Deissertoh, K. (2007a). Multimodal fast optical integration of neural circuitry. *Nature* 446(7136):633-639

Zhang, W., Ge, W., Wang, Z. (2007b). A toolbox for light control of *Drosophila* behaviors through channel- rhodopsin 2- mediated photoactivation of targeted neurons. *Eur J Neurosci* 26(9):2405-2416

Zhu, J.J. (2000). Maturation of layer 5 neocortical pyramidal neurons: amplifying salient layer 1 and layer 4 inputs by Ca^{2+} action potentials in adult rat tuft dendrites. *J Physiol.* 526(Pt 3):571-587

Zochowski, M., Wachowiak, M., Chun, X.F, Cohen, L.B., Lam, Y.W., Antic, S., Zecevic, D. (2000). Imaging membrane potential with voltage- sensitive dyes. *Biol.Bull* 198(1):1-21

Zucker, R.S. (1989). Short- term synaptic plasticity. *Annu Rev Neurosci.* 12:13-31

Zucker, R.S. (1999). Calcium- and activity- dependent synaptic plasticity. *Curr Opin Neurobiol.* 9(3):305-313

http://www.course1.winona.edu/sberg/ILLUST/DABreaction.gif

http://www.products.invitrogen.com

http://www.hi.helsinki.fi/amu/AMU Cf_tut/

Chapter 8

Publications

Groh, A., Bokor, H., Mease, R.A., Plattner, V.M., Hangya, B., **Sharifullina, E.,** Stroh, A., Deschenes, M., Sakmann, B. and Acsády, L. (2011). Dual cortical and sensory drive of single thalamocortical relays. *Submitted.*

Elvira Sharifullina, Bert Sakmann and Arthur Konnerth. (2011). Spine signaling in the apical tuft of thick- tufted L5 pyramidal neurons of the mouse vibrissal cortex. *In preparation.*